NASA CR- 144683

22409-6015-RU-00

STUDY OF MONOPROPELLANTS FOR ELECTROTHERMAL THRUSTERS

(NASA-CR-144683) STUDY OF MONOPROPELLANTS FOR ELECTROTHERMAL THRUSTERS Final Report, Mar. 1973 - May 1974 (TRW Systems Group) 145 p HC $6.00 CSCL 21I

N76-12192

Unclas
G3/28 04787

J.D. Kuenzly

TRW Systems Group
One Space Park
Redondo Beach, Calif. 90278

JUNE 1974

FINAL REPORT

MARCH 1973 – MAY 1974

Prepared for
GODDARD SPACE FLIGHT CENTER
Greenbelt, Maryland 20771

22409-6015-RU-00

STUDY OF MONOPROPELLANTS FOR ELECTROTHERMAL THRUSTERS

J.D. Kuenzly

TRW Systems Group
One Space Park
Redondo Beach, Calif. 90278

JUNE 1974

FINAL REPORT

MARCH 1973 – MAY 1974

Prepared for
GODDARD SPACE FLIGHT CENTER
Greenbelt, Maryland 20771

1. Report No.	2. Government Accession No.	3. Recipient's Catalog No.
22409-6015-RU-00		

4. Title and Subtitle	5. Report Date
STUDY OF MONOPROPELLANTS FOR ELECTROTHERMAL THRUSTERS	June 1974
	6. Performing Organization Code
7. Author(s)	8. Performing Organization Report No.
J. D. Kuenzly	22409-6015-RU-00
9. Performing Organization Name and Address	10. Work Unit No.
TRW Systems Group One Space Park Redondo Beach, California 90278	11. Contract or Grant No. NAS5-23202
12. Sponsoring Agency Name and Address	13. Type of Report and Period Covered
Goddard Space Flight Center Greenbelt, Maryland 20771 R. Callens - Technical Monitor	Final Report March 1973 - May 1974
	14. Sponsoring Agency Code

15. Supplementary Notes

Prepared under the direction of C. K. Murch, Program Manager

16. Abstract

A 333 mN electrothermal thruster designed for operation with MIL-grade hydrazine was demonstrated to be suitable for operation with low freezing point monopropellants containing hydrazine azide, monomethylhydrazine, unsymmetrical-dimethylhydrazine and ammonia. The steady-state specific impulse was greater than 200 sec for all propellants. An azide blend exceeded 175 sec pulsed-mode specific impulse for pulse widths greater than 50 ms; propellants containing carbonaceous species delivered 175 sec pulsed-mode specific impulse for pulse widths greater than 100 ms. Longer thrust chamber residence times were required for the carbonaceous propellants; the original thruster design was modified by increasing the characteristic chamber length and density of screen packing.

Specific recommendations were put forth for the work required to design and develop flight worthy thrusters. These recommendations included methods to increase propellant dispersal at injection, thruster geometry changes to reduce holding power levels and methods to initiate the rapid decomposition of the carbonaceous propellants.

17 Key Words (Selected by Author(s))	18. Distribution Statement
Monopropellant Electrothermal Thruster Hydrazine Substitutes	

19. Security Classif. (of this report)	20. Security Classif. (of this page)	21. No. of Pages	22. Price*
Unclassified	Unclassified	145	

*For sale by the Clearinghouse for Federal Scientific and Technical Information, Springfield, Virginia 22151.

PREFACE

The objective of the "Study of Monop opellants for Electrothermal Thrusters" program was to determine the feasibility of operating small thrust level electrothermal thrusters with monopropellants other than MIL-grade hydrazine. The work scope included analytical study, design and fabrication of demonstration thrusters, and an evaluation test program wherein monopropellants with freezing points lower than MIL-grade hydrazine were evaluated and characterized to determine their applicability to electrothermal thrusters for spacecraft attitude control; a data correlation phase culminated in the proposal of specific recommendations for the work required to design and develop flight worthy electrothermal thrusters using low freezing point monopropellants for space flight applications.

The 333 mN electrothermal thruster designed for operation with MIL-grade hydrazine is suitable for operation with propellants having lower freezing points. These propellants are 76% hydrazine - 24% hydrazine azide, Aerozine-50, 50% hydrazine - 50% monomethylhydrazine, and a TRW-formulated mixture of 35% hydrazine - 50% monomethylhydrazine - 15% ammonia. The program goal of 200 sec steady-state specific impulse was exceeded by all propellants. The pulsed-mode program goal of 175 sec was exceeded by the azide blend for pulse widths greater than 50 ms and was met by the carbonaceous propellants for pulse widths greater than 100 ms.

Longer thrust chamber residence times were required for the carbonaceous propellants; the original thruster design was modified by increasing the characteristic chamber length and density of screen packing. A substantial amount of thermal energy must be supplied to initiate decomposition of propellants containing unsymmetrical-dimethylhydrazine and monomethylhydrazine.

Carbon deposition was minimal with the TRW-formulated mixture, whereas that observed with Aerozine-50 may pose problems for long term operation.

The original baseline thruster configuration gave non-optimal hydrazine performance. Performance was increased by promoting homogeneous,

gas-phase decomposition kinetics in a larger head space. Hydrazine operation with thruster configurations derived for the carbonaceous propellants generated significant data. An analysis of these data greatly increased an understanding of the hydrazine decomposition process.

Advanced development of electrothermal thrusters using low freezing monopropellants is warranted. Specific design recommendations were put forth in a program to develop flight worthy thrusters. These recommendations included methods to increase propellant dispersal at injection, thruster geometry changes to reduce holding power levels and methods to initiate the rapid decomposition of carbonaceous propellants.

Additional development work is recommended for the high performing electrothermal hydrazine thruster. One demonstration thruster produced 236 sec steady-state specific impulse at a thrust level of 400 mN. Pulsed-mode performance was in excess of 200 sec for a 50 ms pulse.

TABLE OF CONTENTS

LIST OF FIGURES

Page

LIST OF TABLES

LIST OF ABBREVIATIONS AND SYMBOLS

Propellants

Aerozine-50 (AERO-50)	fifty percent hydrazine-fifty percent unsymmetrical-dimethylhydrazine
HA	(N_5H_5), hydrazine azide
MHM	mixture of hydrazine monopropellants
MMH	Monomethylhydrazine
MIL-grade	military grade
NVR	non-volatile residue

Units

S I	International System
N	Newtons (thrust), or normality in context of solution chemistry
sec	specific impulse

Miscellaneous

DOD	Department of Defense
ICC	Interstate Commerce Commission
ICRPG	Inter-Agency Chemical Rocket Propulsion Group
JANNAF	Joint-Army-Navy-NASA-Air Force
LD_{50}	lethal dosage required for fifty percent of test subjects
MAC	maximum allowable concentration
RGA	residual gas analyzer

Symbols

α	ammonia dissociation fraction
A	frequency or pre-exponential factor
A_h	homogeneous frequency factor

Symbols (Continued)

A_{het}	heterogeneous frequency factor
A_S	surface area
d	diameter
ε	nozzle area ratio
I_{sp}	specific impulse
K_α	characteristic X-ray emission
K.E.	kinetic energy
k_h	homogeneous reaction rate constant
k_{het}	heterogeneous reaction rate constant
L*	characteristic thrust chamber length
m	mass (when followed by s or N, context is milli or 10^{-3})
P_c	chamber pressure
Q	activation energy
Q_h	homogeneous activation energy
Q_{het}	heterogeneous activation energy
R	universal gas constant
ρ	density
S.E.	surface energy
σ	surface tension
T	absolute temperature
T_{hold}	holding temperature
v	velocity
v*	critical velocity

1.0 INTRODUCTION

Hydrazine is currently the accepted standard for spacecraft low-thrust propulsion systems. However, the relatively high freezing point of 274.5°K inherently restricts its use and/or complicates the spacecraft's thermal control system. Numerous low freezing point monopropellants are not compatible for operation with conventional catalytic thrusters. The development of electrothermal hydrazine thrusters has eliminated many problems characteristic of catalytic hydrazine thrusters. The "Study of Monopropellants for Electrothermal Thrusters" was undertaken to determine the feasibility of operating small thrust level electrothermal thrusters with monopropellants other than MIL-grade hydrazine.

The work scope included analytical study, design and fabrication of demonstration thrusters, an evaluation test program and recommended approach for the design and development of flight worthy electrothermal thrusters using low freezing point monopropellants for spacecraft applications.

The analytical studies phase reviewed the characteristics of available low freezing point monopropellants and identified four such propellants that did not require an excessive trade-off between freezing point and performance. They were monomethylhydrazine, Aerozine-50, 77% hydrazine-23% hydrazine azide, and TRW-formulated mixed hydrazine monopropellant consisting of 35% hydrazine-50% monomethylhydrazine-15% ammonia. Eight demonstration thrusters were fabricated using a modular design which allowed the rapid characterization of the candidate monopropellants. The work performed during the evaluation test program included the initial steady-state characterization of the candidate monopropellants and an optimization phase wherein the thruster configuration was changed to meet the specific requirements of each propellant. Simulated high altitude performance measurements were obtained for the optimized thruster configurations and compared to operation with MIL-grade hydrazine. Each propellant utilized was subjected to a chemical analysis.

Specific recommendations were proposed for the work required to design and develop flight worthy electrothermal thrusters using low freezing point monopropellants for spaceflight applications. These recommendations were the product of a critical review and analysis of the information derived from the Analytical Studies, Design and Fabrication, and Evaluation Test phases.

2.0 PROPELLANT CHEMISTRY STUDIES

2.1 PROPELLANT REQUIREMENTS

A useful monopropellant other than hydrazine is one which has a lower freezing point and which may provide improvements in performance or density impulse. The consideration of various propellants for spacecraft applications also requires that equal importance be given to propellant properties related to materials compatibility, thermal stability, shock sensitivity, toxicity, handling, and transfer. These propellant requirements have been summarized and are presented in Table 1. They are representative of requirements for a system whose thrust functions are typical for spacecraft attitude control and station keeping applications.

Imposition of these characteristics may represent a set of partially contradictory requirements which must be reasonably satisfied by the candidate propellants. Each requirement has therefore been graded as "requirement" or "goal," depending on whether the characteristic is a firm requirement or a design goal which may be compromised.

The requirement of the propellant freezing point (less than that of hydrazine) was amplified to include a design goal of 255.2°K or lower. This value is a reasonable lower temperature limit which may be expected in a typical spacecraft application. It also provides a substantial improvement in comparison to hydrazine. Propellant storability, materials compatibility and thermal stability were classified as requirements in consideration of typical spacecraft missions lasting five years. The criteria for propellant shock sensitivity, toxicity, and safety characteristics were assumed to be the need for handling properties and hazard characteristics no worse than those presently established and accepted for hydrazine.

The designation of program "goal" was chosen for propellant performance, density and commonality. The optimization of each of these characteristics is desirable, but may be compromised to meet a different propellant requirement.

Table 1. Monopropellant Requirements

1.	**Ambient Temperature:** maximum	Requirement	324.7°K
	Freezing Point:	Goal	255.2°K
		Requirement	less than 274.5°K
2.	**Performance:** Steady State, minimum	Goal	I_{sp} = 200 sec
	Pulse Mode, minimum	Goal	I_{sp} = 175 sec
3.	**Density (room temperature)**	Goal	1.0 gm/cm^3 or higher
4.	**Storability**	Requirement	5 years
5.	**Shock Sensitivity**	Requirement	0 cards on JANNAF card gap test
6.	**Materials Compatibility**	Requirement	5 years
7.	**Toxicity**	Requirement	No worse than N_2H_4
8.	**Safety**	Requirement	Handling and transfer characteristics similar to N_2H_4 (DOD hazard classification Group III)
9.	**Thermal Stability**	Requirement	No worse than N_2H_4
10.	**Commonality**	Goal	"On-board" propellant in bipropellant propulsion systems

2.2 PROPELLANT PROPERTIES

Past studies to develop monopropellant substitutes for hydrazine have included the evaluation of hydrogen peroxide, organic nitrates, nitro paraffins and hydrazine derivatives such as MMH and UDMH. Efforts to lower the freezing point of hydrazine led to studies of binary monopropellants utilizing hydrazine with its derivatives as well as inorganic salts such as nitrates and azides. The freezing point of hydrazine is depressed by the addition of amines (ammonia, aniline), alcohols and water. Similar studies have been conducted with hydrazine based ternary and quarternary mixtures. All such mixtures characteristically exhibit a freezing point lower than that of hydrazine. However, the freezing point depression is associated with significant physical property and performance changes. The basic propellant selection criteria applicable to this study require the simultaneous control of the mixture's properties, performance and freezing point. The additional propellant properties requiring evaluation are vapor pressure, viscosity, density impulse, decomposition temperature, boiling point and detonation propagation.

The task of propellant selection was simplified by the rejection of those propellants which are not compatible with the requirements specified in Table 1:

a) hydrogen peroxide: this propellant has a high freezing point of 272.4°K. The decomposition and thermal stability characteristics are unsuitable for extended periods of storage.

b) hydrazine nitrate: mixtures of hydrazine and hydrazine nitrate impose stability and handling-safety problems more severe than hydrazine. Standard JANNAF card gap and drop weight tests have shown a value of zero cards and negative results, respectively, for mixtures up to 16% hydrazine nitrate. Standard ICRPG detonation propagation tests have resulted in partial propagation in 6.35 mm tubing at 296°K and 20% hydrazine nitrate concentration. The non-volatile residues are definitely shock sensitive. The presence of nitrate ions in the hydrazine blends promotes chemical reactions with materials and rapid burning.

c) other inorganic salts with the exception of azides: mixture freezing point can be depressed with the addition of hydrazine sulfide, cyanide, perchlorate, fluoride or carbonate. Performance and physical data on these mixtures are limited or non-existent and none of these has apparently been considered as a likely monopropellant.

d) organic nitrates: n-propyl nitrate has a drop-weight shock sensitivity of 7.0 kg-cm. The corresponding value for hydrazine is 120 kg-cm (minimum). Ethyl nitrate may be added to reduce the shock sensitivity of n-propyl nitrate, but improvements in performance are not expected. Other organic nitrates such as methyl nitrate and diethylene glycol dinitrate exhibit shock sensitivity similar to that of nitroglycerin.

e) nitro paraffins: nitromethane has a freezing point of 244.5°K and can provide a density impulse* of approximately 250 sec at 298°K. The high combustion temperature of 2450°K and oxygen bearing decomposition products (H_2O, CO_2, CO) preclude its use as a monopropellant. The anticipated temperatures are in excess of noble metal alloy limits. Although refractory metals (Re, etc.) have sufficient thermal capability, their reaction with CO_2 and H_2O will result in adverse material degradation. Tetranitromethane is undesirable by virtue of its high freezing point of 286.3°K. The addition of freezing point depressants increases the explosive sensitivity to unacceptable levels.

*Density impulse is expressed as the product of specific impulse (sec) and the propellant specific gravity at a specified temperature.

The remaining propellants that were evaluated are grouped into three major categories.

1. Hydrazine Derivatives. This group includes monomethylhydrazine, unsymmetrical-dimethylhydrazine and Aerozine-50. The latter, a 50-50 blend of N_2H_4 and UDMH, is included with the other monopropellants because it is a unique propellant often used in bipropellant propulsion. The performance and physical properties of these propellants are compared to hydrazine in Table 2. The data, in general, are for ambient room conditions. The safety, storage and handling characteristics are summarized in Table 3.

2. Binary Mixtures. This category considers the binary monopropellant characteristics which result from blending hydrazine with UDMH, MMH, water, ammonia, hydrazine azide and hydrazine nitrate. The latter is included for informative reasons although it has been excluded previously.

Propellant performance and physical property (298°K) data are summarized in Table 4 for mixtures of hydrazine with hydrazine azide, ammonia and hydrazine nitrate, respectively. Corresponding safety, storage and handling characteristics appear in Table 5. The mixture compositions are typical of those considered for propulsion applications.

The freezing point, density, specific impulse, and density impulse dependence on propellant composition are illustrated in Figures 1 - 4, respectively. The freezing point of hydrazine is lowered by all additives in this section (Figure 1). The minimum freezing point, 255.5°K, of hydrazine-hydrazine azide mixtures occurs at the eutectic composition of 77% N_2H_4 - 23% N_5H_5. The density is increased by the addition of water, hydrazine azide or hydrazine nitrate, whereas, additions of ammonia, MMH or UDMH decrease mixture densities. The specific and density impulse data shown in Figures 3 and 4 were computed for a chamber pressure of 1.034 MN/m^2 and expansion to vacuum through a nozzle having an area ratio of 50 to 1. The TRW Rocket Chemistry Computer Program was used to obtain the performance parameters in Figures 3 and 4. The data are for adiabatic thermodynamic equilibrium. The fraction of dissociated ammonia at equilibrium corresponds to the maximum possible. An analysis

Table 2. Performance and Physical Characteristics of Pure Monopropellants

Characteristic	Units	Propellant			
		N_2H_4	MMH	UDMH	Aero-50
1. Freezing Point	°K	274.53	220.8	215.8	267.4
2. Density (298°K)	gm/cm^3	1.00	0.87	0.79	0.90
3. Vapor Pressure (298°K)	$10^3 N/m^2$	1.89	6.58	22.2	17.9
4. Viscosity (298°K)	Poise	0.0091	0.0078	0.0049	0.0081
5. Theoretical Vacuum I_{sp} $P_c = 1.03\ MN/m^2$ $\epsilon = 50$	Sec	231	225	217	226
6. Density Impulse (298°K)	Sec	231	196	171	203
7. Adiabatic Flame Temperature	°K	1089 $\alpha = 0.72$	1058	1021	1062

ϵ = Nozzle Area Ratio

α = Fraction of Ammonia Dissociation

Performance Data for MMH, UDMH and Aero-50 are at Thermodynamic Equilibrium

Table 3. Safety/Storage/Handling Characteristics of Pure Monopropellants

		Propellant			
Characteristic	Test Method*	N_2H_4	MMH	UDMH	AERO-50
Shock Sensitivity	Drop-weight	120 kg-cm (minimum)	N/A	N/A	N/A
	JANNAF card gap	0	0	0	0
Detonation Propagation	Standard ICRPG	No propagation in 0.64 cm line at 296°K	No propagation	No propagation	No propagation
Thermal Stability	Differential Scanning Calorimeter	445°K	N/A	N/A	N/A
	Standard ICRPG	441°K	N/A	N/A	N/A
Long Term Storability	Gas Evolution Rate	1.19×10^{-4} $CC_{NTP}/kg\text{-}min$	6.89×10^{3} N/m^2-day at 344.1°K 6061 aluminum	68.9 N/m^2-day at 34. .1°K 5250 aluminum	N/A
Toxicity	MAC (PPM for 8 hr)	1.0	0.5	0.5	0.5
Safety/Handling	DOD Hazard	Group III	Group III	Group III	Group III
	ICC Rating	Corrosive liquid	Flammable liquid	Flammable liquid	Flammable liquid
Materials Compatibility**	Aluminum alloys	A	A	A	A
	300 CRES	A&B	A	A	A
	Titanium alloys	A	A	A	A

*Specific Test Methods are described in Appendix A.

**Compatibility classifications are listed in Table A1.

N/A - Not available

Table 4. Performance and Physical Property Characteristics of Pure Binary Monopropellants

Characteristic	Units	Propellant		
		77% N_2H_4 23% N_5H_5	80% N_2H_4 20% NH_3	72% N_2H_4 28% HN
1. Freezing Point	°K	255.5	258	255.2
2. Density (298°K)	gm/cm^3	1.08	0.92	1.12
3. Vapor Pressure (298°K)	$10^3 N/m^2$	1.33	424	N/A
4. Viscosity (298°K)	Poise	0.02	N/A	0.015
5. Theoretical Vacuum I_{sp} P_c = 1.03 MN/m^2 ε = 50	Sec	230	218	252
6. Density Impulse (298°K)	Sec	248	201	282
7. Adiabatic Flame Temperature	°K	1089	1039	1194
		α = 0.92	α = 0.7	Equilibrium

N/A = Not Available

Table 5. Safety/Storage/Handling Characteristics of Pure Binary Monopropellants

		Propellant Mixture		
Characteristic	Test Method	N_2H_4 - NH_3	N_2H_4 - $N_2H_5NO_3$	N_2H_4 - N_5H_5
Shock Sensitivity	Drop-weight	120 kg-cm (minimum)	N/A	120 kg-cm (23% HA)
	JANNAF card gap	0	0 up to 25% HN	0
Detonation Propagation	Standard ICRPG	Not available No propagation expected	Partial propagation in 0.64 cm tubing at 296°K (40% HN)	No propagation in 0.64 cm tubing at 296°K
Thermal Stability	Differential scanning calorimeter	N/A	N/A	Endotherm 441°K Exotherm 455°K
	Standard ICRPG	N/A	N/A	Exotherm 402°K (Peak 450°K)
Long Term Storability	Gas evolution rate	N/A	N/A	5.73×10^{-3} cc_{NTP}/kg-min 333°K, 23% N_5H_5
Toxicity	MAC(PPM for 8hr)	1.0	1.0	1.0
Safety and Handling	DOD Hazard	Group III	Group III up to 25% HN Group IV above 25% HN	Group III
	ICC rating	Corrosive liquid	Corrosive liquid up to 25% HN	Corrosive liquid
Materials Compatibility	Aluminum alloy	A	A or B	A
	300 CRES	A or B	A or B	A or B
	Titanium alloy	A	A or B	A

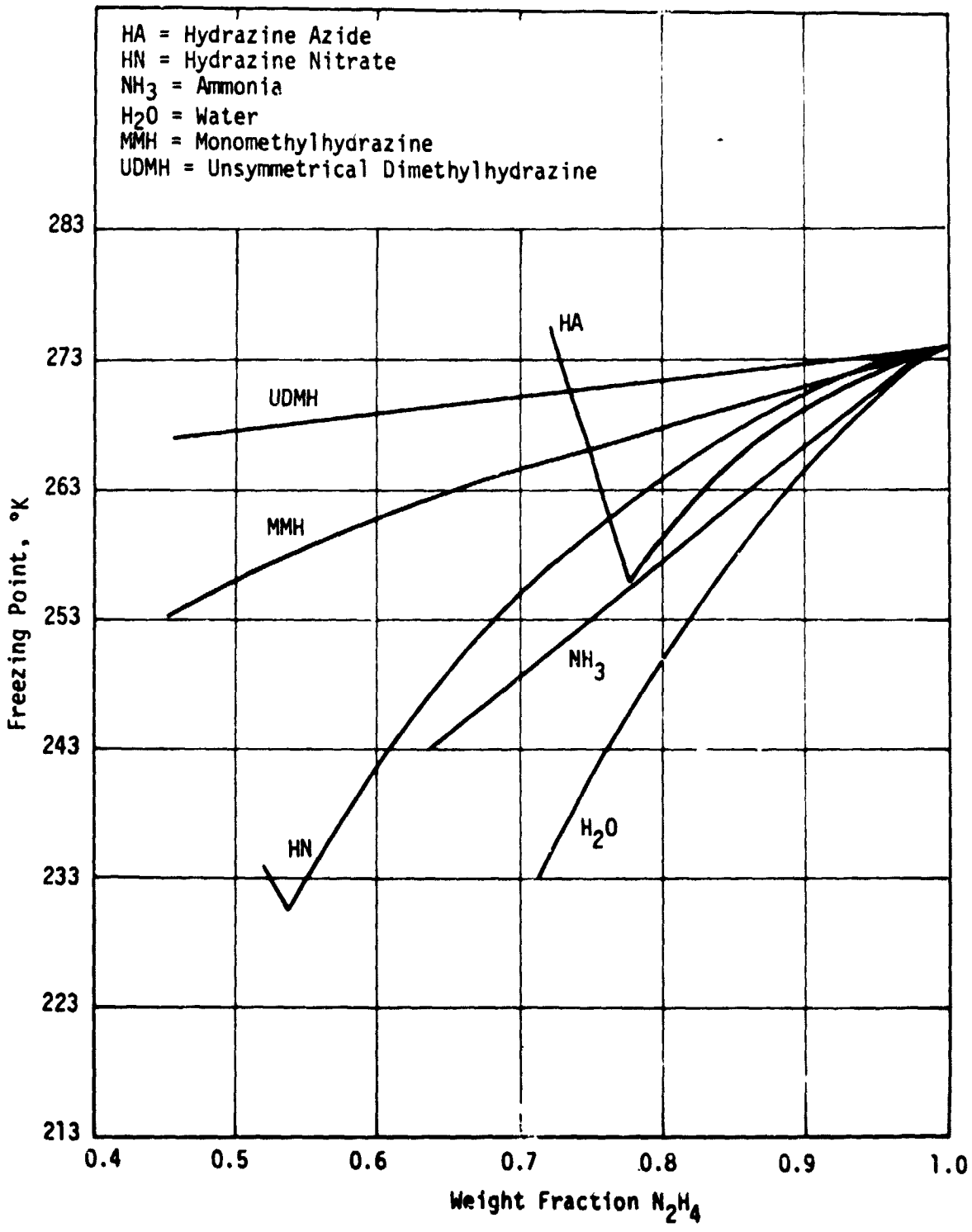

Figure 1. Freezing Point Temperatures of Pure Binary Monopropellants

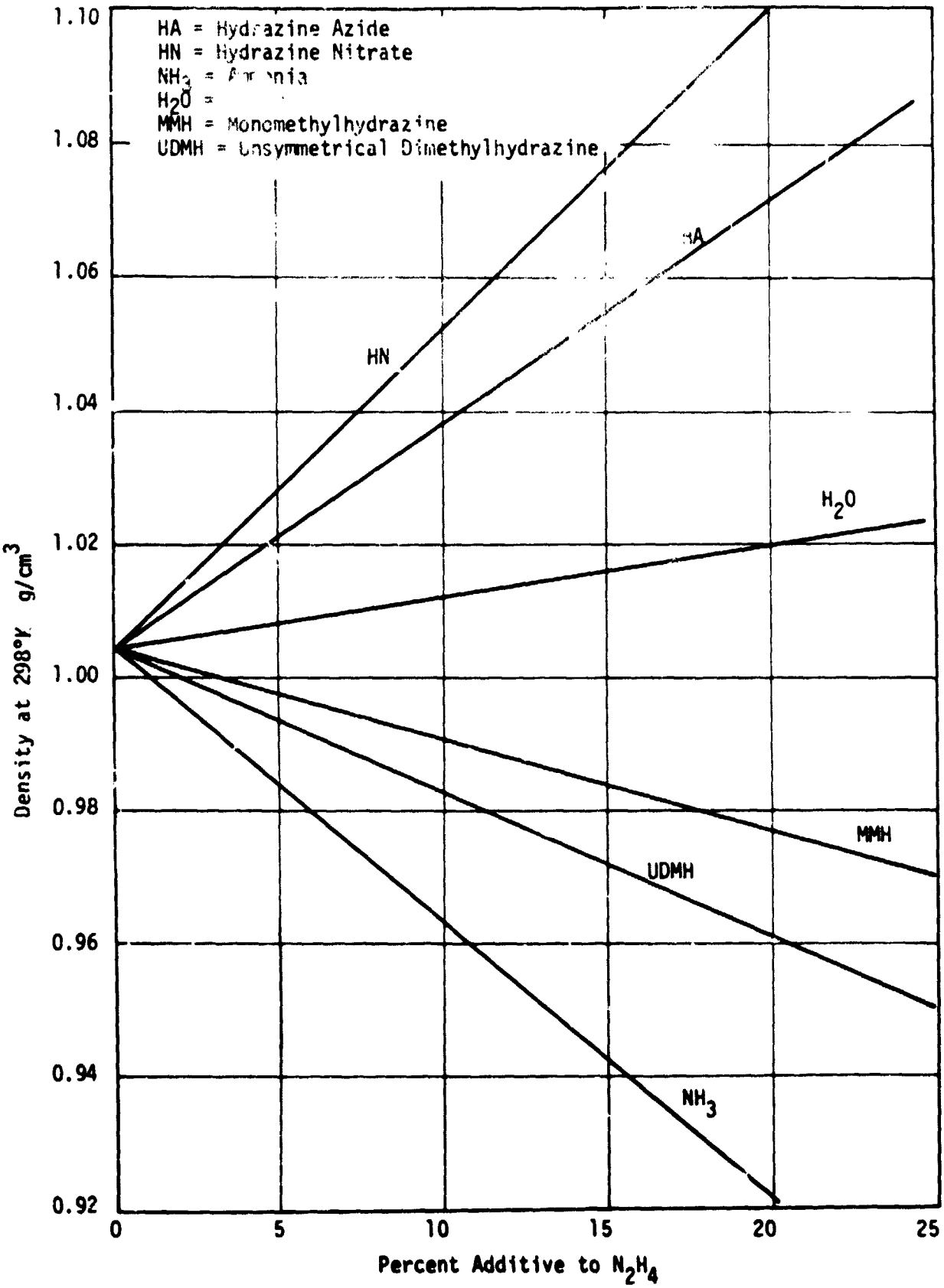

Figure 2. Density of Pure Binary Monopropellants

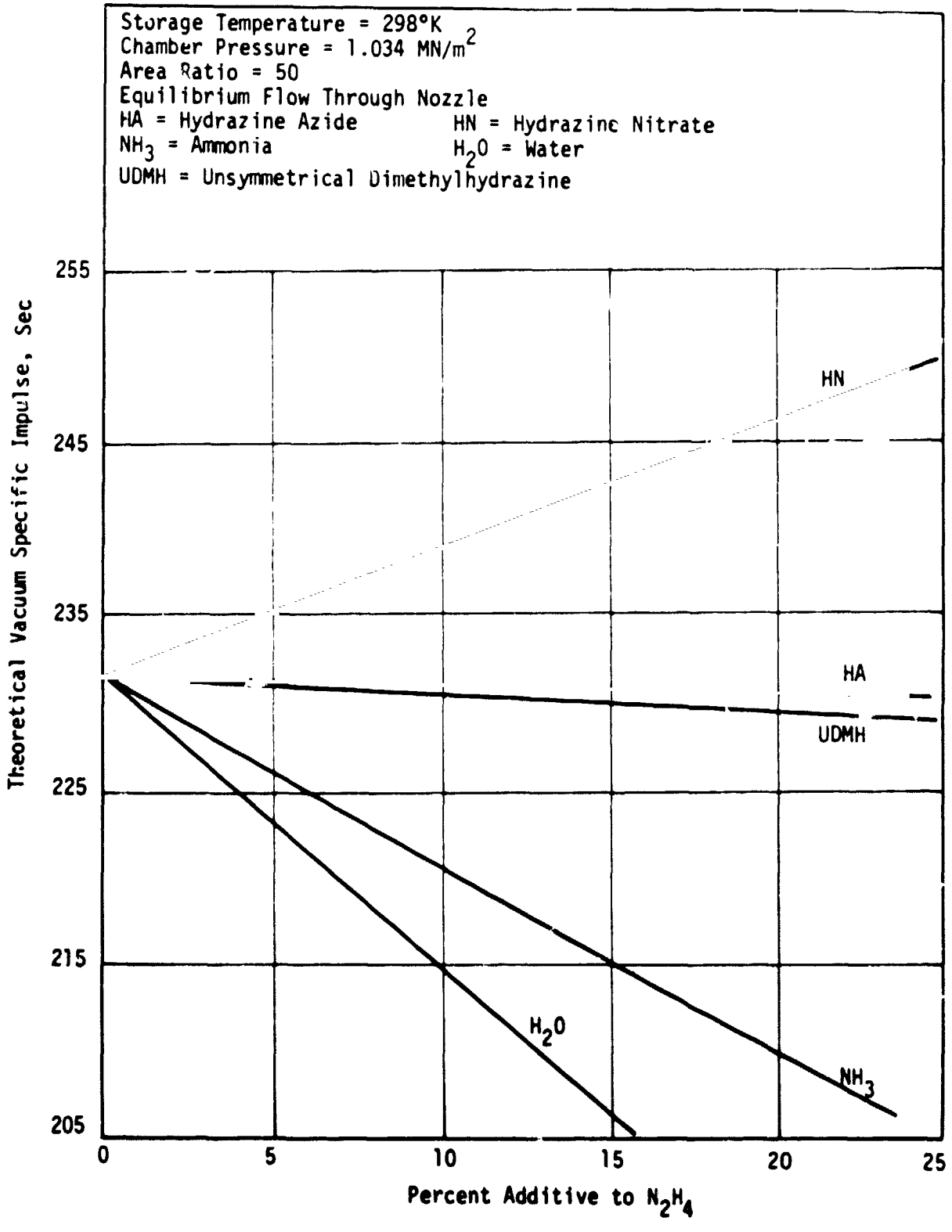

Figure 3. Theoretical Vacuum Specific Impulse of Pure Binary Monopropellants

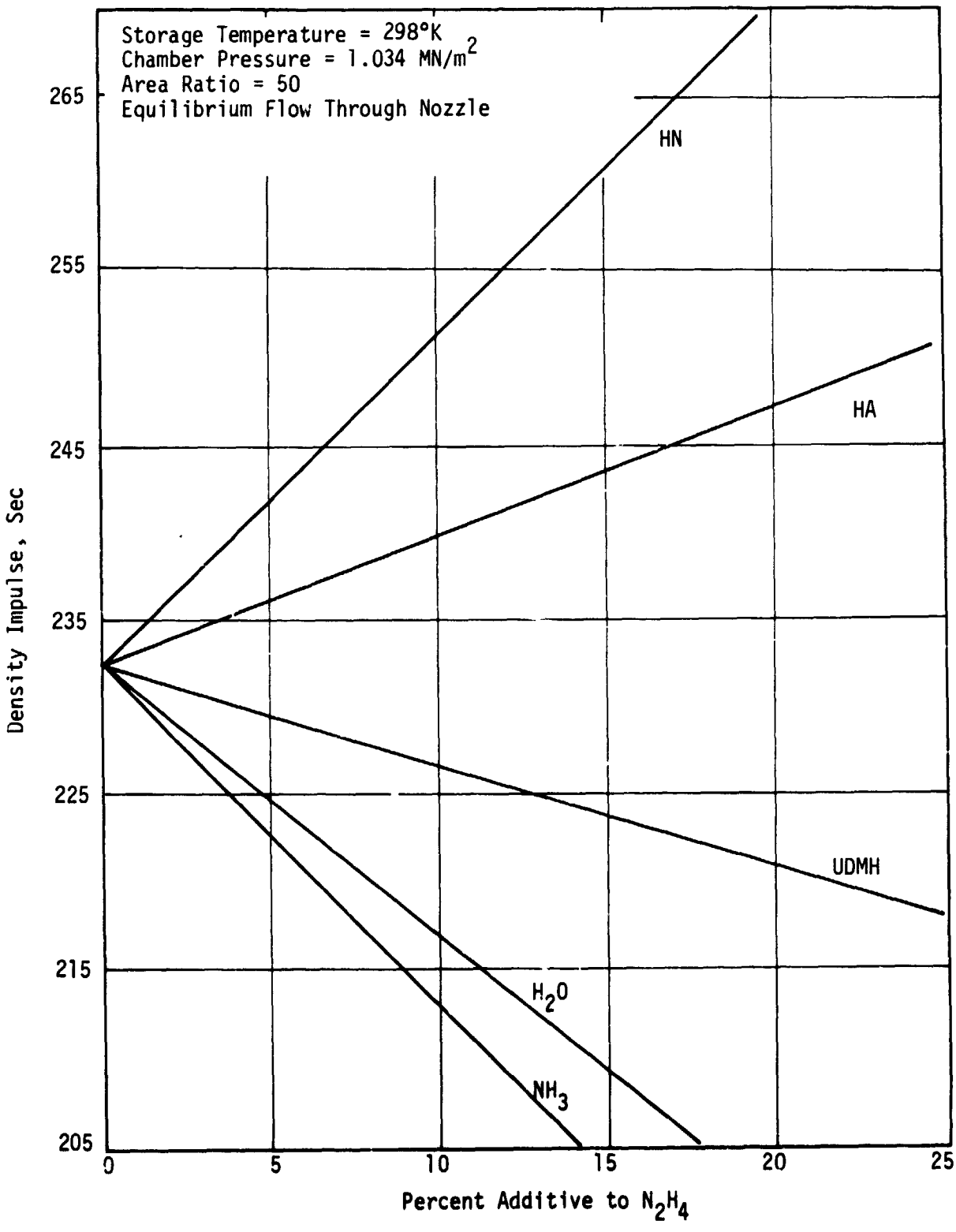

Figure 4. Density Impulse of Pure Binary Monopropellants

of the kinetic environment in most thrusters reveals that thermodynamic equilibrium is rarely achieved. Hydrazine thrusters are designed to provide a minimum amount of ammonia decomposition. Higher performance results when the energy of ammonia dissociation is retained to increase the hydrazine decomposition product enthalpy. The effect of ammonia dissociation on performance is best illustrated by assuming the condition of frozen flow. The hydrazine decomposition product compositions and phases are arbitrarily fixed and no consideration is given to equilibrium. The performance parameters are expressed as a function of ammonia dissociation fraction, α. The decomposition of hydrazine may be described by

$$3N_2H_4 \longrightarrow 4\ (1-\alpha)NH_3 + (2\alpha + 1)\ N_2 + 6\alpha H_2 \qquad (1)$$

The corresponding descriptive decomposition reaction for hydrazine azide (N_5H_5) is

$$3N_5H_5 \longrightarrow 5\ (1-\alpha)NH_3 + (2.5\alpha + 5)\ N_2 + 7.5\alpha H_2 \qquad (2)$$

The effect of ammonia decomposition on the performance of azide blends is illustrated in Figure 5 (specific impulse) and Figure 6 (density impulse). Pure hydrazine is included as a comparison. Only data for practical ammonia decomposition fractions are shown (α = 0.3 to 0.8).

3. Ternary Mixtures. This group includes three component mixtures of hydrazine, MMH, UDMH, hydrazine azide, ammonia and water. The performance and physical properties of three mixtures are shown in Table 6. A comparison of the two hydrazine-hydrazine azide based ternary blends illustrates the trade-off between freezing point and performance for nearly equal additions of ammonia (7%) and water (8%). The mixture containing water (freezing point = 253°K) has a density impulse 7.8% below that of hydrazine, whereas, the mixture containing ammonia (freezing point 255°K) has a 6.1% increase in density impulse. A freezing point of 219.1°K is realized for the MHM blend while retaining performance levels similar to that of the hydrazine-hydrazine azide-water mixture. Figure 7 compares the theoretical vacuum specific impulse as a function of ammonia dissociation of the two N_2H_4-N_5H_5 ternary blends with that of hydrazine. The lower combustion temperatures of the ternary blends should result in a

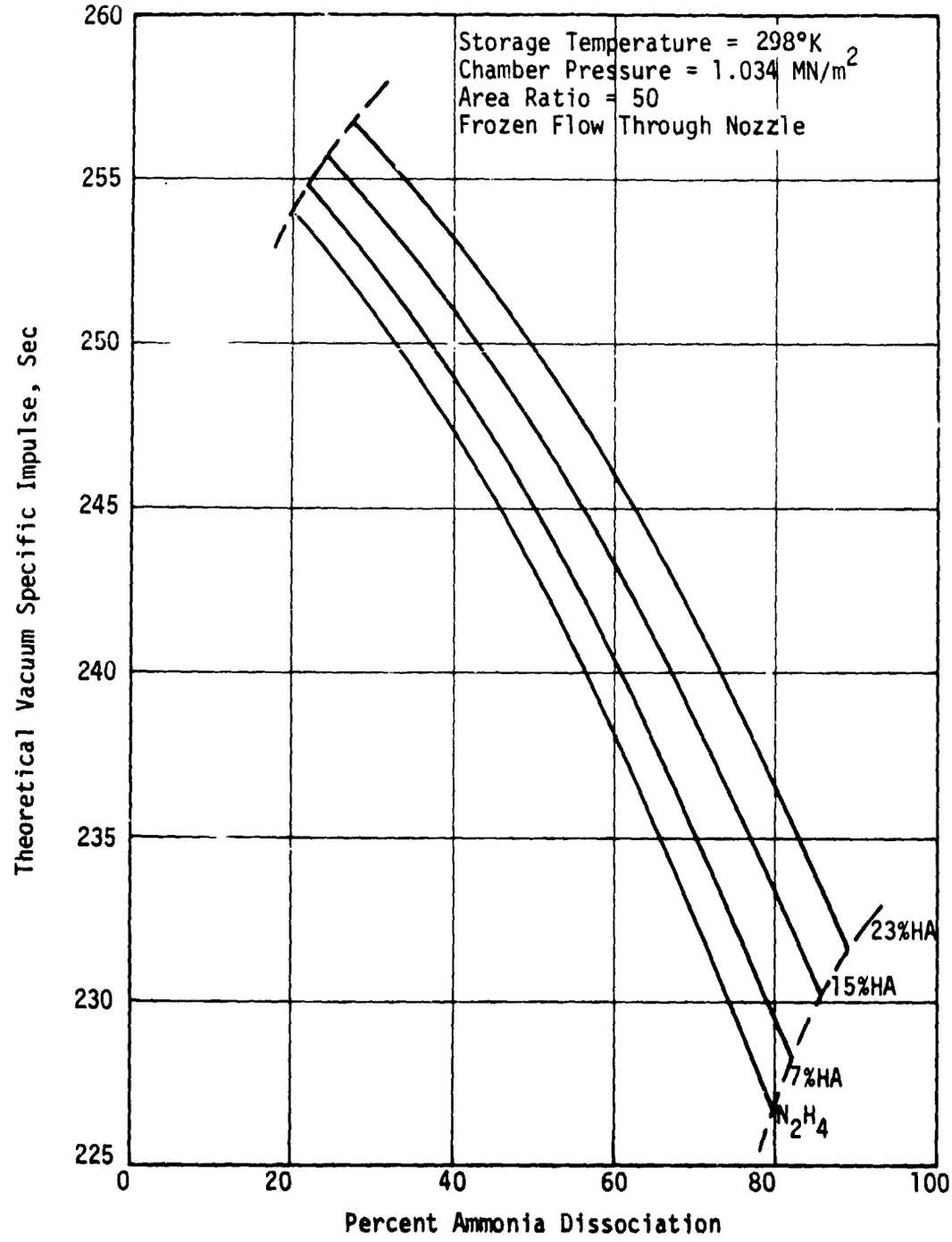

Figure 5. Theoretical Vacuum Specific Impulse of Hydrazine-Hydrazine Azide Mixtures as a Function of Ammonia Dissociation

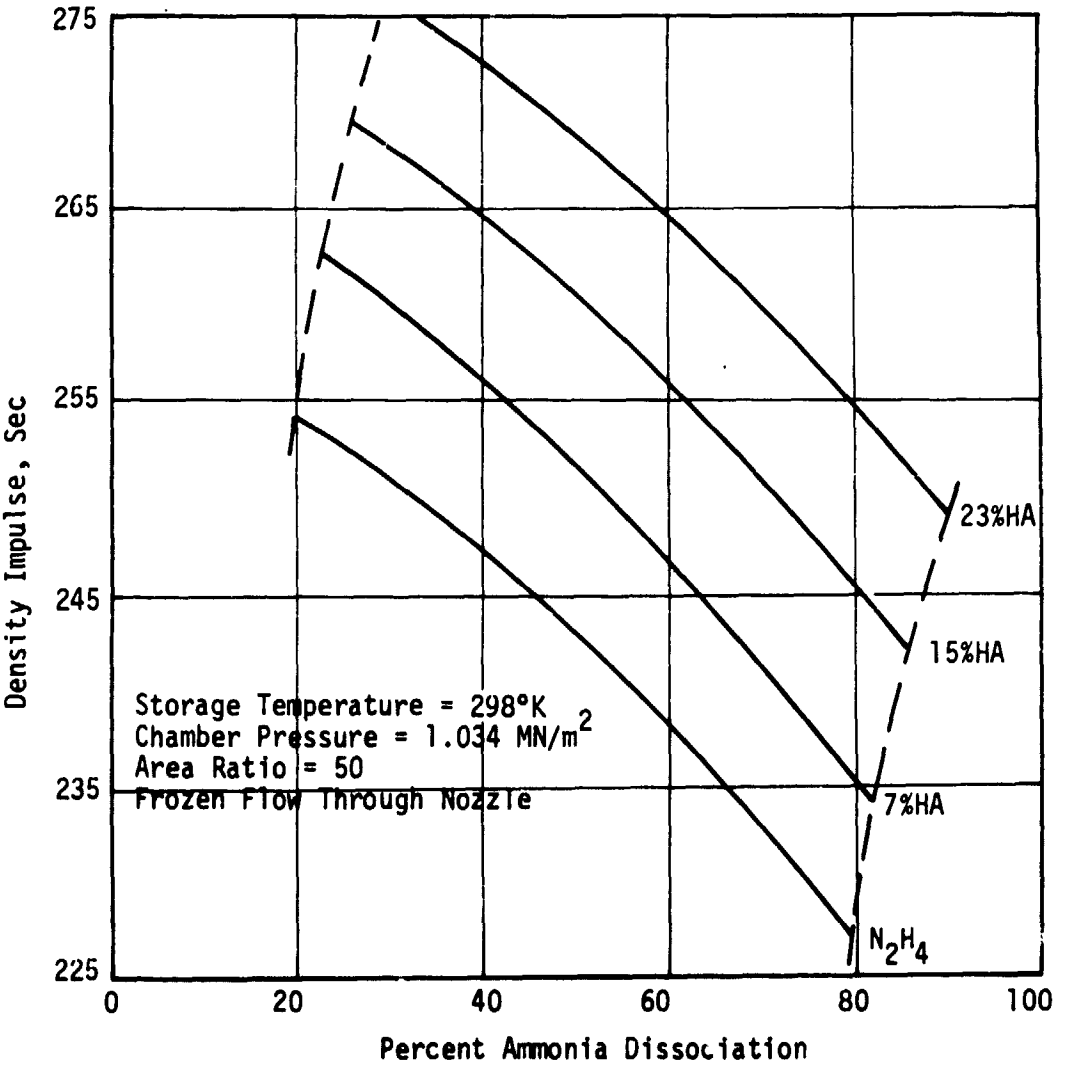

Figure 6. Density Impulse of Hydrazine-Hydrazine Azide Mixtures as a Function of Ammonia Dissociation

Table 6. Performance and Physical Characteristics of Pure Ternary Monopropellants

Characteristic	Units	Propellant			
		N_2H_4	1	2	3
1. Freezing Point	°K	274.53	255	253	219.1
2. Density (298°K)	gm/cm^3	1.00	1.1	1.06	0.88
3. Vapor Pressure (298°K)	$10^3 N/m^2$	1.89	111	1.46	343
4. Viscosity (298°K)	Poise	0.0091	N/A	0.02	N/A
5. Theoretical Vacuum I_{sp} P_c = 1.03 MN/m^2 ϵ = 50	Sec	231	222	201	200
6. Density Impulse (298°K)	Sec	231	245	213	176
7. Adiabatic Flame Temperature	°K	1089	1083	1077	1077
		α = 0.72	α = 0.65	α = 0.65	α = 0.65

1. 74% N_2H_4 - 19% N_5H_5 - 7% NH_3
2. 75% N_2H_4 - 17% N_5H_5 - 8% H_2O
3. MHM, 35% N_2H_4 - 50% MMH - 15% NH_3

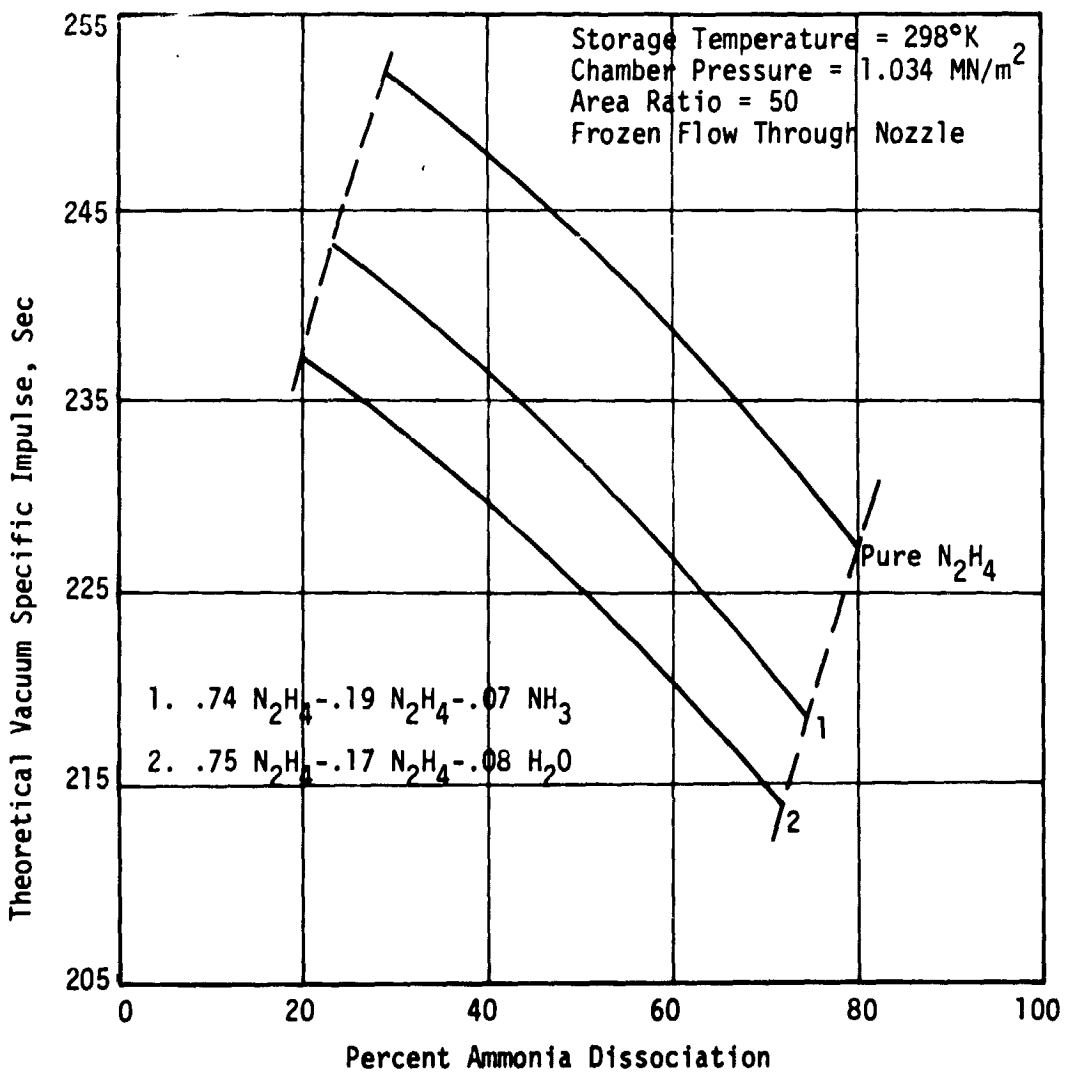

Figure 7. Theoretical Vacuum Specific Impulse of Pure Ternary Monopropellants as a Function of Ammonia Dissociation

smaller percentage of dissociated ammonia in actual engine operation. The relative difference in operating performance between hydrazine, N_2H_4 - N_5H_5 - H_2O and N_2H_4-MMH-NH_3 should be reduced to less than 5%.

Although numerous other ternary blends could be formulated from the six components considered in this section, the three blends presented appear to be the best compromise between freezing point depression and performance.

2.3 PROPELLANT SELECTION

The two hydrazine derivatives, MMH and UDMH, are attractive by virtue of very low freezing points (220.8°K and 215.8°K, respectively), theoretical values of specific impulse near that of hydrazine (<5% below), and of being "on board" in many spacecraft for use in high thrust bipropellant systems. However, both propellants perform poorly with catalytic thrusters. Carbon deposition from propellant decomposition has led to rapid clogging, poisoning and degradation of the catalyst bed. Large concentrations of MMH and UDMH are required to significantly depress the freezing point of hydrazine (Figure 1). Consequently, electrothermal thrusters utilizing these mixtures may also have problems associated with carbon deposition. However, the potential advantages of low freezing point and high theoretical performance warranted their selection for the evaluation test program. Carbon accumulation in the thrust chamber can be best evaluated by using one propellant unmixed or "pure," and the other blended with hydrazine. The logical selections were Aerozine-50 (50% N_2H_4 - 50% UDMH) and MMH. Aerozine-50 has the advantage of being a commonly used bipropellant. The total carbon content of both propellants is identical.

Binary mixtures obtained from blending hydrazine with ammonia or water exhibit 255.2°K freezing points at additive concentrations of 21.5% (NH_3) and 17% (H_2O). However, the large loss of density impulse (11% for H_2O, 20% for NH_3) excluded them from further consideration. The eutectic blend of 77% N_2H_4 - 23% hydrazine azide offers a substantial performance increase over hydrazine and has an acceptable freezing point of 255.5°K. Previous TRW experience with catalytic thrusters using azide blends has been negative. Higher thruster temperatures and a more severe nitriding

environment resulted in premature catalyst, thrust chamber and injector failures. These adverse characteristics will be absent for the electrothermal thruster; no catalyst (such as Shell 405) is used, and the thruster design allows the fabrication of noble metal alloy components capable of withstanding the higher temperature environment. For these reasons, the eutectic hydrazine-hydrazine azide mixture was selected for evaluation in the test program phase.

Performance levels of the N_2H_4 - N_5H_5 - NH_3 ternary mixtures are similar to those of the binary N_2H_4 - N_5H_5 blend. The degree of self-pressurization (0.11 MN/m^2) and slightly lower freezing point of 255°K are not considered significant enough to include this ternary blend in addition to or in lieu of the binary azide mixture.

The N_2H_4 - N_5H_5 - H_2O mixture has a freezing point (253°K) below the program goal. The performance characteristics of this blend have been severely compromised by a slight reduction in freezing point when compared to the other ternary blend. Ignition delay times are increased by the addition of water to hydrazine fuels. The trade-off between performance and freezing point of the ternary azide - water mixture results in an unacceptable candidate for the scope of this program.

The TRW-formulated ternary blend (MHM), 35% N_2H_4 - 50% MMH - 15% NH_3, has numerous advantages that offset the reduction in specific impulse (≈13% below N_2H_4). The MHM has a density impulse comparable to the derivatives of hydrazine, has no solid exhaust products or condensable combustion species. Faster start transients are expected for the MHM blend than mixtures containing water. Thus, the MHM blend was a logical candidate for the evaluation test program.

3.0 THRUSTER DESIGN AND FABRICATION

3.1 DESIGN OBJECTIVES

The thruster design was based on the Electrothermal Hydrazine Thruster (EHT) developed by TRW for NASA/GSFC on NASA Contract No. NAS5-11477.[1] The upgraded design and performance requirements are listed below.

1. Thrust: 0.333 ± 0.0267N at 1.724 MN/m^2 nominal feed pressure
2. Vacuum specific impulse: 200 sec steady-state
   (goals) 175 sec pulsed-mode
3. Pulse duration: 0.050 second to steady-state
4. Pulse mode duty cycle: that typical for attitude control including "wheel dump"
5. Holding power: 5 watts maximum
6. Nominal voltage: 24 to 32 vdc
7. Maximum steady-state on-time: 30 hours
8. Total number of pulses: 3×10^5
9. Weight: to be determined
10. Size: to be determined

The specific impulse values have been designated as program goals rather than a firm requirement.

3.2 DESCRIPTION OF DESIGN

The original electrothermal hydrazine thruster (EHT) upon which the present thruster is based is shown in Figure 8. The EHT design was modified by replacing the braze joint between the thrust chamber and nozzle with a threaded screen pack sleeve arrangement. This design, as illustrated in Figure 9, provided significant cost savings in thruster fabrication and greatly implemented performance optimization during the Evaluation Test Program. The design provides for:

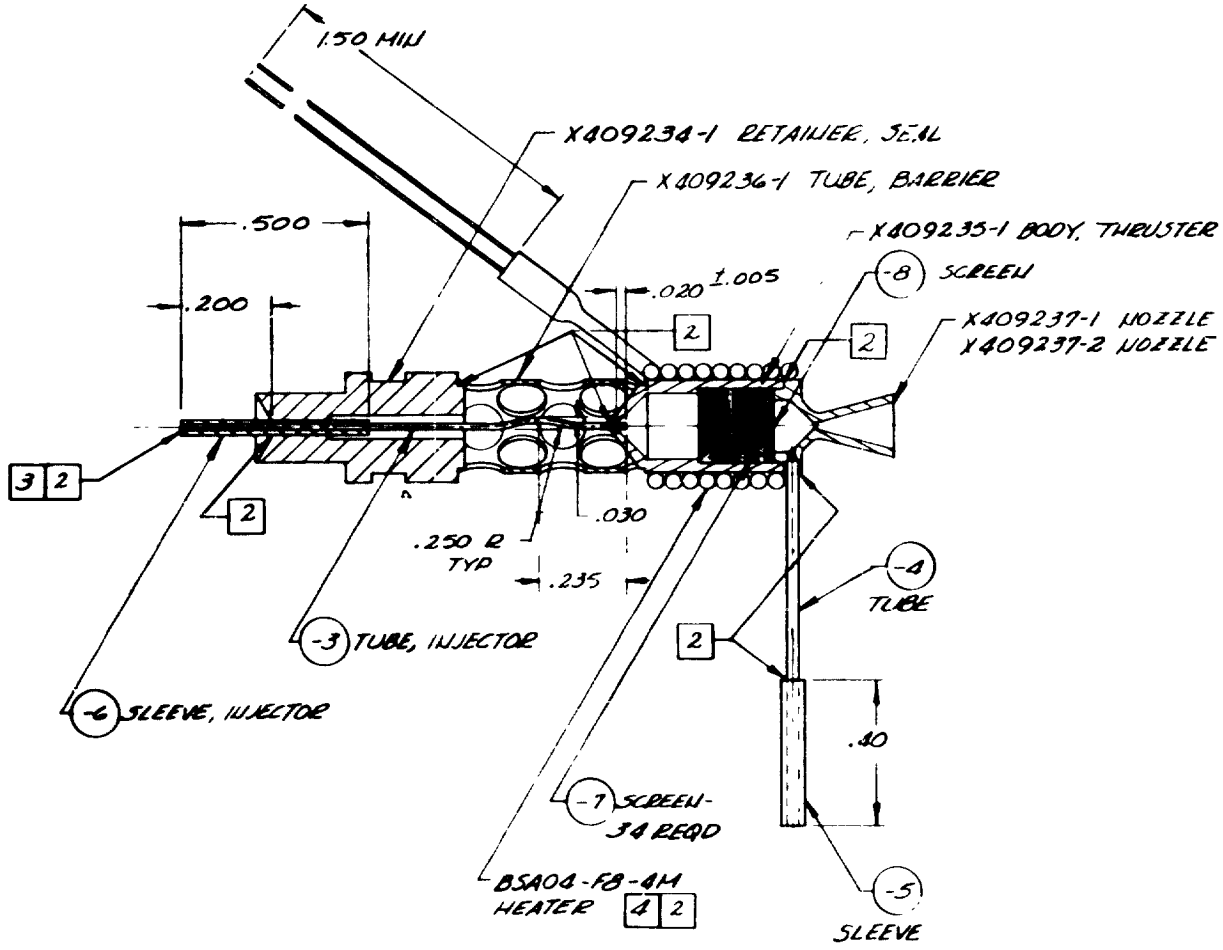

Figure 8. Electrothermal Hydrazine Thruster

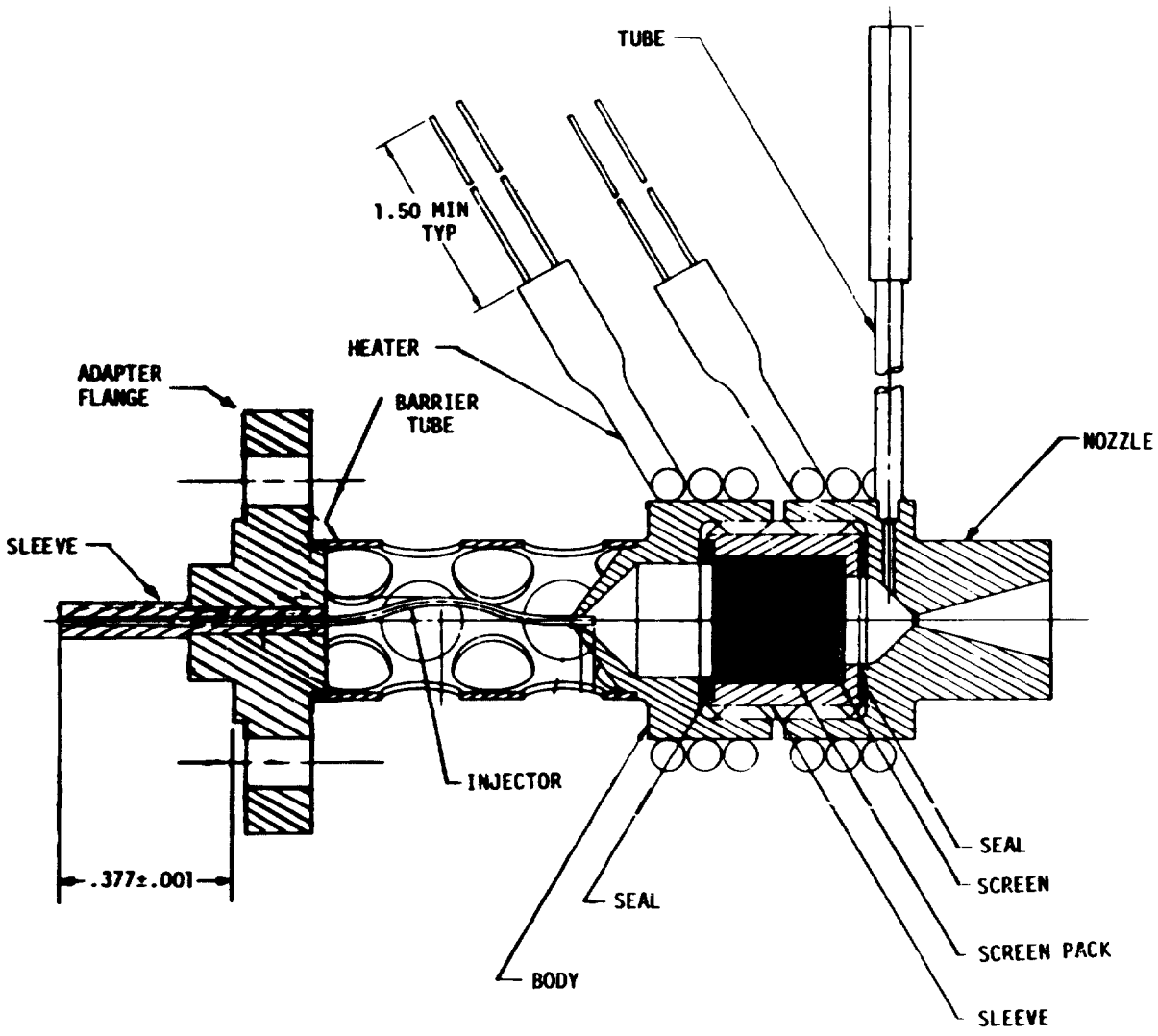

Figure 9. Monopropellant Demonstration Thruster

1. Component interchangeability

2. Changes in screen pack geometry

3. Changes in characteristic chamber length, L*, by varying the screen pack length or nozzle section length, or both

4. Nondestructive inspection, analysis, and cleaning of internal thruster components.

3.3 THRUSTER COMPONENTS

The thruster solenoid valve used during the Evaluation Test Program was the Wright Components, Inc. Model No. 15650 valve. This valve was successfully used on NASA/GSFC Contract No. NAS5-11477. The injector-to-valve seal is accomplished by a Teflon compression sleeve.

Two 10.2 cm long by 0.114 cm diameter sheathed Aerorod heater elements are used to heat the thrust chamber and nozzle. These heater elements were sized to maintain holding temperatures in excess of 800°K for sea level operation during portions of the Evaluation Test Program phase. Thruster insulation was provided by wrapping layers of Microquartz felt around the thrust chamber.

The nozzle is of standard convergent-divergent design with an area ratio of 50. The throat diameter is 0.046 cm. The screen pack sleeve is sized to accept 0.51 cm diameter platinum screens. The initial sleeve length is 0.51 cm. The chamber head end has a 90° included angle and a tapered wall thickness to limit heat transfer to the injector. The thrust chamber - screen pack - nozzle seals are of thin hardened copper.

The thruster is mated to the Wright Components, Inc. valve through a 0.025 cm thick thermal barrier tube and adapter flange.

Engineering drawings for the various demonstration thruster components are included in Appendix B.

3.4 FABRICATION

The fabricated components for five thrusters are shown in Figure 10. Included are the nozzle, screen pack sleeve, body, barrier tube, valve adapter flange and gasket seals. An assembled but not brazed view of

the demonstration thruster configuration is presented in Figure 11. All parts were fabricated from Haynes alloy L605 (Haynes 25) with the exception of the adapter flange (Type 304 stainless steel) and the gasket seals (No. 102 copper).

The injector tubes were fabricated from Haynes 25 tubing (0.0356 cm OD by 0.0152 cm ID). All injectors were built with a thermal relief bend rather than a complete loop. The chamber end of the injector was trimmed square and deburred on a jeweler's lathe.

The heater elements were wound in one layer on a mandrel slightly smaller than the outer diameter of the thruster body.

The screen packs were fabricated from 52 mesh platinum gauze and 40 mesh Haynes 25. The platinum screens (60) were punched and pre-compressed in a forming die. A single Haynes 25 screen was used as a retainer for the platinum screen pack. The Haynes 25 retainer was inserted into the screen pack sleeve towards the nozzle end of the thruster. The compacted platinum screen pack was then transferred directly from the compression die into the sleeve.

The split-chamber design allowed the thruster to be assembled in one high-temperature braze cycle. Nicrobraze alloy 210 was used for the entire assembly. A brazed thruster is shown in Figures 12 and 13 as disassembled and assembled views, respectively.

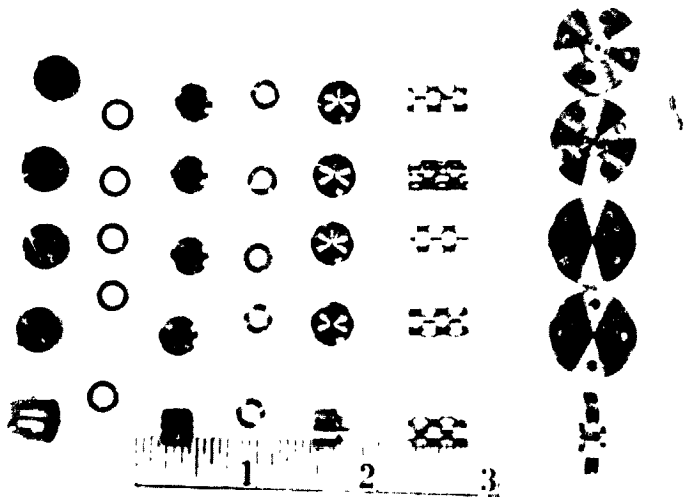

Figure 10. Demonstration Thruster Components

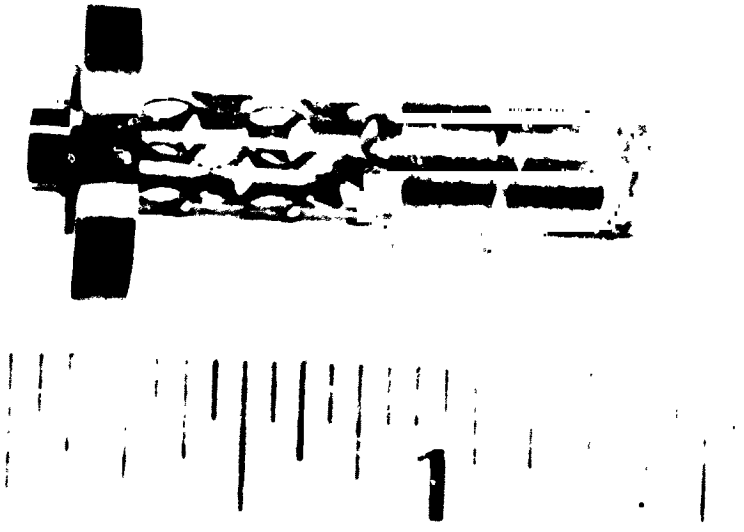

Figure 11. Demonstration Thruster Configuration

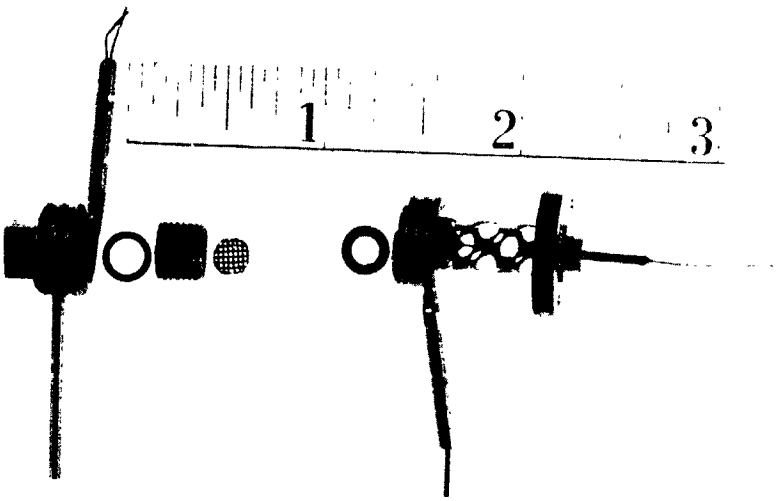

Figure 12. Disassembled Demonstration Thruster

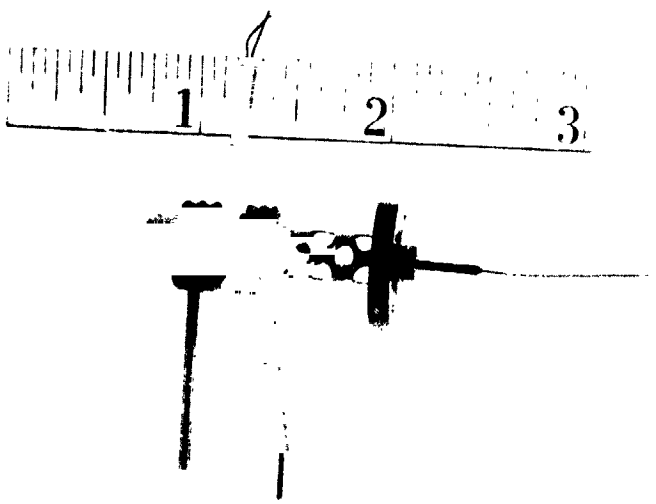

Figure 13. Assembled Demonstration Thruster

4.0 PROPELLANT EVALUATION

4.1 TEST PROGRAM

The evaluation test program was comprised of five interacting subtasks. These tasks are illustrated schematically in the flow diagram of Figure 14. Each propellant was subjected to a chemical analysis for conformance to appropriate specifications. The demonstration thrusters were operated with MIL-grade hydrazine prior to testing with the candidate monopropellants. Preliminary operation with the monopropellants was performed under sea level conditions for reasons of safety. Thruster configurations were varied to satisfy the different decomposition characteristics of each propellant. These variable configurations were also operated with MIL-grade hydrazine. Simulated high altitude performance measurements were obtained for the candidate monopropellants with "optimized" thruster configurations.

4.1.1 Test Methods

The preliminary sea level measurements were performed using the equipment shown schematically in Figure 15. The propellants MMH, AERO-50, and HA were supplied in 500 cc interchangeable Type 304 stainless steel sample cylinders. A separate piston tank (Figure 16) was required to prevent the loss of ammonia from the MHM blend. Two additional cylinders of water and alcohol were incorporated in the propellant supply manifold. This enabled the convenient flushing and cleaning of the thruster valve and propellant lines (thruster removed during such operations). A semi-open canister was mounted around the thruster. Argon was flowed through the canister to reduce oxidation of the thruster components. The thruster, thruster valve and filter were securely attached to an aluminum plate. A water shower head was installed directly over the thruster and valve assembly as a precautionary measure in the event of a propellant fire. The sea level tests were monitored visually by a closed-circuit television hook-up (control block-house located 16 m from test cell). The parameters recorded during sea level testing are indicated in Table 7.

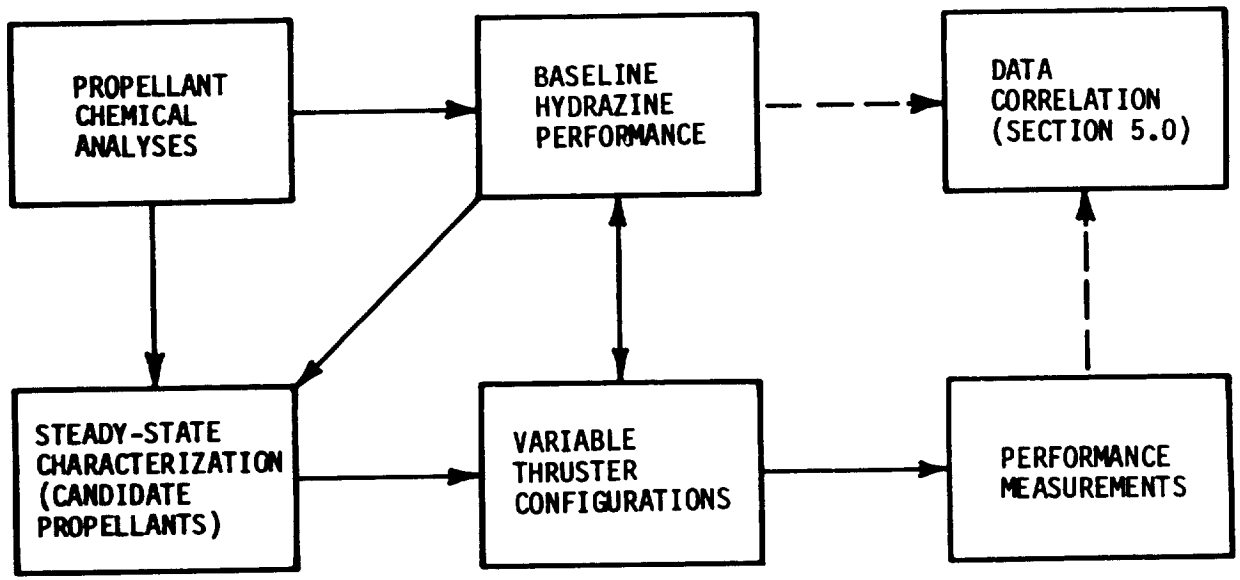

Figure 14. Evaluation Test Program Schematic

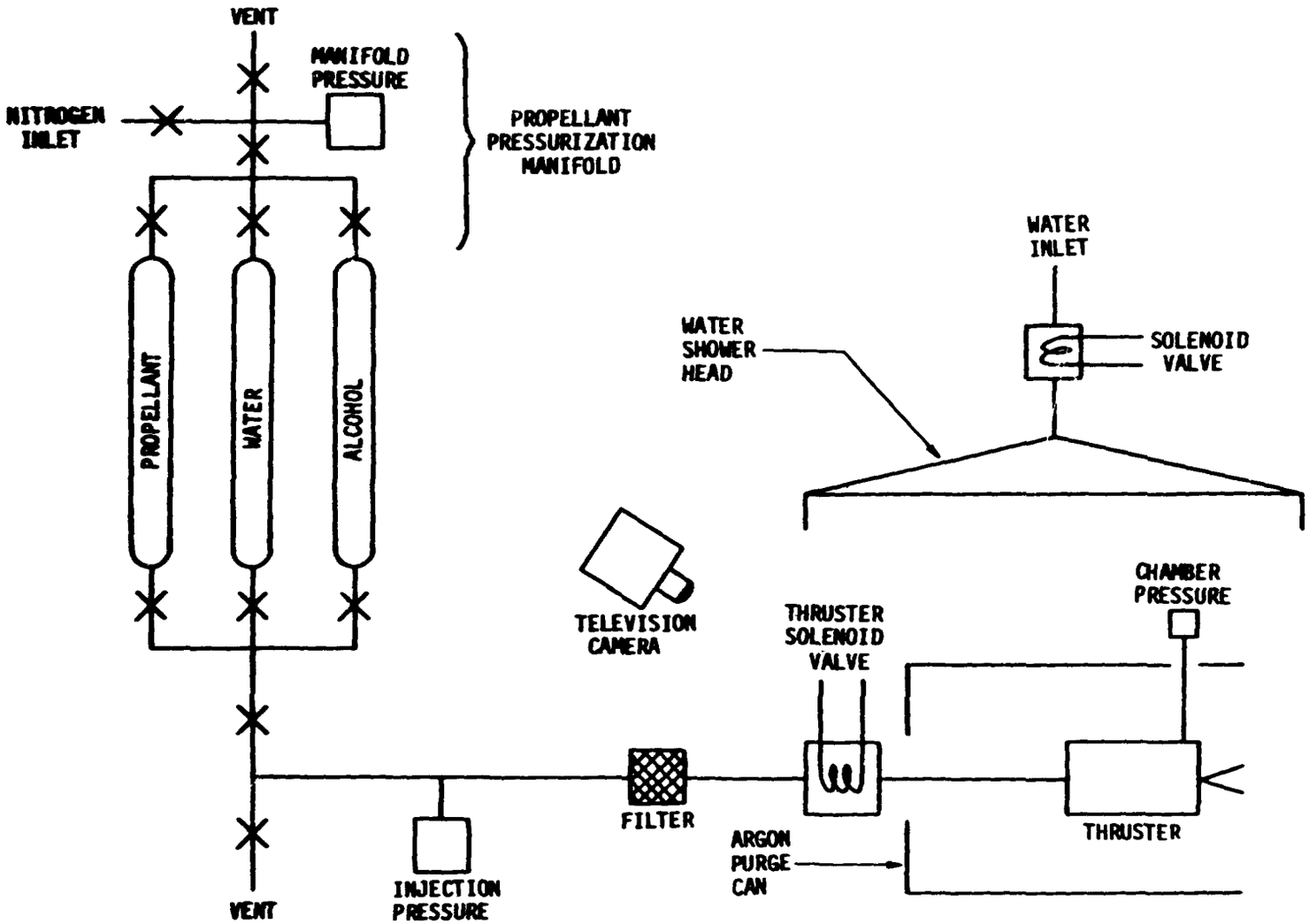

Figure 15. Sea-Level Test Schematic

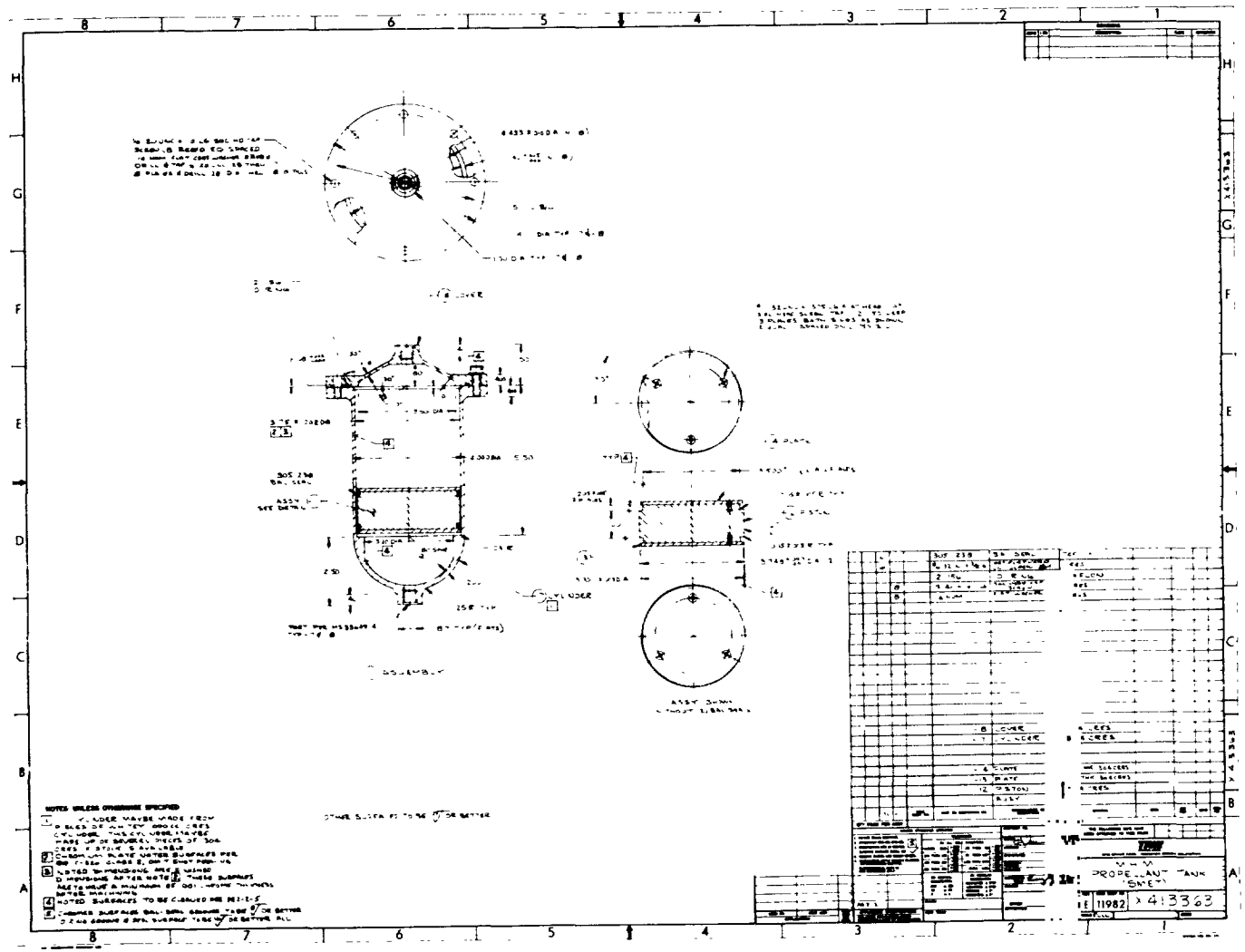

Figure 16. Mixture of Hydrazine Monopropellants (MHM) Piston Tank

Table 7. Sea Level Test Instrumentation

Pressures	Temperatures	Heater	Valve
Manifold	Nozzle	Voltage	Voltage
Injection	Chamber	Current	Current
Chamber	Injector		
	Barrier Tube		
	Valve		

The simulated high altitude performance measurements were conducted in a facility incorporating a 1.22 m x 1.22 m cylindrical vacuum chamber. High vacuum ($<1.3 \times 10^{-4}$ N/m^2) is maintained by two 0.254 m diffusion pumps. A chevron cyro baffle is mounted at the inlet port of each diffusion pump and is cooled with liquid nitrogen during operation. The diffusion pump assemblies exhaust to a 38 l/s mechanical pump through 5.1 cm tubing. The mechanical pump is used in lieu of the diffusion pumps for steady-state operation and high duty cycle pulsed-mode operation. The mechanical pump maintains the chamber at a pressure of 130 N/m^2 or less during such operations.

The internal chamber configuration is shown in Figure 17. The chamber contains two independent thrust and propellant supply systems (one system was installed during this program reporting interval). The dual systems satisfied the need to test more than one propellant without delays normally encountered in changing propellants. A fully instrumented demonstration thruster is shown mounted on one thrust stand in Figure 18. The propellant supply and mass flow measuring system is represented schematically in Figure 19. Dry, filtered nitrogen is used as the propellant pressurant. The flow measuring device consists of a piston that displaces propellant stored within a small diameter cylinder. The piston displacement is measured by a linear potentiometer.

The data acquisition equipment in Figure 20 was used to obtain performance data. Operating and performance data were recorded on an oscillograph or on magnetic tape. Three additional parameters were recorded for the high altitude tests. They were thrust (steady-state) or integral of thrust (impulse-bit in the case of pulsed-mode), mass flow and integral of chamber pressure.

The thrusters were routinely disassembled and inspected throughout the test program phase. Several screen pack assemblies were subjected to electron probe microanalysis for the identification of deposits formed on the screens during high temperature operation.

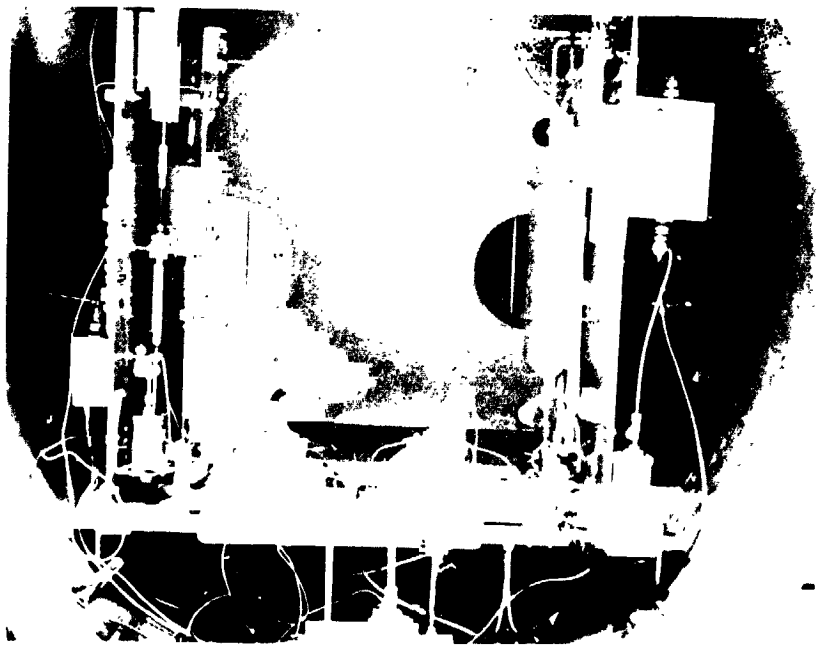

Figure 17. Vacuum Chamber Test Apparatus

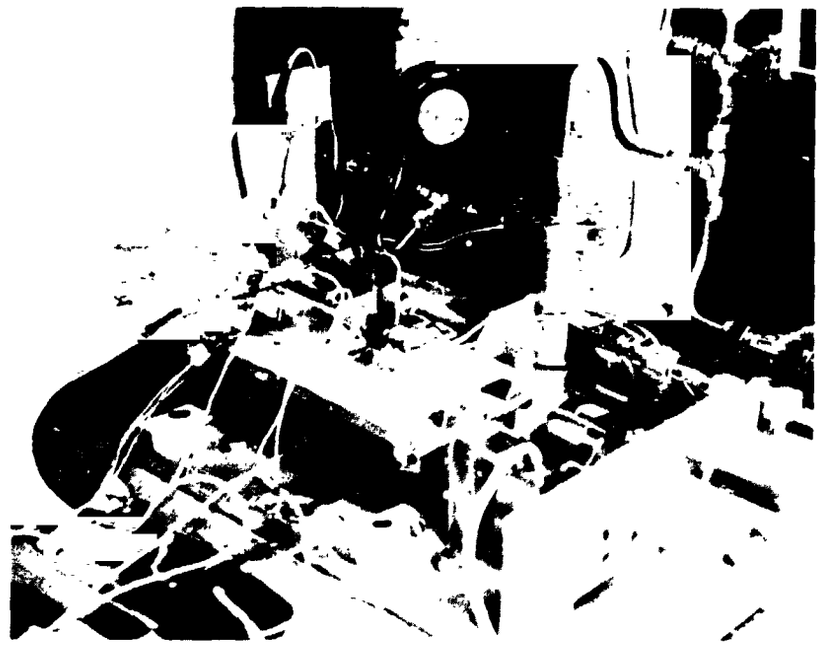

Figure 18. Thruster Mounted for Performance Measurements

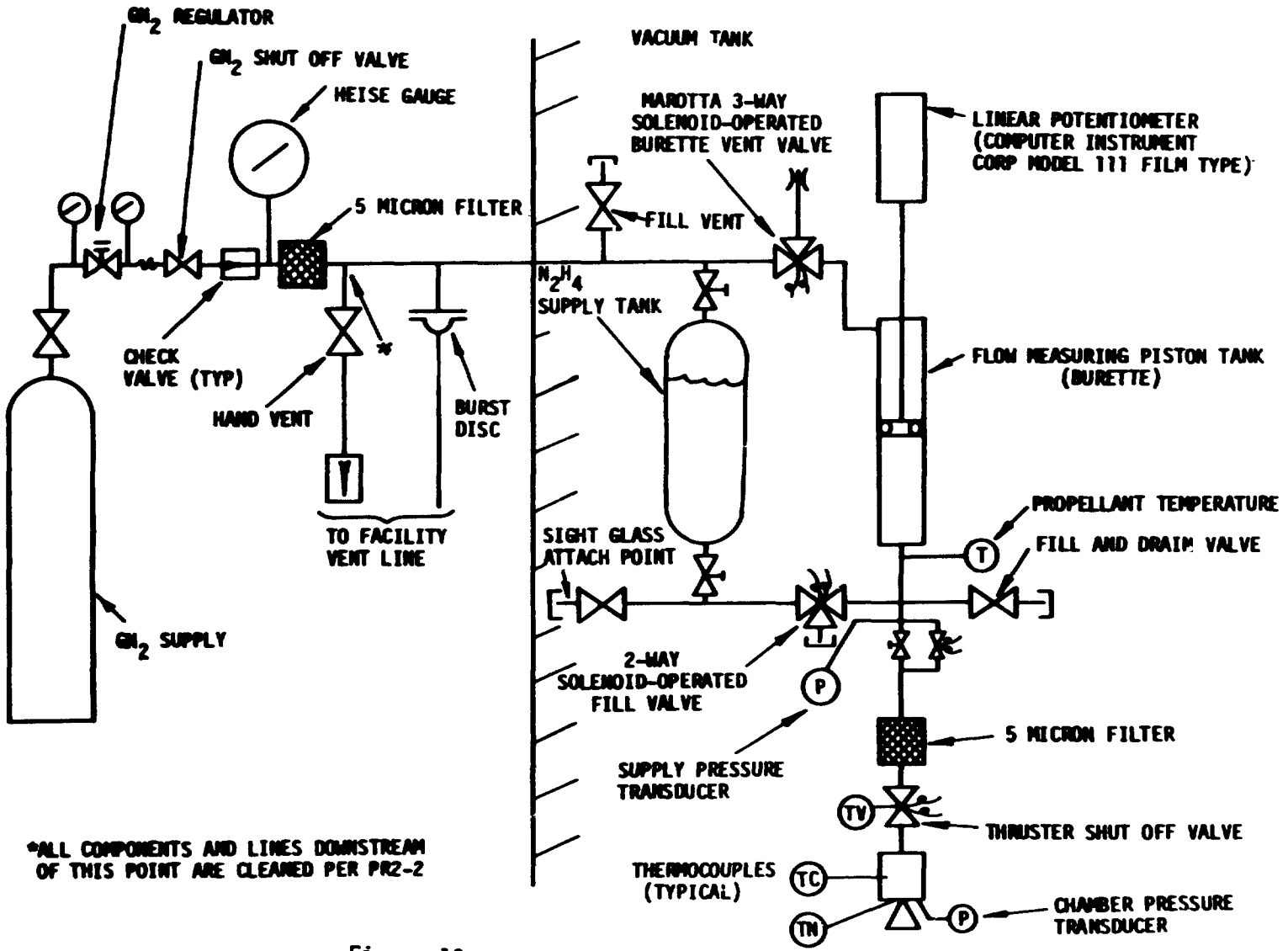

Figure 19. Propellant Supply System

Figure 20. Data Acquisition System

Original performance measurements were acquired in British Engineering units (foot-pound-second-degree Fahrenheit). The data in this report have been converted to the International System of Units (SI) or to more convenient metric units.

4.1.2 Chemical Analysis

Standard analytical methods were used to determine the chemical composition, particulate weight, particle size distribution and non-volatile residues for the propellants hydrazine, Aerozine-50, monomethylhydrazine, and hydrazine-hydrazine azide. An analysis of the ammonia used for the mixture of hydrazine monopropellants (MHM) was supplied by the manufacturer. The chemical composition of the MHM propellant was determined by the charging sequence. A pre-mixed and weighed charge of hydrazine and MMH was introduced into the piston tank. Both sides of the piston tank were evacuated to remove a protective nitrogen blanket. Ammonia was transferred to the propellant tank in the vapor phase and allowed to saturate the pre-mixed hydrazine and MMH to the vapor pressure corresponding to an aqueous solution content of 15% ammonia. Both ends of the propellant tank were then sealed under pressure.

Results of the propellant chemical analyses are presented in Tables 8 through 11 for MIL-grade hydrazine, Aerozine-50, monomethylhydrazine, and hydrazine-hydrazine azide, respectively. The hydrazine azide content was determined by potentiometric titration with 0.1 N NaOH and ammonia liberated from the addition of a weighed sample to acetone. The non-volatile residue (NVR) for the hydrazine-hydrazine azide blend was determined by propellant decomposition with hydrogen peroxide and slow evaporation on a hot plate to dryness. The NVR contents of hydrazine, Aerozine-50, and MMH were determined by weighing the matter remaining after distilling 100 ml of propellant at 313°K and a pressure of 133 N/m^2. An analysis of the anhydrous ammonia used for the MHM blend is presented in Table 12.

Table 8. Analysis of MIL-Grade Hydrazine Propellant

Results	(Ref. 2) Spec. Limits	Analysis
Density at 298°K, g/ml	NR*	1.0047
Hydrazine, %	98 Min	99.50
Unknown, %	NR	Trace
Water, %	1.5 Max	0.50
No. of Particles Per 100 ml	(Ref. 3)	
6 - 10 microns	9700 Max	361
11 - 25 microns	2680 Max	247
26 - 50 microns	380 Max	133
51 -100 microns	56 Max	9
101 -250 microns	5 Max	0
Fibers	None	None

Non-Volatile Residue, mg/100 ml - 6.0

Element	Analysis, ppm
Fe	0.26
Ni	0.09
Cr	0.11

*NR: Not Required

Table 9. Analysis of Aerozine-50 Propellant
(50% N_2H_4 - 50% UDMH)

Results	(Ref. 4) Spec. Limits	Analysis
Density at 298°K, g/ml	NR*	0.8996
N_2H_4, %	51 ± 0.8	51.58
UDMH, %	47 Min	47.81
Ammonia, %	NR	Trace
Water, %	1.8 Max	0.61
No. of Particles Per 100 ml	**(Ref. 3)**	
6 - 10 microns	9700 Max	960
11 - 25 microns	2680 Max	320
26 - 50 microns	380 Max	108
51 -100 microns	56 Max	18
101 -250 microns	5 Max	1
Fibers	None	None

Non-Volatile Residue, mg/100 ml - 24.4

Element	Analysis, ppm
Fe	0.79
Ni	0.22
Cr	0.66

*NR: Not Required

Table 10. Analysis of Monomethylhydrazine Propellant

Results	(Ref. 5) Spec. Limits	Analysis
Density at 296.9°K, g/ml	0.870 to 0.874	0.8725
Monomethylhydrazine, %	98.3 Min	99.02
Unknown, %	NR*	Trace
Water, %	1.5 Max	0.98
No. of Particles Per 100 ml	(Ref. 3)	
6 - 10 microns	9700 max	1460
11 - 25 microns	2680 max	520
26 - 50 microns	380 max	122
51 -100 microns	56 max	31
101 -250 microns	5 max	4
Fibers	None	None

Non-Volatile Residue, mg/100 ml - 0.8

Element	Analysis, ppm
Fe	0.39
Ni	0.10
Cr	0.03

*NR: Not Required

Table 11. Analysis of Hydrazine-Hydrazine Azide Propellants

Results	
Density at 298°K, g/ml	1.0759
Hydrazine Azide, %	24.38
Water, %	Trace

No. of Particles Per 100 ml	(Ref. 2) Spec. Limits	Analysis
6 - 10 microns	9700 Max	1220
11 - 25 microns	2680 Max	486
26 - 50 microns	380 Max	130
51 -100 microns	56 Max	16
101 -250 microns	5 Max	5
Fibers	None	None

Non-Volatile Residue mg/100 ml - 392.0

Element	Analysis, ppm
Fe	44.8
Ni	7.68
Cr	12.72

Table 12. Analysis of Anhydrous Ammonia

Ammonia, %	99.99 Min
Non-Basic Gas in Vapor Phase	25 ppm Max
Non-Basic Gas in Liquid Phase	10 ppm Max
Water	33 ppm Max
Oil (as soluble in petroleum ether)	2 ppm Max
Salt (calculated as NaCl)	None
Pyridine, Hydrogen Sulfide, Napthalene	None

The NVR contents of hydrazine, Aerozine-50 and MMH were normal for these propellants. However, the high NVR content of the azide blend indicated that the propellant was contaminated. The non-volatile residues of the four propellants were extracted with 3N HCl and subjected to atomic adsorption analyses for iron, nickel and chromium (major storage vessel constituents). The metallic contaminant level of the azide blend (Table 11) was 100 to 200 times that of MIL-grade hydrazine (Table 8). Although hydrazine-hydrazine azide propellants are more reactive than hydrazine, the large difference in contaminant levels should be viewed with caution. The hydrazine test system and storage containers used during the evaluation test program phase were maintained at the highest cleanliness levels applicable to TRW flight-oriented programs. The hydrazine-hydrazine azide blend had been used on a previous program where the cleanliness levels, storage and handling methods were less stringent. The high azide blend contaminant level may have been due to prior handling.

4.2 PROPELLANT CHARACTERIZATION

4.2.1 Baseline Hydrazine Performance

Performance characterization and baseline testing with MIL-grade hydrazine were performed on five demonstration thrusters prior to operation with the candidate monopropellants. These baseline configurations (Figure 9) contained sixty 0.5 cm dia. platinum screens (52 mesh, 0.1 mm wire diameter) and one 0.5 cm dia. Haynes 25 retaining screen (40 mesh, 0.28 mm wire diameter).

The pulsed-mode and steady-state performance characteristics for one baseline thruster configuration are presented in Figures 21 and 22, respectively. The steady-state data were taken at maximum operating temperatures which varied between 1213 and 1238°K over the range of inlet pressures studied. The nominal design thrust of 0.333 N at 1.724 MN/m^2 feed pressure was met by a delivered thrust of 0.32 N. Chamber pressure roughness (thrust variation) varied from $\pm$ 3% to $\pm$ 6% among the five baseline thrusters. The design requirement of $\pm$ 7.8% thrust variation was easily met. The specific impulse variation between the five baseline thrusters was negligible. Larger variation in thrust and chamber pressure levels were noticed due to different injector flow tube characteristics.

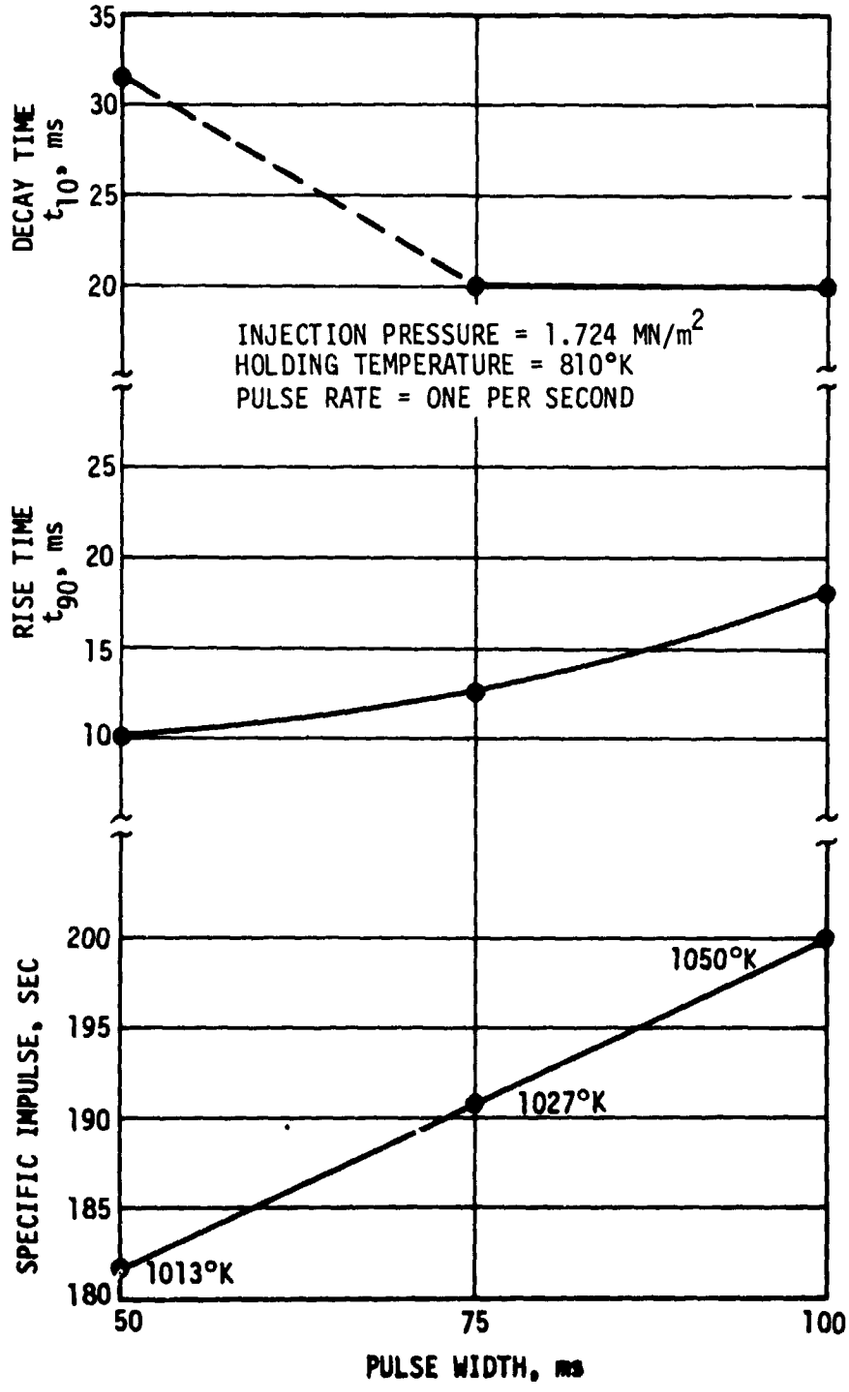

Figure 21. Baseline Pulsed-Mode Performance

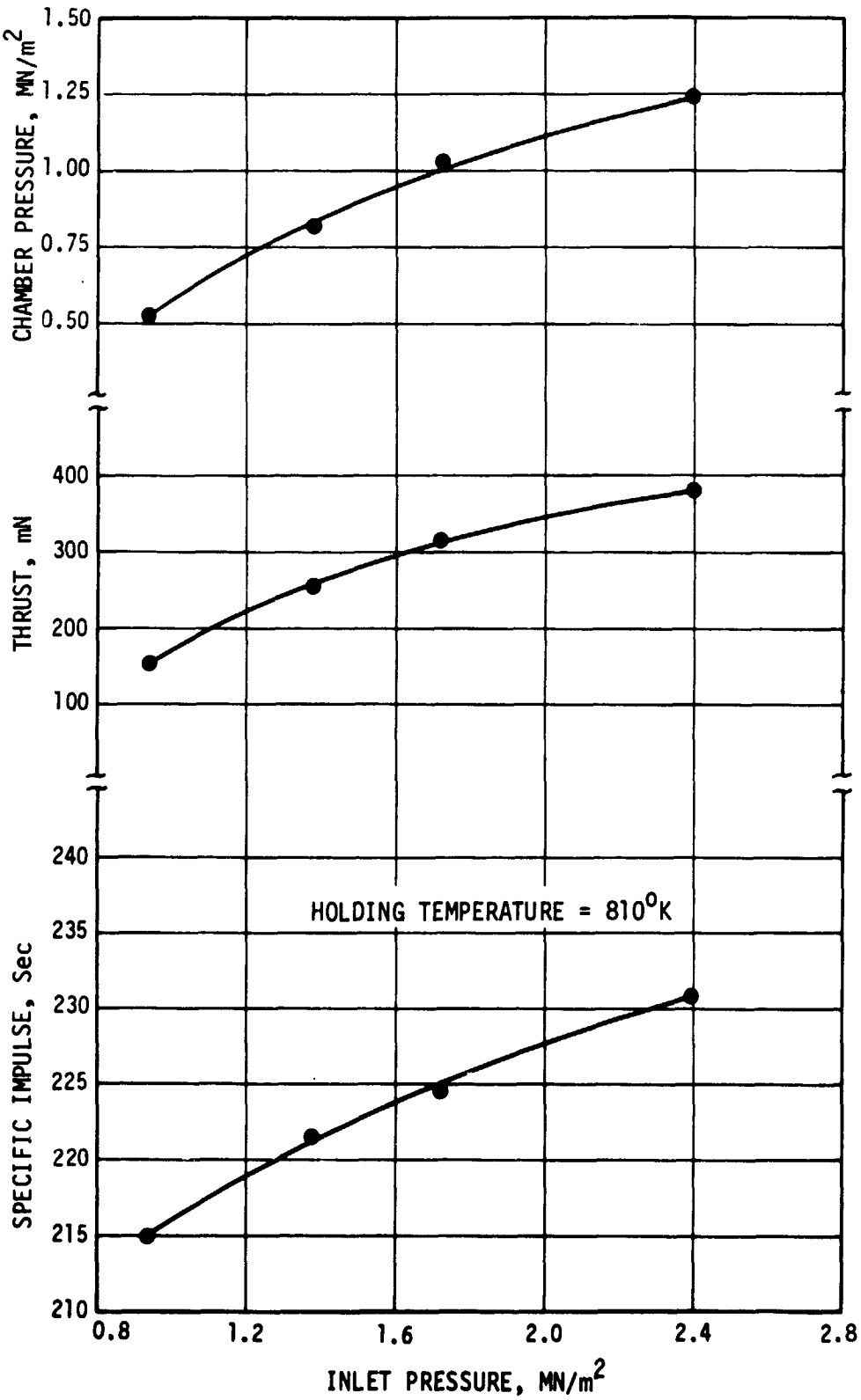

Figure 22. Baseline Steady-State Performance

One demonstration thruster was disassembled after baseline testing to examine the internal thrust chamber components. This provided a reference point for post-test examinations following operation with other propellants. All interior components revealed minimal reaction with the combustion products. The screen pack remained intact within the sleeve. A dark deposit was noticed on the middle of the top platinum screens (those nearest the injector). Low magnification photomicrographs of Figure 23 reveal this deposit. The Haynes 25 screen at the bottom of the pack assembly (nearest nozzle) retained its structural and chemical integrity. The platinum screen pack deposit was subjected to electron-probe microanalysis. A backscattered electron micrograph of the top platinum screen center appears in Figure 24. A spectral analysis of the X-rays emitted when the electron beam was positioned directly on the deposit revealed that the major contaminants were Fe, Ni and Cr. The relative intensity of elements present are summarized in Table 13. The Fe content in the screen center was approximately four to five times that measured on the outer periphery of the top screen. An iron K_α X-ray image, Figure 25, confirmed that the iron detected by the spectral analysis was localized on the platinum screen (Figures 24 and 25 are of the same region). The region of highest contamination is at the lower right of each figure.

A spectral analysis of the bottom Haynes 25 retaining screen revealed the presence of W, Ni, Co, Fe, Cr, Mn and Si. The intensity of Fe-K_α radiation from the Haynes 25 screen was considerably smaller than that obtained from the top platinum screen. Iron was present on both screen materials in a disproportionate amount to that possibly present in Haynes 25. The presence of Ti on the top screen deposit indicated that the cause was not due to propellant attack and corrosion of the Haynes 25 thruster materials. The logical sources of contamination were the stainless steel storage vessels, feed lines, filters and propellant valves. The nominal compositions of stainless steels used for propellant handling is given in Table 14. Haynes 25 is also included.

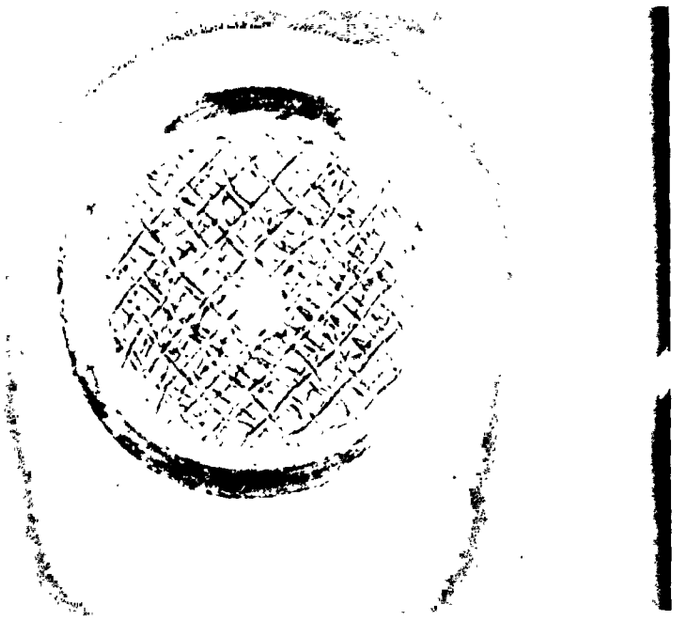

(a) 10X

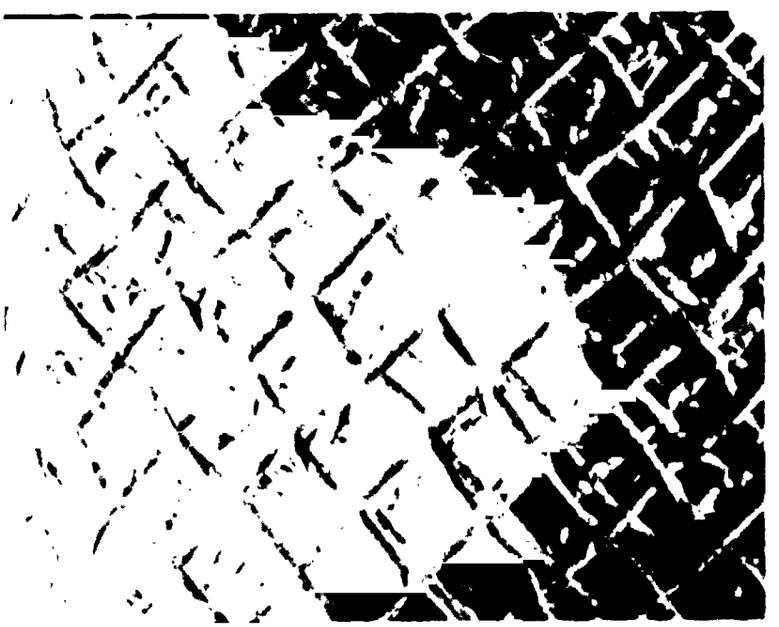

(b) 27X

F gure 23. Deposit on Top Platinum Screen

Figure 24. Backscattered Electron Image of the Top Platinum Screen Center

Table 13. Spectral Analysis of Platinum Screen Deposit

Relative X-Ray Intensity

Very Strong	Strong	Medium	Weak	Trace
Pt	Fe	Cr	Ti	Ca
	Ni		Co	Si
				Cl
				S
				Na
				Mn

NOTE: Carbon below instrument detection limits.

Oxygen below instrument detection limits.

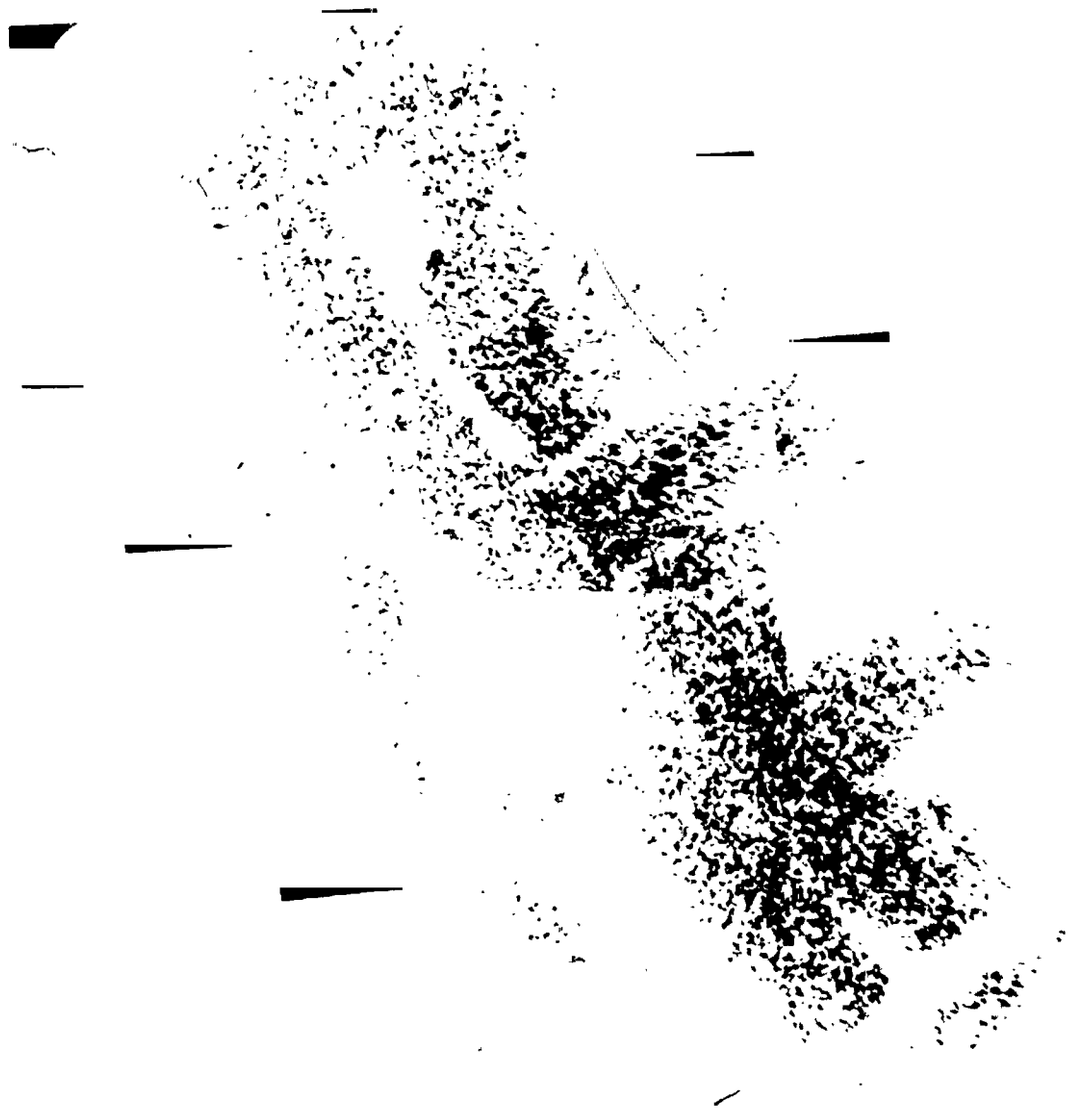

Figure 25. Iron K_α X-Ray Image of the Top Platinum Screen Center

Table 14. Nominal Compositions of Stainless Steels and Haynes 25

Steel	C	Cr	Ni	Mn	Si,max	P,max	S,max	Others
303	0.015 max	17.00-19.00	8.00-10.00	2.00 max	1.00	0.02	0.15 min	0.060 max Mo(a)
304	0.08 max	18.00-20.00	8.00-12.00	2.00 max	1.00	0.045	0.03	...
321	0.08 max	17.00-19.00	9.00-12.00(b)	2.00 max	1.00	0.045	0.03	5 x C min Ti

Haynes 25, 0.10C, 20Cr, 10Ni, 15W, 1.5Mn, 0.5Si, Balance Co.

(a) Optional

(b) A nickel content of 9 to 13% is permitted for tubular products.

The mechanism of the storage vessel material dissolution into hydrazine has not been well defined. However, a very likely cause is the presence of carbazic acid in propellant grade hydrazine. Carbazic acid can react to form metal or hydrazine salts, e.g., $(N_2H_3COO)_3$ Fe and $N_2H_3COON_2H_5$. These salts will be present as residues after propellant vaporization. The salt residue may undergo subsequent decomposition at the high thruster operating temperatures. This would result in a highly localized metallic concentration.

4.2.2 Preliminary Sea-Level Operation With Selected Monopropellants

This section presents the operating characteristics of hydrazine-hydrazine azide, Aerozine-50 and monomethylhydrazine with the baseline thruster configuration. Initial tests with these three propellants were performed under sea-level conditions. Initial characterization tests with 50% MMH-50% N_2H_4 and MHM were performed during the later stages of the evaluation test program with thruster configurations derived from satisfactory operation with Aerozine-50. The test results with these propellants are included in the performance measurements section.

Hydrazine-Hydrazine Azide

A total of 23.5 minutes steady-state operation was accumulated before testing was terminated by an injector failure (revealed by post-test inspection). The thruster exhibited metastable operation during this period. This mode is illustrated by the chamber pressure trace in Figure 26. Ignition at the holding temperature of 1000°K was very erratic. The large chamber pressure fluctuations were significantly reduced when the energy supplied by decomposition raised the thruster temperature to 1155°K. Chamber pressure roughness continued to decrease with time. High speed oscillograph chamber pressure traces reproduced in Figure 27 illustrate the roughness decrease.

Stable operation could not be achieved at injection pressures above 0.83 MN/m^2. The injection pressure was reduced to 0.72 MN/m^2 and an additional 18 minutes steady-state time was accumulated when an abrupt loss of chamber pressure occurred. Operation during this period was

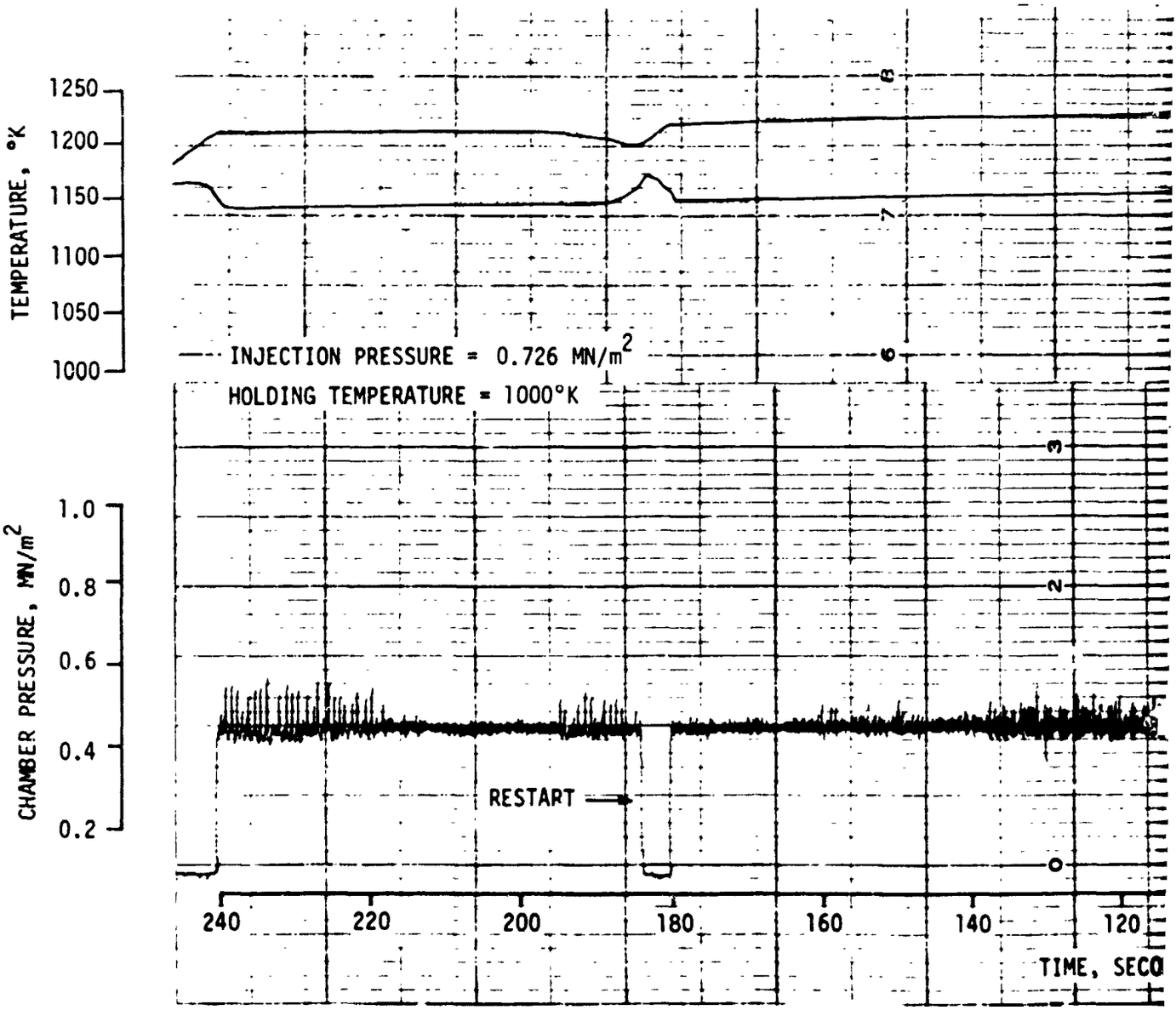

FOLDOUT FRAME 1

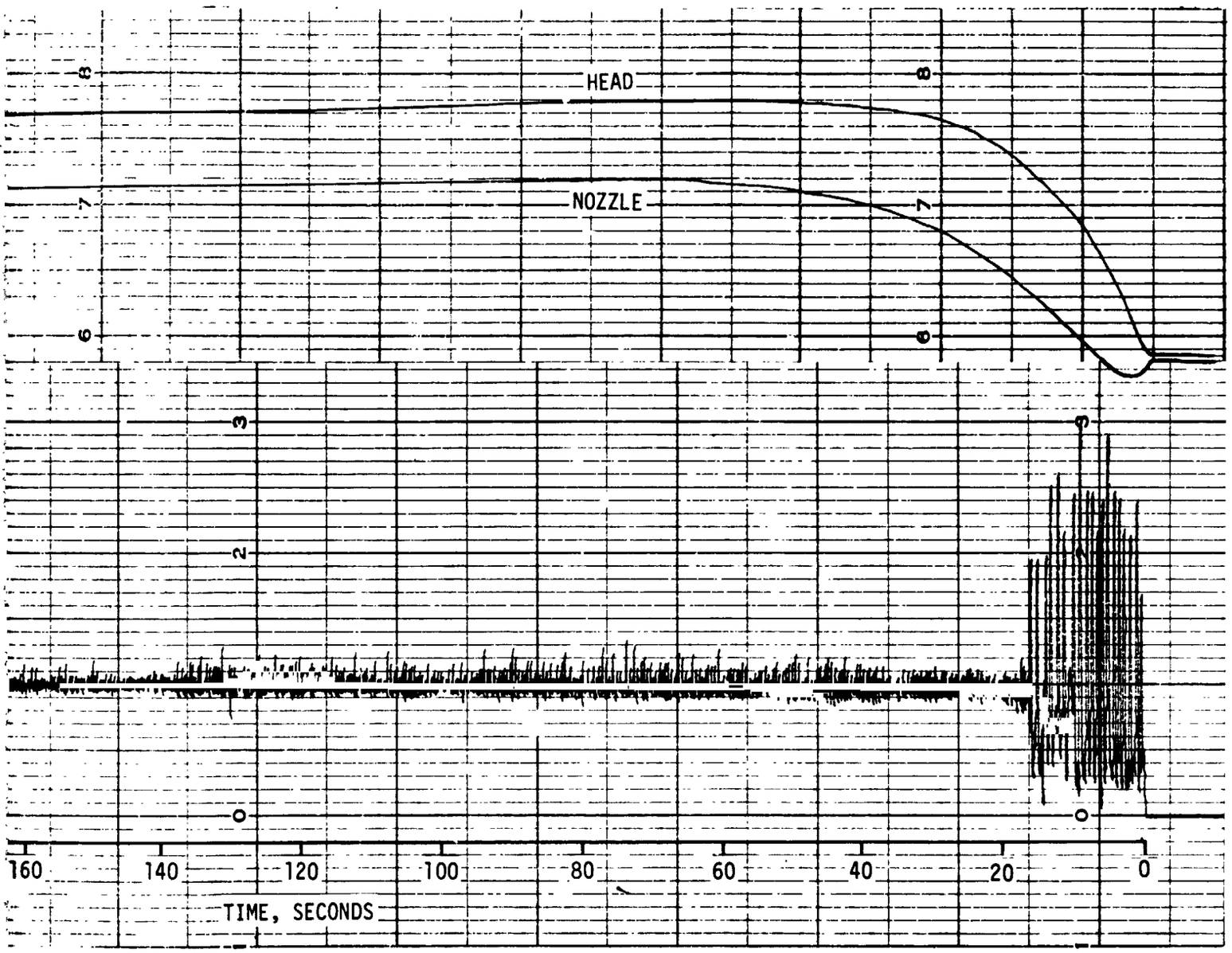

Figure 26. Preliminary Sea-Level Steady-State Operation with 76 Percent Hydrazine —— 24 Percent Hydrazine Azide

FOLDOUT FRAME 2

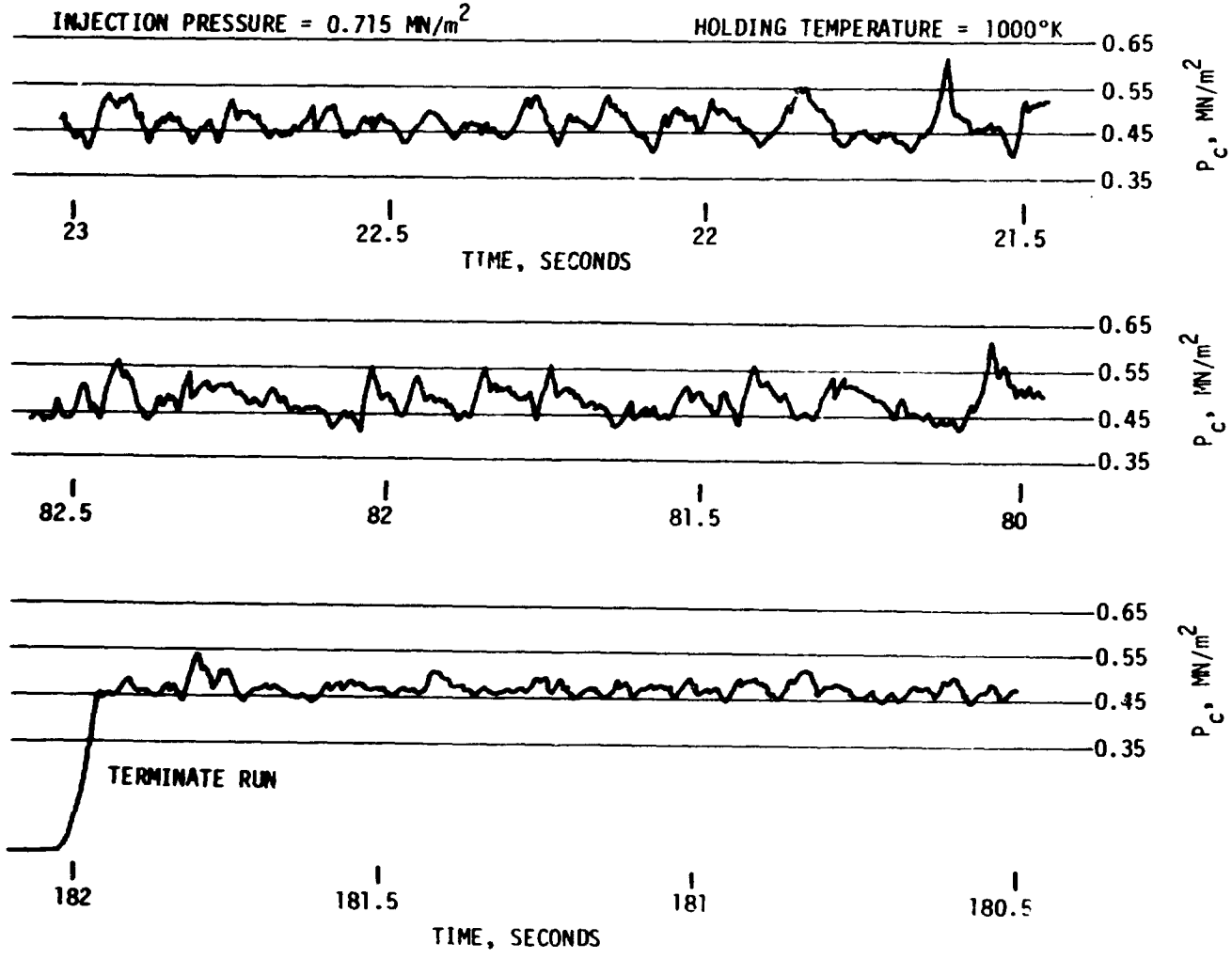

Figure 27. Steady-State Oscillograph Chamber Pressure Traces at Times Corresponding to Those of Figure 26

characterized by smooth and very rough behavior. The chamber pressure trace just prior to and at injector failure is shown in Figure 28. Post-test inspection revealed that the injector ruptured at the first portion of the thermal relief bend (Figure 29).

Disassembly of the thruster revealed a considerable amount of screen pack rearrangement and compaction (Figure 30). A two-zoned contamination region is indicated in the plan view (Figure 30a). The individual screen wires were bent and kinked from their original geometry. The oblique view in Figure 30b illustrates the screen pack compaction. These effects were caused by the large chamber pressure fluctuations which occurred during unstable operation. Negligible chamber corrosion was observed. An interior view of the nozzle end appears in Figure 31. The Haynes 25 retaining screen (Figure 31b) remained intact during testing.

An electron microprobe analysis of the post-test screen pack condition indicated that the major contaminant was iron. A backscattered electron image of the central area of Figure 30a appears in Figure 32. An Fe-K_α X-ray image of the same area is shown in Figure 33. A spectral analysis also revealed the presence of chromium, nickel and cobalt. The iron content was significantly higher than that observed on the screen pack following operation with hydrazine.

Aerozine-50

A total of seven minutes steady-state operation was accumulated with the baseline thruster configuration. Injection pressures were varied between 0.31 and 1.03 MN/m^2, and initial holding temperatures of 993 and 1073°K were used. The thruster exhibited stable operation under all test conditions. Ignition could not be sustained for any reasonable length of time with injection pressures above 0.31 MN/m^2 at either holding temperature. Chamber pressure (P_c) traces during steady-state operation are illustrated in Figure 34 for an injection pressure of 1.03 MN/m^2 and holding temperatures of 993 and 1073°K, respectively. Large chamber pressure fluctuations were absent. The gradual decrease in P_c after two seconds run time was accompanied by a decrease in thruster temperature (monitored visually on digital

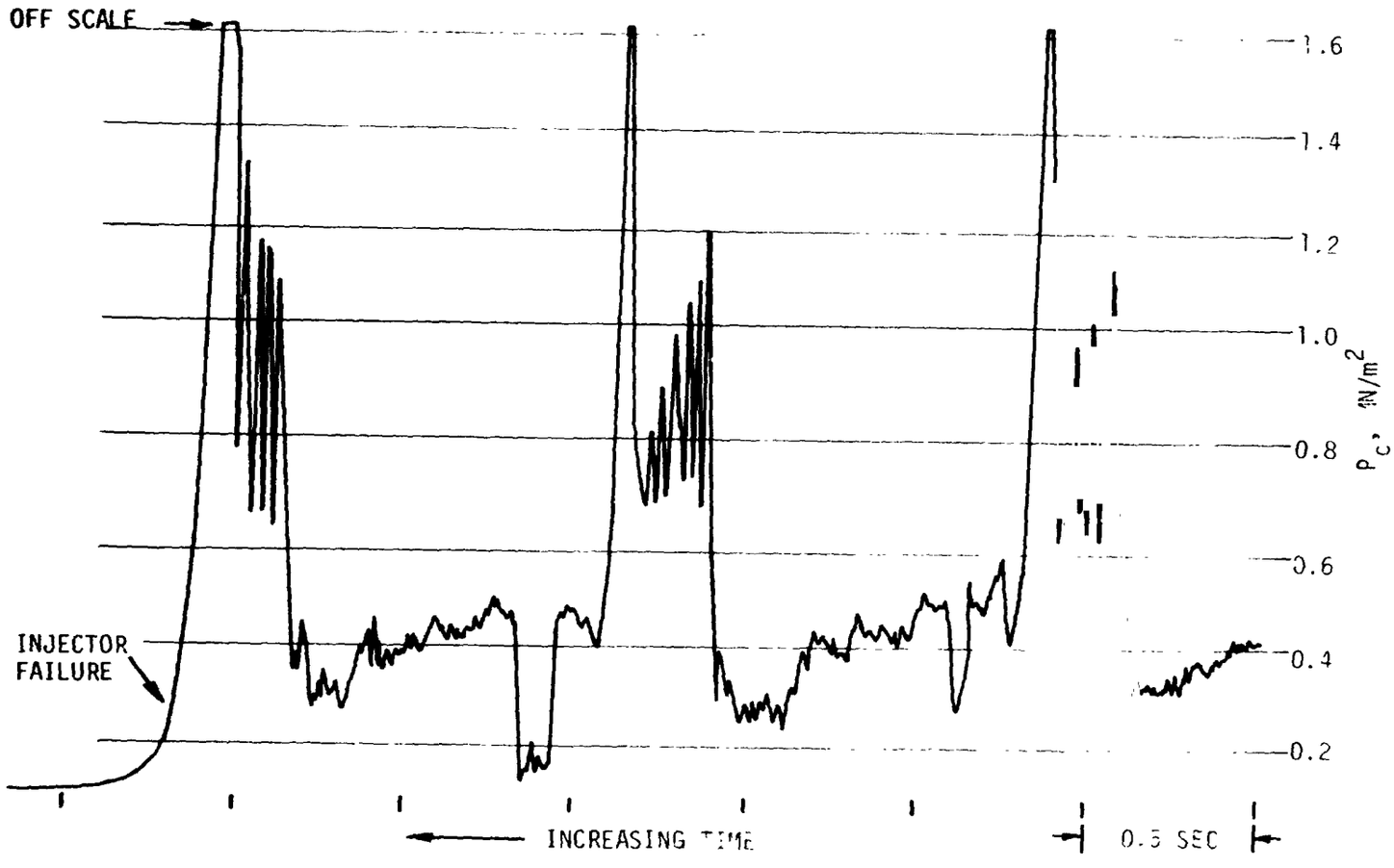

Figure 28. Oscillograph Trace of Chamber Pressure Prior to and at Injector Failure

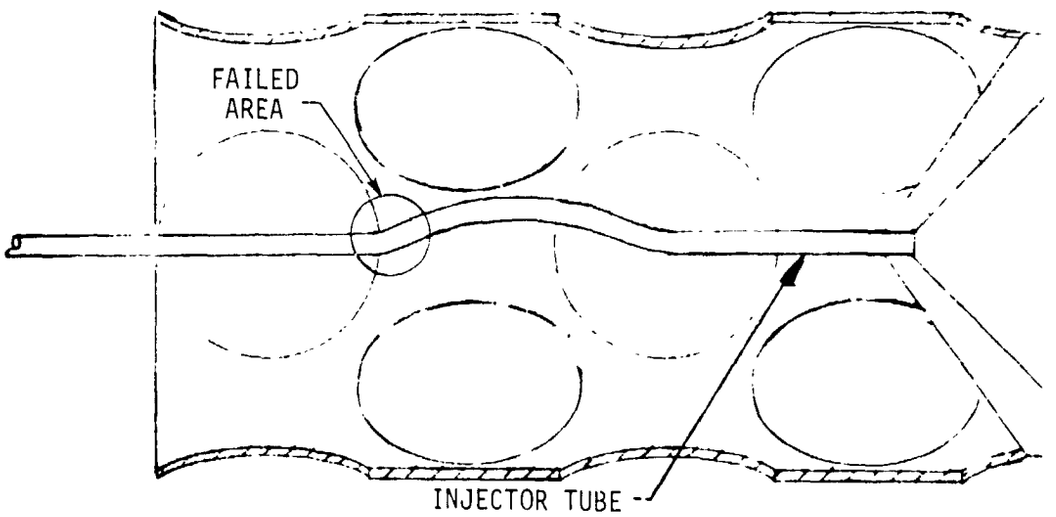
FAILED
AREA
INJECTOR TUBE

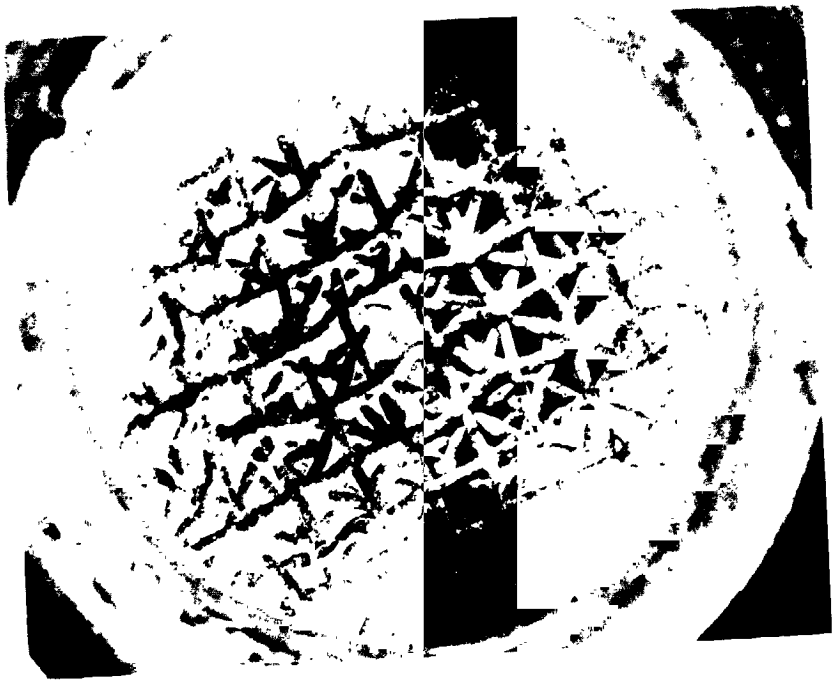

(a) Plan View

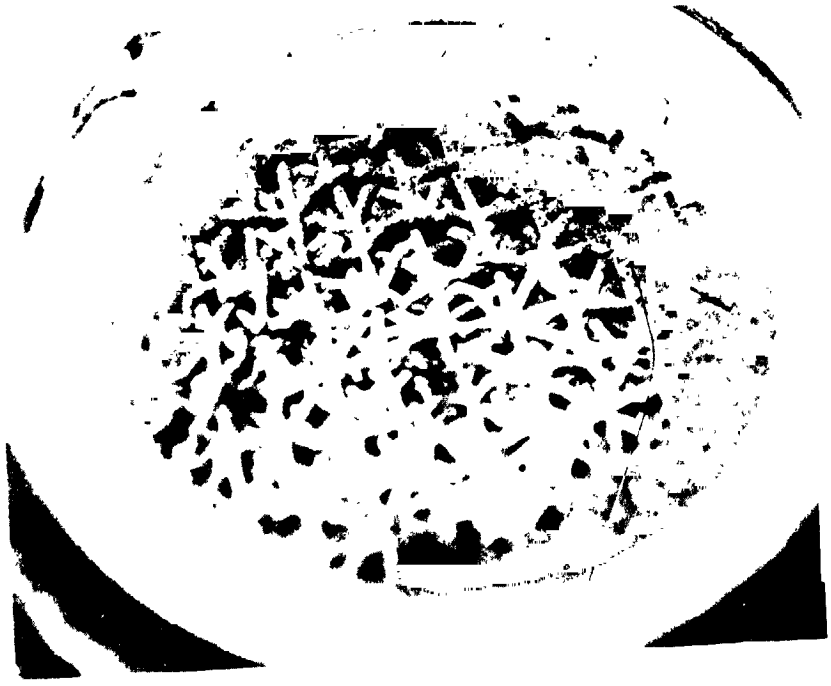

(b) Oblique View

Figure 30. Post-Test Condition of Screen Pack from Thruster Operated on 76 Percent Hydrazine - 24 Percent Hydrazine Azide

(a) Interior View of Nozzle End and Throat

(b) Haynes 25 Retaining Screen

Figure 31. Downstream Thrust Chamber Components of Thruster Operated on 76 Percent Hydrazine - 24 Percent Hydrazine Azide

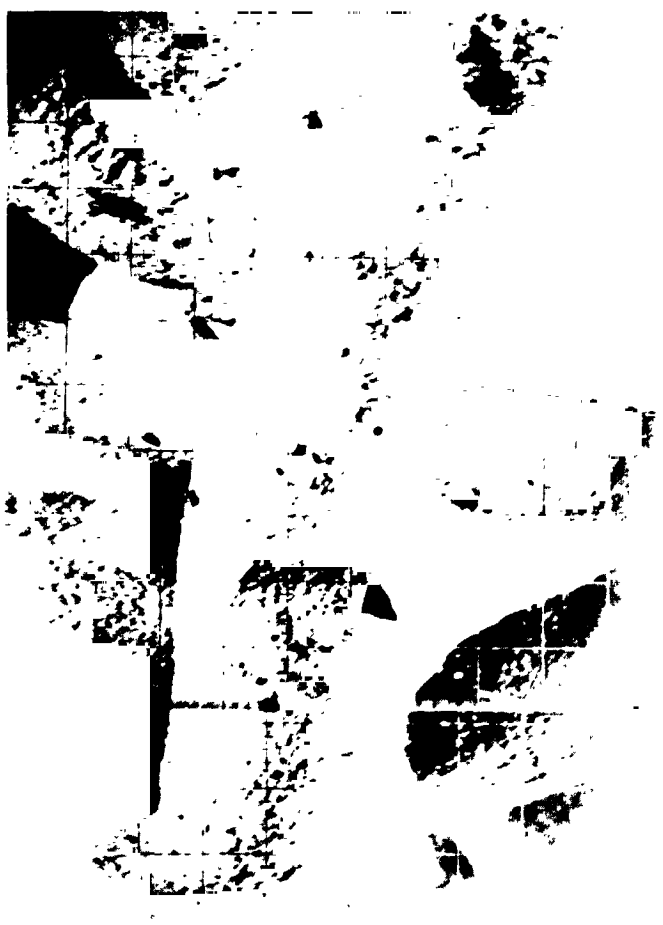

Figure 32. Backscattered Electron Image of the Top Platinum Screen Center from Thruster Operated With Hydrazine-Hydrazine Azide

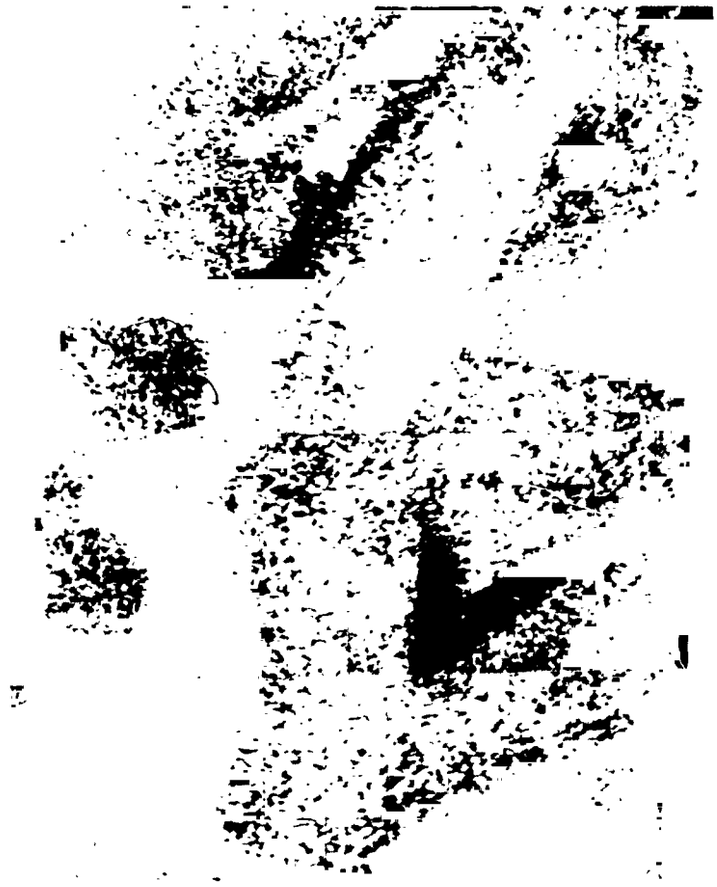

Figure 33. Iron K_α X-Ray Image of the Top Platinum Screens of Figure 32

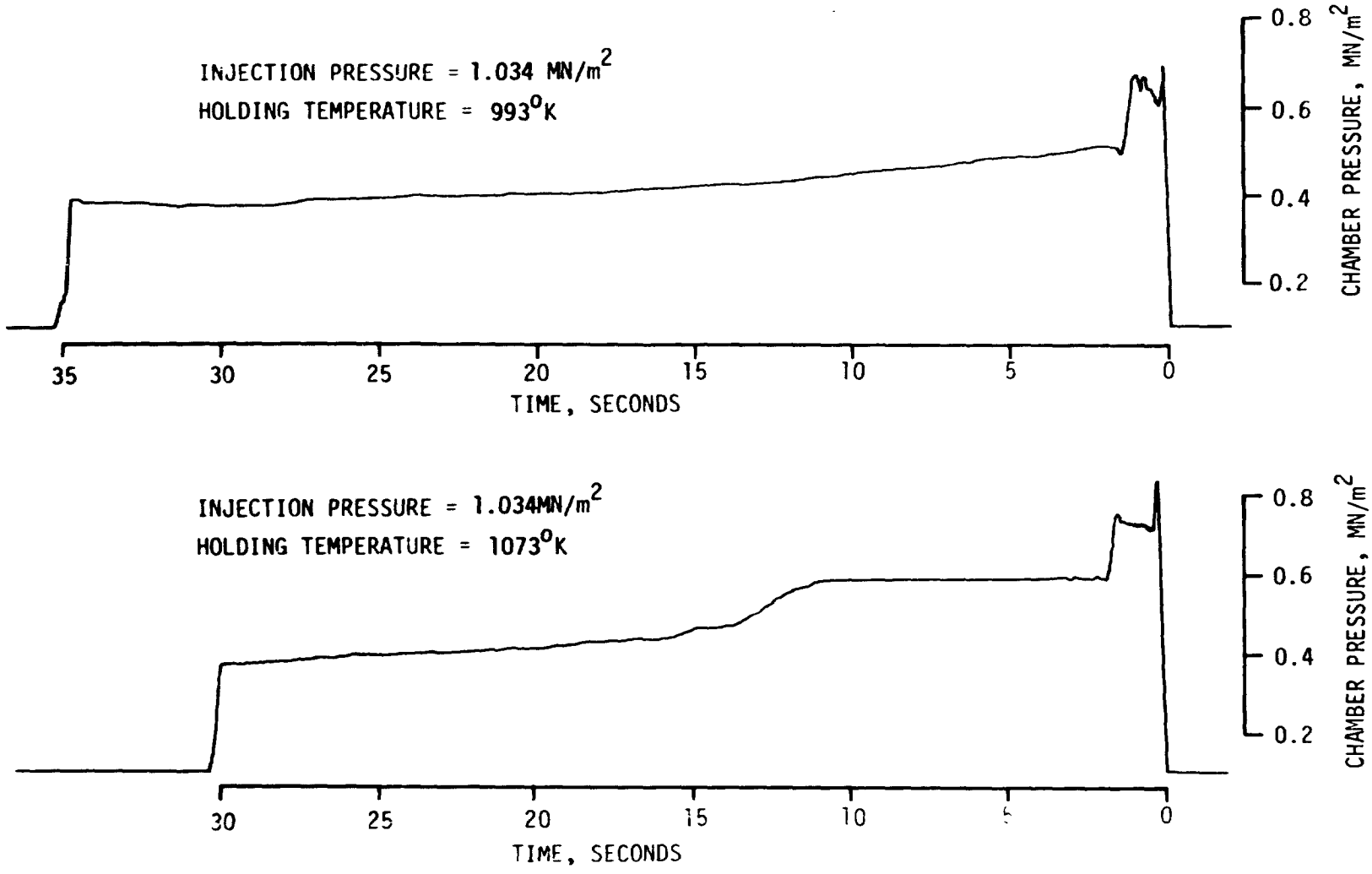

Figure 34. Preliminary Sea-Level Steady-State Thruster Operation With Aerozine-50

readout). Limited decomposition occurred at a low injection pressure of 0.31 MN/m^2 for about 45 seconds before the thruster temperatures were observed to decrease.

Post-test thruster disassembly and inspection revealed negligible chamber corrosion. Carbon deposition was not observed on the chamber walls or in the nozzle section. No evidence of carbon deposition was noticed on the platinum screens. The bottom Haynes 25 retaining screen had a dark deposit buildup. The top and bottom portions of the screen pack appear in Figure 35. X-ray imaging in the electron microprobe confirmed that the deposit on the retaining screen was carbon.

Monomethylhydrazine

Preliminary sea-level steady-state operation with MMH was similar to that with Aerozine-50. The rate of decrease in thruster temperature was more severe than that with Aerozine-50. This rapid performance degradation is illustrated in Figure 36. Screen pack flooding also occurred at lower injection pressures and higher holding temperatures. The only difference was the time required to produce the same level of thruster quench. These steady-state tests were terminated prior to the condition of liquid propellant flow through the nozzle. The total steady-state operation amounted to about five minutes.

The thruster was pulsed (50 ms pulse, one pulse per second) with an injection pressure of 0.34 MN/m^2 and holding temperatures of 1000, 1061 and 1144°K, respectively. Two hundred pulses were accumulated at holding temperatures of 1000 and 1061°K (one hundred each). There were no indications of abnormal operation at these temperatures. Rapid chamber pressure degradation occurred after ten pulses at the high holding temperature of 1144°K. Post-test inspection revealed that the injector was plugged with carbon. Thermal soakback between pulses was sufficient to cause vaporization and decomposition in the injector. No carbon deposits were observed on any of the interior thrust chamber surfaces.

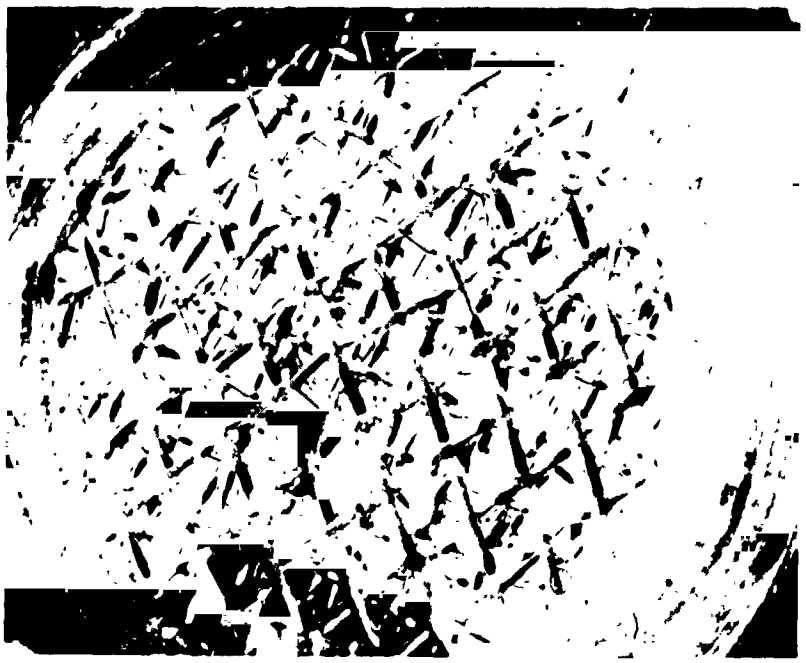

(a) Top Platinum Screens, 20X

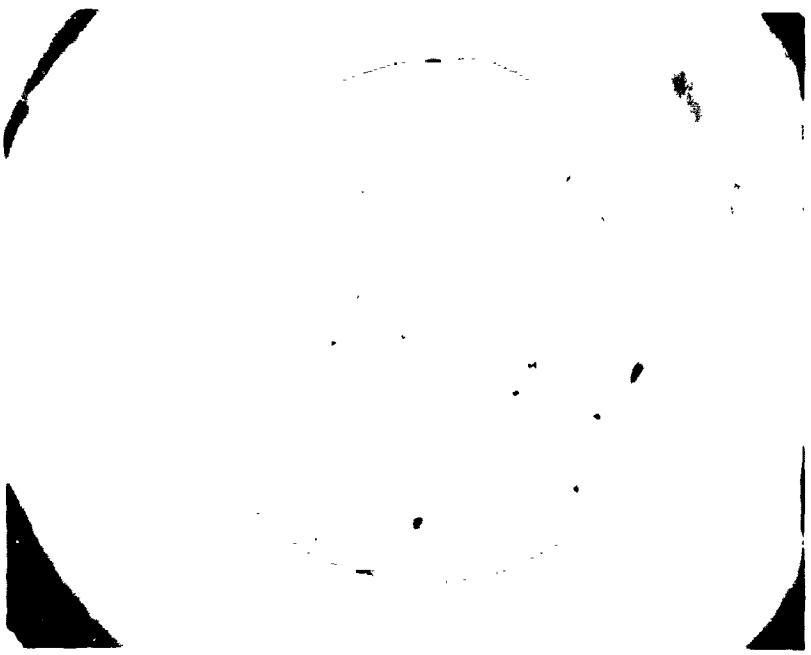

(b) Haynes 25 Retaining Screen, 20X

Figure 35. Aerozine-50 Post Test Screen Pack Appearance

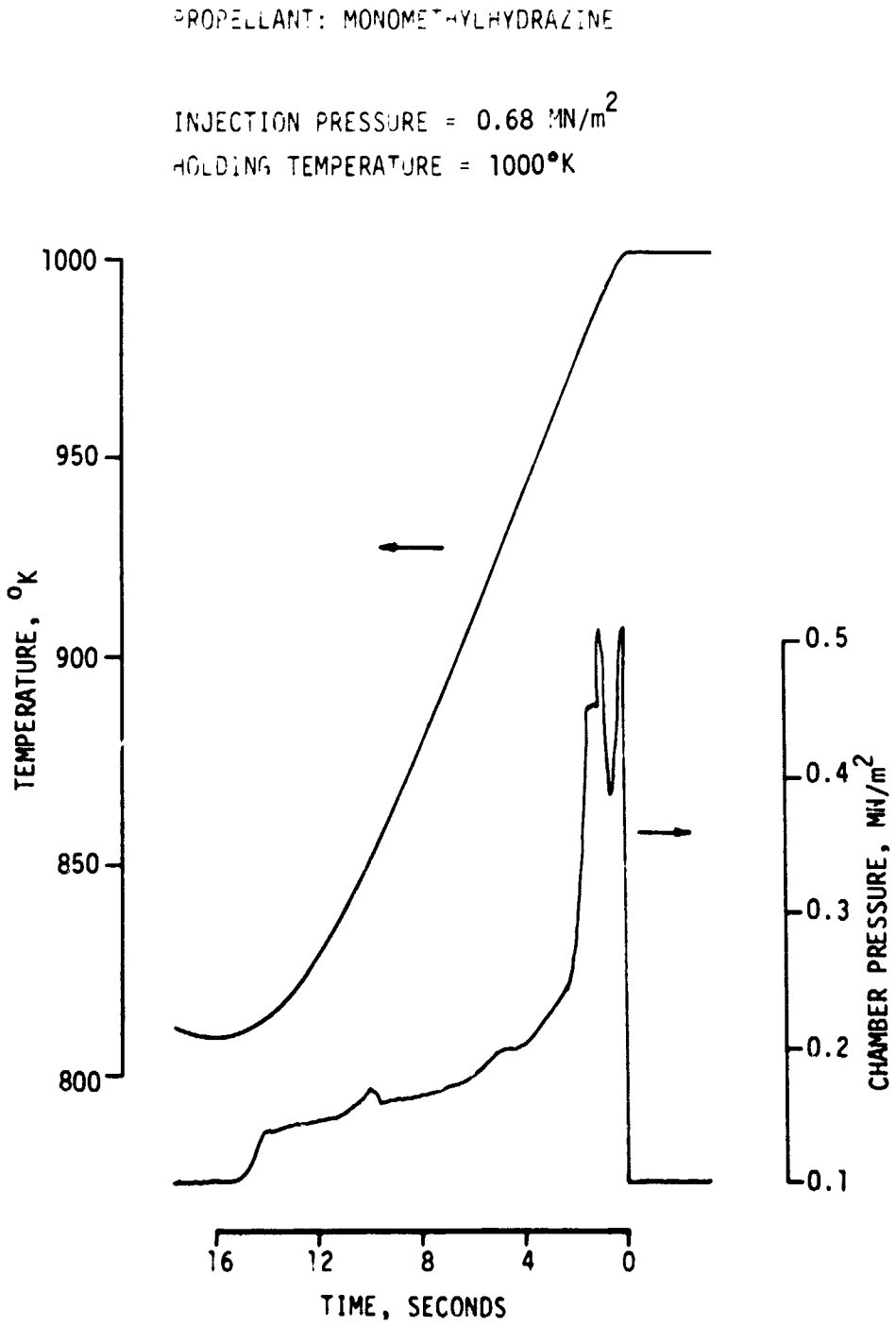

Figure 36. Preliminary Sea-Level Steady-State Thruster Operation With Monomethylhydrazine

4.3 VARIABLE THRUSTER CONFIGURATIONS

The initial characterization tests (Section 4.2) indicated that the baseline thruster configuration was marginal for stable operation with the azide blend and inadequate for operation with the carbonaceous propellants (AERO-50, MMH).

All thruster modifications were performed by changing the internal screen pack geometry. A series of tests with the azide blend were performed to determine the relationship between stable modes of operation, screen pack density and characteristic chamber length, L*. Unstable operation was promoted by increases in L* and screen pack density. A configuration using a variable density screen pack produced stable operation and was used for the high altitude performance measurements.

The "flooding" characteristics of propellants containing UDMH and MMH clearly indicated that the thrust chamber residence times were too short with the baseline configuration. Longer and/or higher density screen pack assemblies were necessary to satisfy the heat transfer requirements for sustained steady-state operation.

Each variable thruster configuration was also performance tested with MIL-grade hydrazine. A substantial amount of hydrazine data was gathered during these tests. Although the primary objective of the monopropellant study described herein was to investigate propellants other than hydrazine, the aforementioned hydrazine data was significant enough to warrant a complete analysis.

4.4 PERFORMANCE MEASUREMENTS

4.4.1 Hydrazine-Hydrazine Azide

The unstable operation which led to an injector failure with the baseline thruster configuration indicated that undecomposed propellant traversed a considerable distance into the screen pack. Subsequent decomposition of this propellant caused a pressure wave front to rapidly move towards the injector end of the thruster. The intensity of this wave front promoted rapid decomposition of propellant remaining in the head space. The end result of this process was a large pressure spike.

An empirical test series indicated that the head space "reactivity" controlled the overall thruster performance. A configuration using a variable density screen pack reduced the head space "reactivity." Sixty screens were packed in a 0.5 cm sleeve with the packing density at the head end approximately twice that at the nozzle end. This configuration resulted in a holding temperature reduction of 75°K from the preliminary level of 998°K.

Performance measurements with hydrazine for this thruster configuration were similar to the original baseline configuration. Values of delivered specific impulse were five percent lower. Steady-state performance measurements for the azide blend are given in Figure 37. A higher holding temperature of 923°K was used after the ignition characteristics were rough at a holding temperature of 810°K. Chamber pressure roughness varied from ± 9% at 1.034 MN/m^2 injection pressure to ± 15% at 1.724 MN/m^2 injection pressure. Operation at the high injection pressure of 2.413 MN/m^2 resulted in metastable operation similar to that obtained with the baseline configuration. The data at this injection pressure are approximate. The pulsed-mode performance characteristics are presented in Figure 38. The low value of delivered specific impulse and large rise time to 90% P_c for the 50 ms pulse indicated that vaporization and/or decomposition was occurring in the feed tube.

4.4.2 Aerozine-50

The thrust chamber residence times were increased by a high density screen pack (larger pressure drop). Eighty platinum screens were packed into a 0.5 cm sleeve. Thirty minutes sustained steady-state ignition was obtained using Aerozine-50 with the modified screen pack. An injection pressure of 1.034 MN/m^2 and a holding temperature of 810°K were used. The chamber pressure roughness was ± 3.5% at an average value of 0.637 MN/m^2. The chamber temperature rose to 977°K. The steady-state test was terminated when response from the chamber pressure transducer became sluggish. At this time, however, the thruster was still operating in a normal mode as judged from the chamber temperature traces. The thruster was removed from the test stand and disassembled. The slow transducer response was

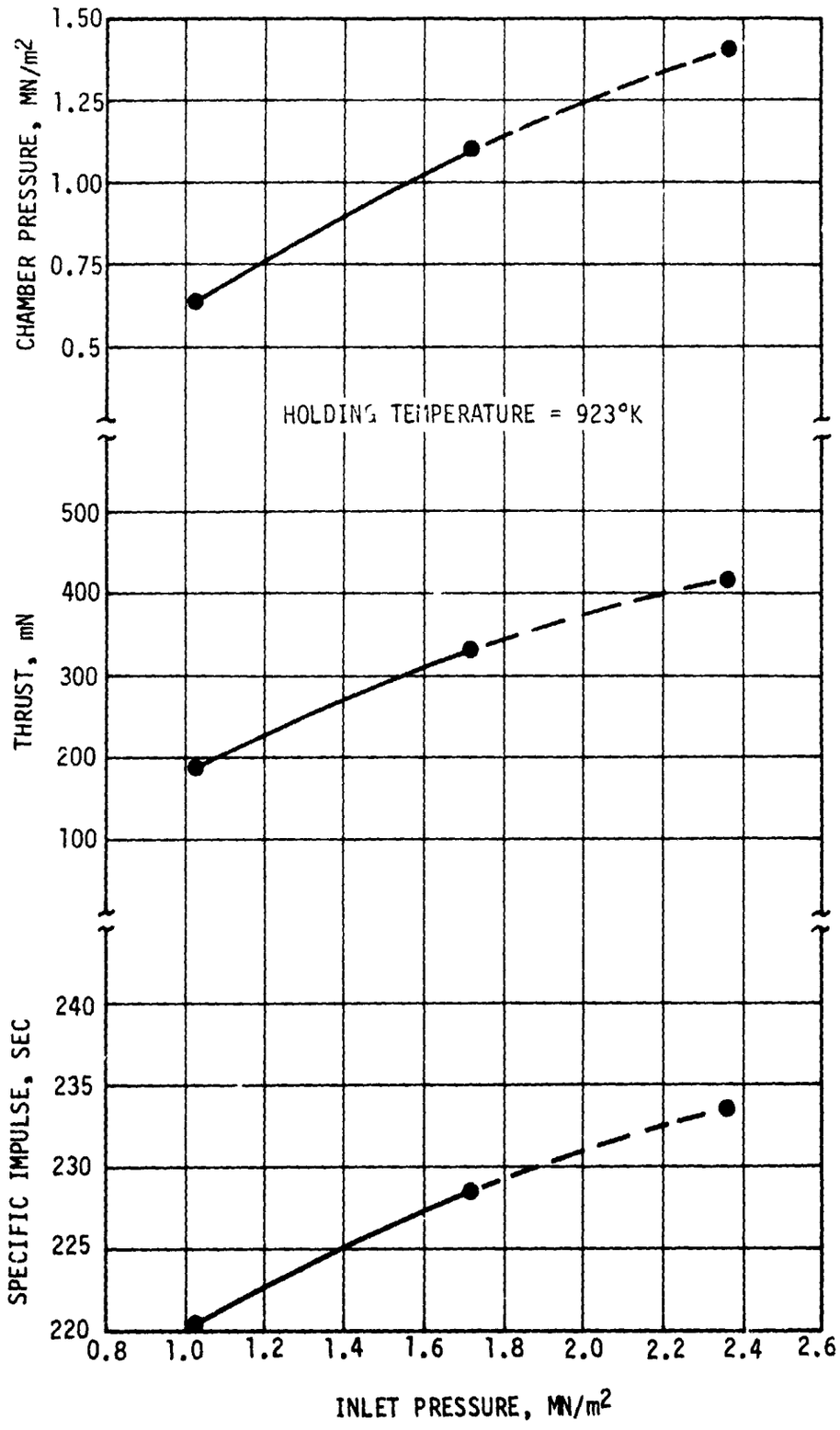

Figure 37. Hydrazine-Hydrazine Azide Steady-State Performance

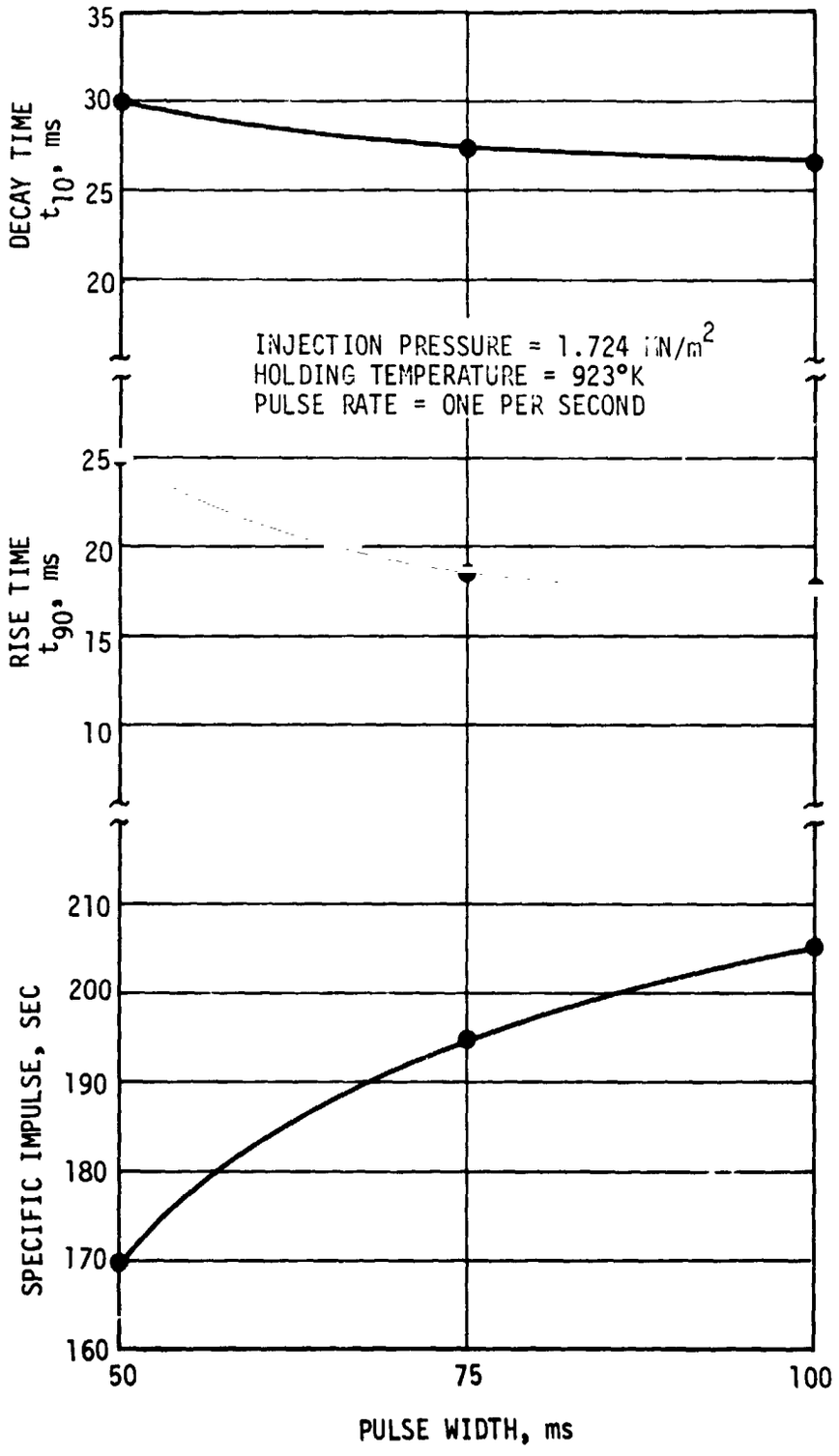

Figure 38. Hydrazine-Hydrazine Azide Pulsed-Mode Performance

caused by a thin layer of carbon buildup in the nozzle section. The nozzle section is shown in Figures 39a and 39b as internal and external views, respectively. The nozzle throat showed no evidence of carbon accumulation; the pre and post-test diameters were identical. Carbon deposits were also observed on the walls of the head space and within the screen pack. The injector showed no signs of carbon buildup. The carbon deposited in the form of a fine powder.

Steady-state performance parameters for Aerozine-50 are compared to those for hydrazine in Figure 40 with the modified thruster configuration. Temperature measurements indicated that considerable decomposition was occurring near the nozzle. The nozzle block and chamber head temperatures were 1061°K and 1027°K, respectively (injection pressure was 1.724 MN/m^2). The corresponding nozzle and head temperatures for operation with hydrazine were 1205°K and 1239°K, respectively. Chamber pressure roughness was $\pm$ 7% for hydrazine and $\pm$ 6% for Aerozine-50.

The pulsed-mode performance of hydrazine versus Aerozine-50 appears in Figure 41. The operating parameters for these data were injection pressure = 1.724 MN/m^2; holding temperature = 810°K; pulse rate = one per second. The maximum thruster temperatures are indicated at each datum point. An oscillograph recording of the pulsed-mode analog data is reproduced in Figure 42 for a 100 ms pulse. The rise and decay times to 90% and 10% P_c were 28 ms and 75 ms, respectively. A 42 ms centroid shift from the command pulse was calculated.

Post-test disassembly and inspection revealed a similar level of carbon deposition as was observed after sea-level testing.

4.4.3 Monomethylhydrazine

Longer thrust chamber residence times were required for MMH than for UDMH. A 1.02 cm sleeve was packed with 160 platinum screens to provide a higher pressure drop. An additional heater element was wrapped around the longer sleeve to prevent temperature gradients along the thruster assembly. A separate power supply was used to equalize the temperature distribution. Steady-state operation was marginal at a

(a) Interior View of Nozzle Section

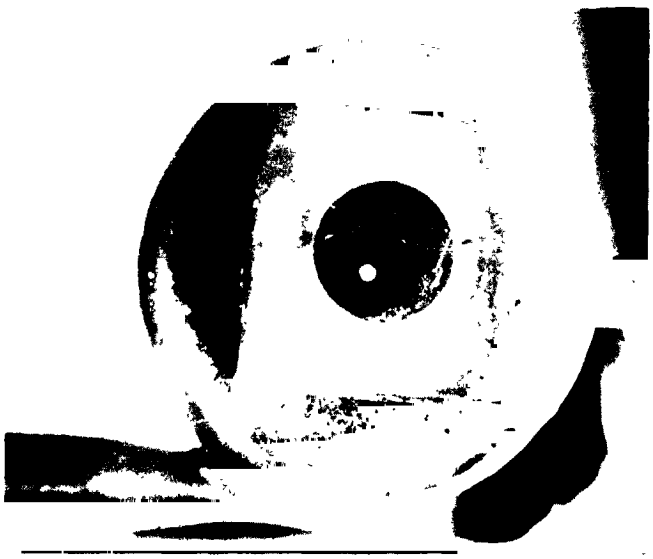

(b) Exterior View of Nozzle Section

Figure 39. Post-Test Appearance of Nozzle Section From Thruster Operated 30 Minutes Steady-State With Aerozine-50

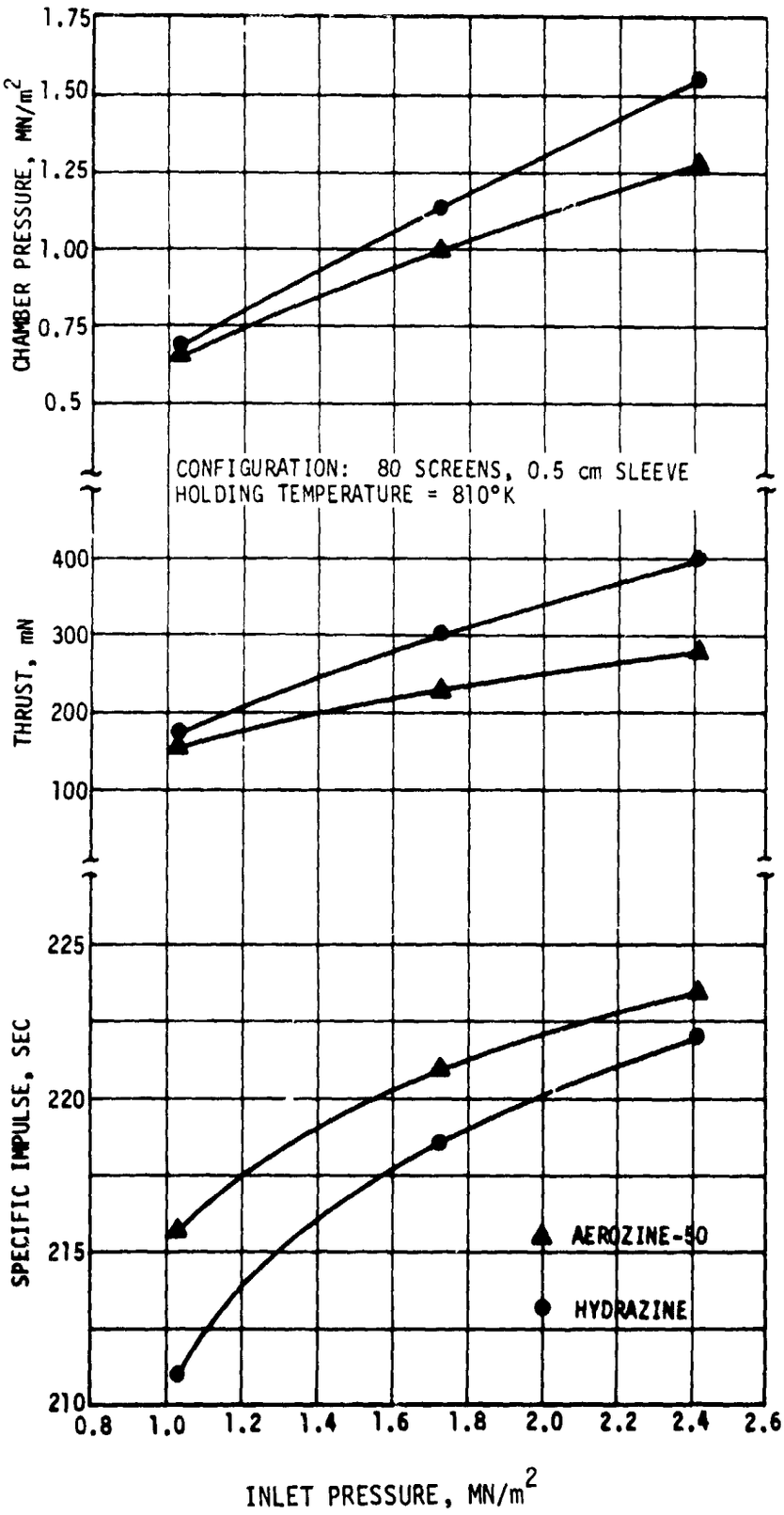

Figure 40. Steady-State Performance Measurements With Aerozine-50

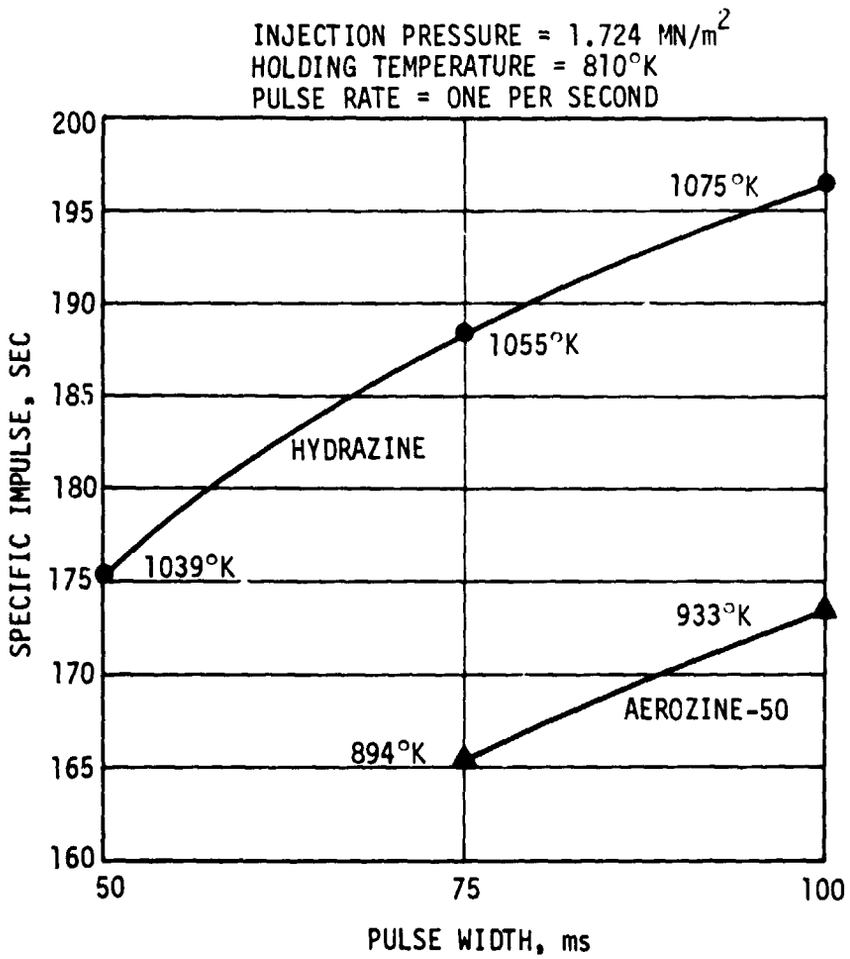

Figure 41. Pulsed-Mode Performance With Aerozine-50

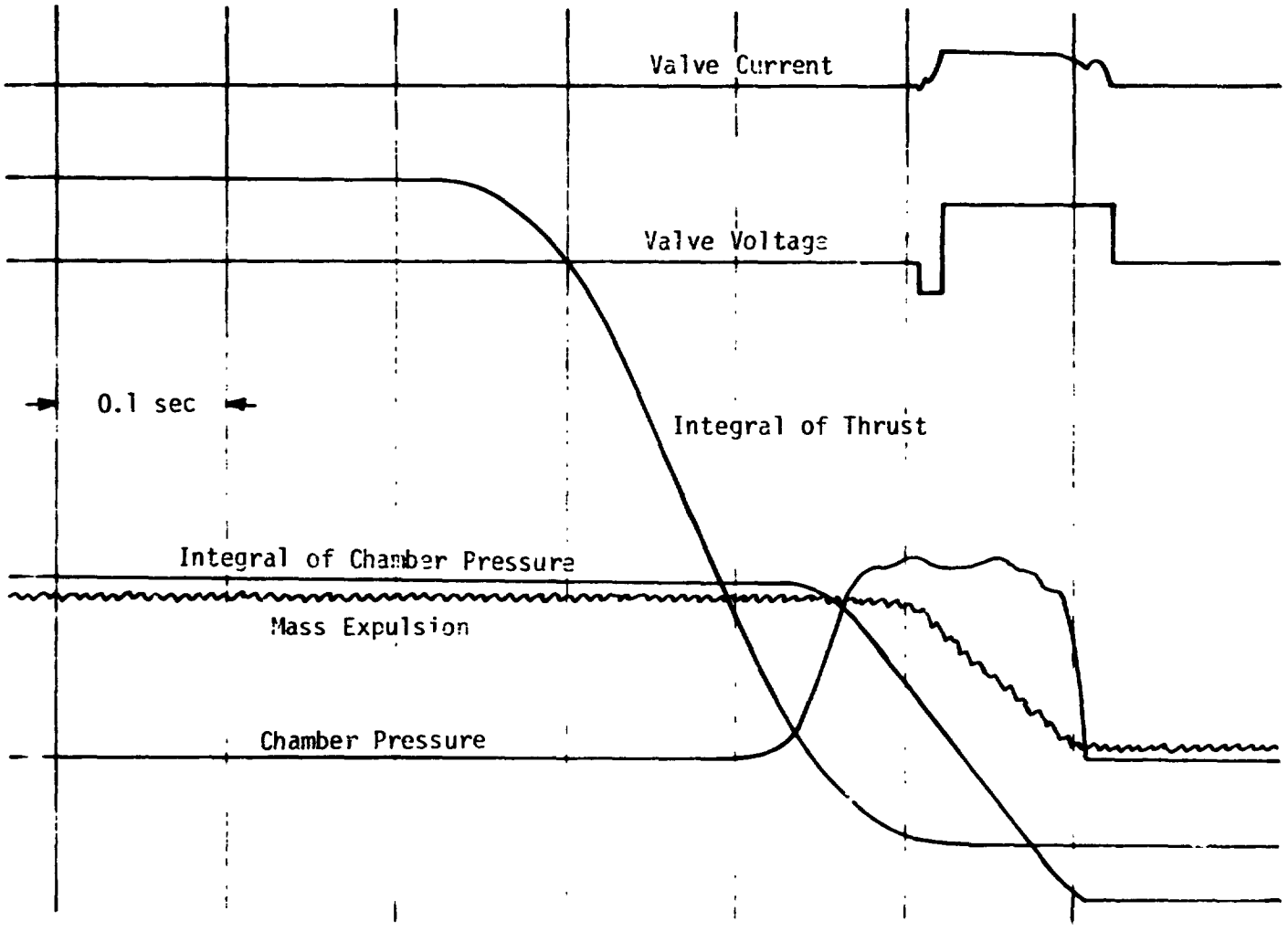

Figure 42. Aerozine-50 Pulsed Mode Analog Data Recording

holding temperature of 1198°K and an injection pressure of 1.034 MN/m^2. The nozzle section temperature rose to 1263°K and the head section quenched to 773°K after five minutes of operation. Longer run times resulted in "flooding." Prior to this condition, the thrust level was 154 mN with a delivered specific impulse of 229 sec.

Hydrazine was mixed in a 1:1 ratio with MMH in order to reduce the high holding temperatures necessary to initiate MMH decomposition. Two screen pack configurations were used. One configuration was similar to that used with MMH. The 1.02 cm sleeve was packed with 180 screens. The second thruster had 360 screens packed in a 2.54 cm sleeve. Marginal steady-state decomposition was obtained at a lower holding temperature of 1033°K with the former thruster configuration. The thruster's temperature-time history indicated that the decomposition front was towards the nozzle end. Sustained steady-state decomposition was obtained for ten minutes with the long (2.54 cm) screen pack assembly at a holding temperature of 1033°K and an injection pressure of 1.034 MN/m^2. Thrust and chamber pressure degradation were noticed after ten minutes. The thrust decreased from 168 mN to 52 mN. The specific impulse decreased from 221 sec to 207 sec. A decrease in thruster temperature from 1143°K to 1083°K was recorded. During thrust degradation, the primary decomposition front appeared to move from the middle of the screen pack to the head end. These observations indicated that a high pressure drop was created in the nozzle section. Post-test inspection revealed a substantial carbon deposit on the Haynes 25 retaining screen. Heavy carbon deposits were not noticed elsewhere on the internal thrust chamber components. Pre- and post-test injector water flow characteristics were identical. It was concluded that the thrust degradation was caused by carbon buildup on the Haynes 25 retaining screen.

Limited pulsed-mode data was obtained for the 50/50 N_2H_4-MMH mixture with the 2.54 cm screen pack. A specific impulse of 171 sec was obtained for a 100 ms pulse at a holding temperature of 1033°K and an injection pressure of 1.034 MN/m^2. The pulse rate was one per second; the thruster temperature rose to 1089°K.

4.4.4 Mixture of Hydrazine Monopropellants

The MHM blend was the last propellant investigated during the evaluation test program. Previous tests with Aerozine-50, MMH and the N_2H_4 - MMH mixture indicated that worthwhile data would not be obtained using the baseline thruster configuration. Accordingly, longer screen pack assemblies were used to characterize the MHM blend. The 180 screen, 1.02 cm sleeve was used to obtain data for comparison with MMH and 50% N_2H_4 - 50% MMH. The final configuration consisted of 400 screens in a 2.54 cm sleeve. Both thruster configurations were steady-state baseline tested with hydrazine.

A holding temperature of 1143°K was necessary to sustain MHM decomposition with the shorter screen pack (180 screens, 1.02 cm sleeve) at an injection pressure of 0.965 MN/m^2. Operation at higher injection pressures resulted in "flooding." The steady-state data in Figure 43 shows performance degradation at an injection pressure of 1.655 MN/m^2. The nozzle and head section temperatures remained at the holding temperature while the middle screen pack temperature rose to 1223°K. Fifteen minutes steady-state operation was accumulated with the 1.02 cm screen pack. Post-test disassembly revealed a minimal amount of carbon deposition. Carbon accumulation was not observed in the head space or on the platinum screens. Little to no carbon was noticed in the nozzle section. However, a small deposit was noticed on the Haynes 25 retaining screen.

Operation with the 2.54 cm sleeve containing 400 platinum screens resulted in a reduced holding temperature necessary to initiate and sustain MHM decomposition. The holding temperature was reduced from 1143°K to 1033°K. The maximum thruster temperature (1094°K) at an injection pressure of 1.034 MN/m^2 occurred at the middle of the screen pack. The decomposition front moved towards the nozzle section as the injection pressure was increased. At 1.724 MN/m^2 injection pressure, marginal operation resulted. At higher injection pressures, decomposition could not be maintained and "flooding" occurred. Post-test thruster inspection revealed little carbon deposition. Steady-state performance data for the 2.54 cm screen pack configuration appears in Figure 44. Pulsed-mode data at an injection

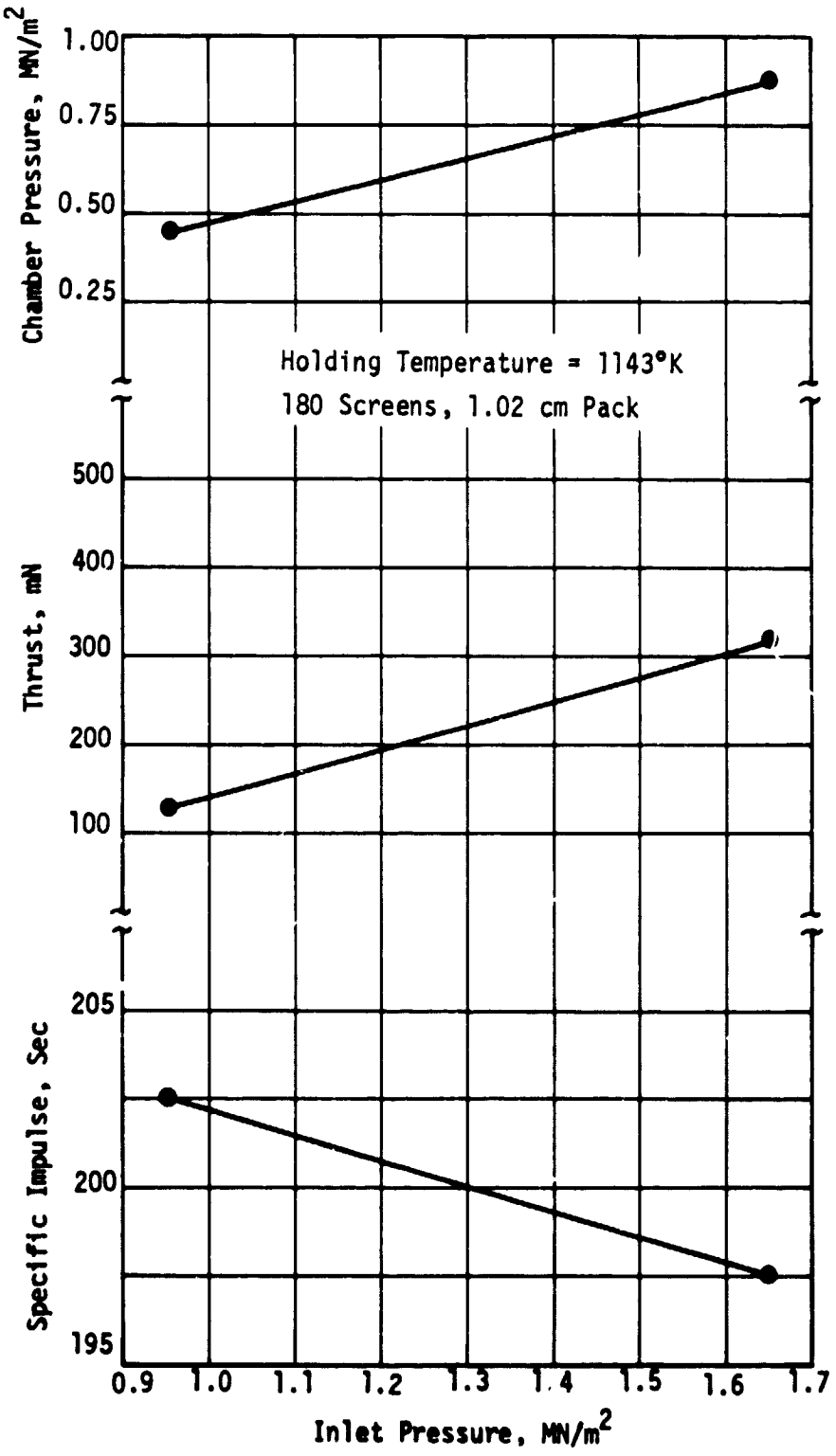

Figure 43. MHM Steady-State Performance with 1.02 cm Screen Pack

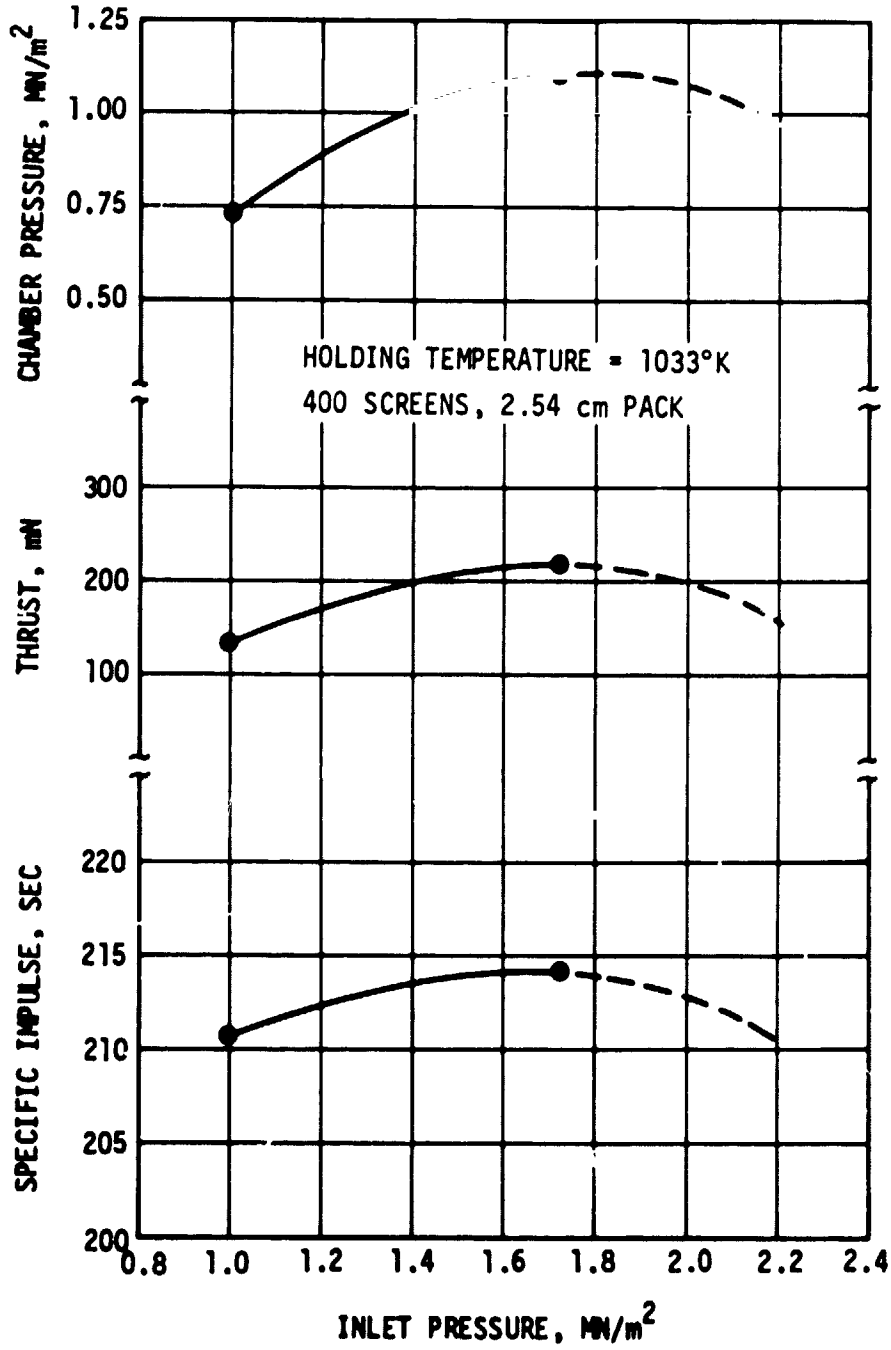

Figure 44. MHM Steady-State Performance With 2.54 cm Screen Pack

pressure of 0.81 MN/m^2 were obtained for pulse widths of 75 and 100 ms. The delivered specific impulse at 75 ms was 162 sec and 173 sec for the 100 ms pulse. The rise and decay times were slightly longer than those observed for Aerozine-50.

5.0 DISCUSSION

5.1 PERFORMANCE CORRELATION

The steady-state and pulsed-mode hydrazine performance characteristics for the standard 60 screen 0.5 cm sleeve were comparable to those obtained with the EHT.[1] The additional thrust chamber and nozzle mass associated with the modular, three piece design increased the times to reach holding and steady-state temperatures. Holding power levels of 8 to 9.1 watts were required to maintain the thruster temperature at 810°K under simulated high altitude conditions. The power requirement for a flight configuration thruster with proper insulation, no pressure tap and only one heater lead has been previously demonstrated to be less than 5 watts.[1]

The general steady-state performance levels predicted by the propellant chemistry studies were verified during the evaluation test program. An exception was the datum point for MMH at an injection pressure of 1.034 MN/m^2. The high holding temperature (1198°K) resulted in a somewhat inflated specific impulse value (228 seconds). A more precise correlation between the thermochemical computations and measured performance levels is difficult to assess, especially with the carbonaceous propellants. Computations based on equilibrium thermodynamics cannot describe the thruster's kinetic environment. The concept of frozen flow has benefited the understanding of hydrazine thruster performance (the hydrazine decomposition product compositions and phases are arbitrarily fixed and no consideration is given to equilibrium). Attempts to correlate similar computations with carbonaceous monopropellant performance have not been successful.

A comparison of the delivered steady-state specific impulse for the candidate monopropellants is presented in Figure 45. The configurations and holding temperatures for each propellant are summarized. Reference data for hydrazine are included. The steady-state program goal of 200 sec specific impulse was met by all propellants studied. A similar comparison of the pulsed-mode specific impulse appears in Figure 46. The pulsed-mode performance levels are best assessed by comparing the ratio of pulsed-mode specific impulse to steady-state specific impulse at comparable injection pressures. Data for four propellants at pulse widths

C-2

PROPELLANT	CONFIGURATION SCREENS	SLEEVE LENGTH, CM	HOLDING TEMPERATURE, °K
Azide	60	0.5	923
AERO-50	80	0.5	810
MHM	400	2.54	1033
50 N_2H_4 - 50 MMH	360	2.54	1033
MMH	160	1.02	1198
N_2H_4	60	0.5	810

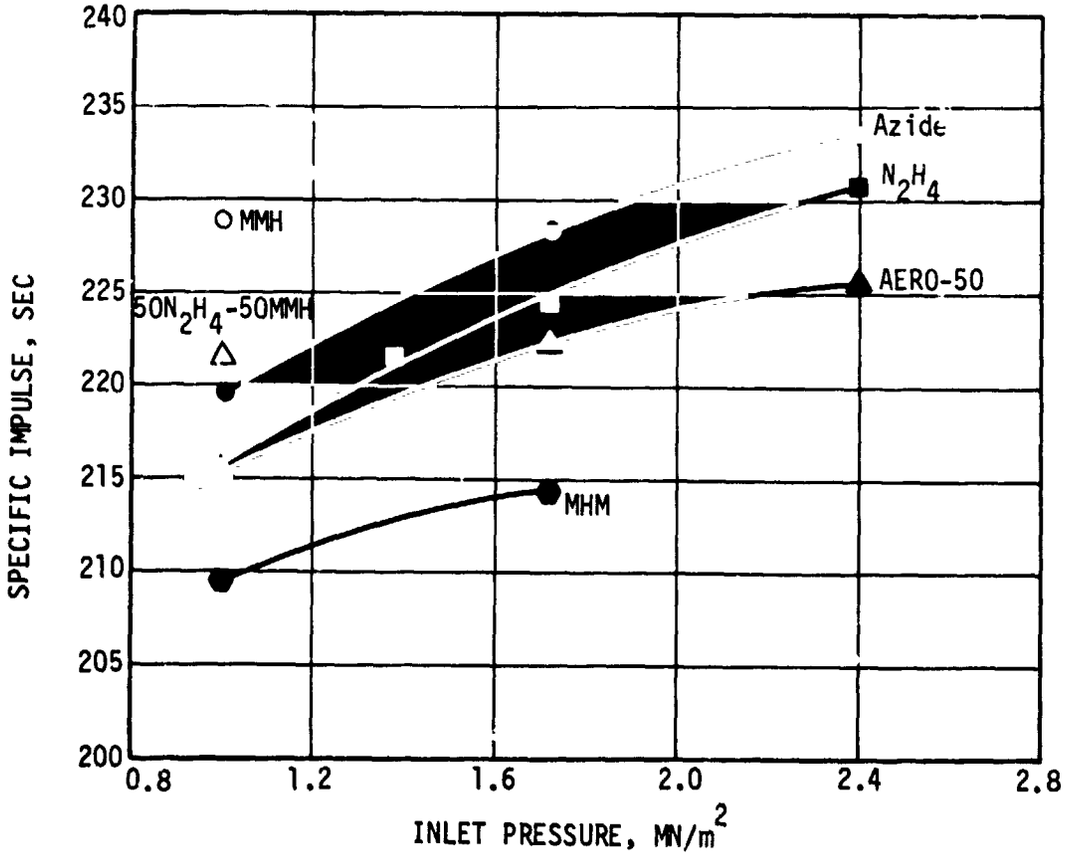

Figure 45. Steady-State Performance Data of Five Candidate Monopropellants

PROPELLANT	INJECTION PRESSURE MN/m^2	HOLDING TEMPERATURE °K
HA	1.724	923
MHM	0.807	1033
AERO-50	1.034	810
50 N_2H_4 - 50 MMH	1.034	1033
Hydrazine	1.724	810

(PULSE RATE = ONE PER SECOND)

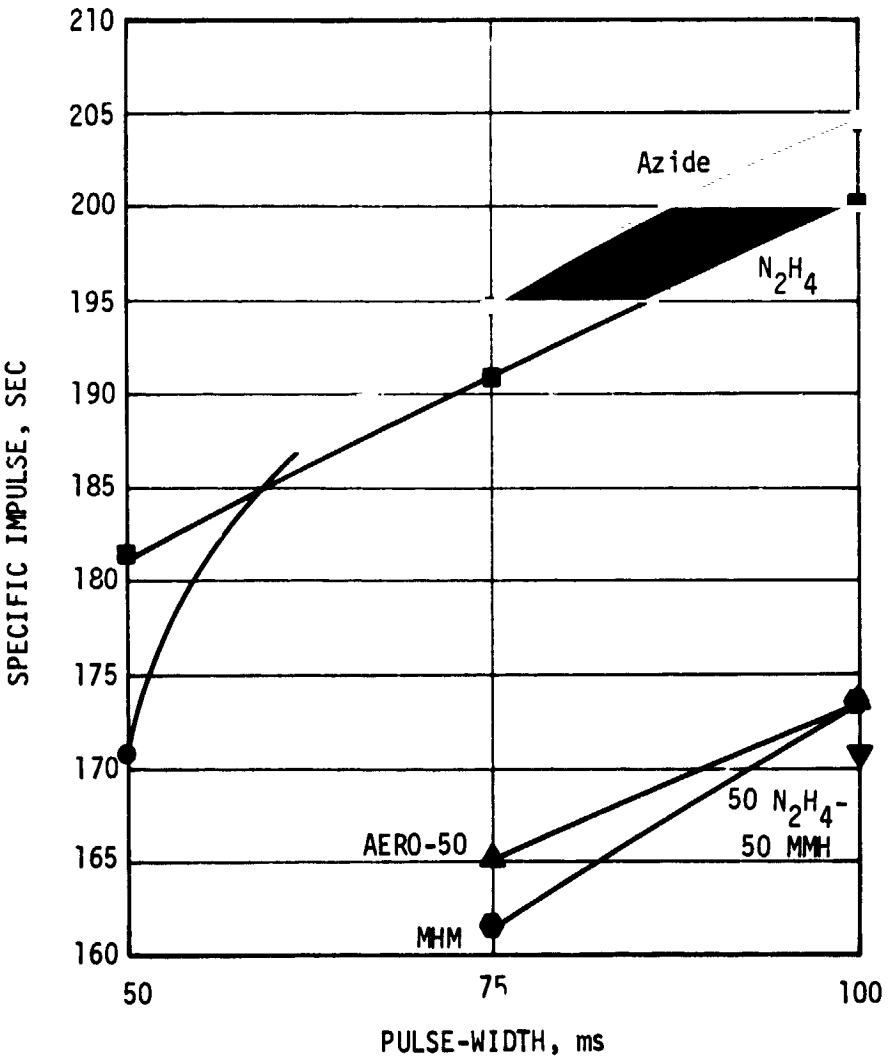

Figure 46. Pulsed-Mode Performance Data of Four Candidate Monopropellants

of 75 and 100 ms appear in Table 15. These data indicate that the pulsed-mode performance of the azide blend is slightly better than that obtained with hydrazine when compared to the steady-state levels. The high density and long screen pack assemblies compromised the MHM and Aerozine-50 pulsed-mode performance. Thrusters using shorter screen pack assemblies pulsed well but steady-state operation could not be sustained. Longer or higher density screen pack assemblies were required to satisfy the heat transfer conditions necessary to initiate decomposition of the carbonaceous propellants. The ease of initiating decomposition decreased in the following order: Aerozine-50, 50% N_2H_4-50% MMH, MHM and MMH.

5.2 DECOMPOSITION KINETICS

The thermal decomposition kinetics of the propellants evaluated during the test program phase are discussed in this section. The discussion is based on the operation of these propellants with the electrothermal thruster concept. The thermal decomposition of hydrazine is first discussed as a reference for comparison. Hydrazine performance data with the variable thruster configurations are also presented and analyzed in detail.

5.2.1 Hydrazine

The following sequence of events describe the operation of TRW's electrothermal hydrazine thruster:

1. Liquid hydrazine is admitted to the injector at thruster valve actuation. The injection design eliminates two-phase flow conditions by maintaining high propellant velocities and suppressing heat transfer from the chamber to the injector (commonly called "soak-back").

2. The liquid propellant stream impinges on the heated screen pack. The screen pack provides the initial energy for propellant vaporization and decomposition. It also serves as an optical barrier by eliminating a line of sight from the injector to the propulsive nozzle, and as a "flame-holder" to provide steady-state stability.

Table 15. Comparison of Pulsed-Mode to Steady-State Specific Impulse

Propellant	Ratio of Pulsed-Mode to Steady-State Specific Impulse 75 ms	100 ms	Remarks
Hydrazine - Hydrazine Azide	0.853	0.895	Short Screen Pack
Hydrazine	0.847	0.884	Short Screen Pack
Aerozine-50	0.766	0.804	High Density Screen Pack
MHM	0.773	0.829	Long Screen Pack

3. Hydrazine vapor decomposition is heterogeneously initiated by thermal excitation and the catalytic effect of the screen pack.

4. Decomposition is maintained by the energy release of the dissociation of hydrazine. The thruster design incorporates a large head space in the vicinity of the propellant injector. This head space promotes a toroidal recirculation of hot decomposition gases which enables a substantial amount of energy to be transferred to the incoming propellant stream. The hot gas recirculation also provides for a uniform distribution of propellant over the screen pack surface.

Hydrazine decomposition is often described by the reaction (Equation 1)

$$3N_2H_4 \longrightarrow 4(1-\alpha)\ NH_3 + (2\alpha + 1)\ N_2 + 6\alpha H_2$$

where α is the ammonia dissociation fraction. The products of Equation (1) (NH_3, N_2, H_2) are the end result of the decomposition process and may be measured quantitatively in the thruster exhaust. The ammonia dissociation fraction, α, is computed and the measured performance level is compared to the thermochemical computations. Unfortunately, Equation (1) yields no information about the actual kinetic processes occurring within the thruster. Design changes proposed to improve or optimize thruster performance require an understanding of the internal kinetic environment. A technique to couple the chemical kinetic rate equations to the modes of thruster operation has not been devised. A simplified approach is used to explain the observed decomposition characteristics of the monopropellants tested.

The decomposition of hydrazine and hydrazine-like propellant begins by an endothermic process although the end result is the liberation of substantial amounts of energy. The temperature dependence of a homogeneous, gas phase reaction rate may be expressed by an Arrhenius relationship of the form

$$k_h = A_h \exp\left(-\frac{Q_h}{RT}\right) \qquad (3)$$

where

k_h = specific reaction rate constant

A_h = frequency factor

Q_h = activation energy of the rate-controlling process

R = universal gas constant

T = absolute temperature

and the subscript h refers to the homogeneous process. A similar relationship may be written for a heterogeneous process as

$$k_{het} = A_{het} \exp\left(-\frac{Q_{het}}{RT}\right) \tag{4}$$

where the terms are analogous to those of Equation (3) with the subscript het referring to the heterogeneous reaction. Table 16 lists Arrhenius parameters for the homogeneous initiation reactions of hydrazine, MMH and UDMH. The frequency factor, A_{het}, may be estimated at approximately 10^4 for a smooth surface. The role of the screen pack in assisting the initial propellant decomposition is assessed by a comparison of the relative heterogeneous and homogeneous rates. The ratio of these two rates is given by

$$\frac{k_{het}}{k_h} = \frac{A_{het}}{A_h} \exp\left(\frac{Q_h - Q_{het}}{RT}\right) \tag{5}$$

Table 16. Arrhenius Parameters for the Homogeneous Decomposition of Hydrazine, MMH and UDMH[6]

Propellant	Initiation Reaction	Frequency Factor A	Activation Energy Q, Kcal/mole
Hydrazine	$N_2H_4 \rightarrow 2\ HN_2$	4.98×10^{16}	71.2
MMH	$CH_3\ NHNH_2 \rightarrow CH_3NH + NH_2$	5.01×10^{16}	63.8
UDMH	$(CH_3)_2NNH_2 \rightarrow (CH_3)_2N + NH_2$	7.94×10^{16}	62.7

The heterogeneous rate refers to a surface to volume ratio of unity and the homogeneous rate refers to a unit volume of the reacting propellant. The heterogeneous activation energy, Q_{het}, is the homogeneous activation energy, Q_h, reduced by the heat of adsorption of the reacting propellant. The energy of a strongly absorbed specie can be as high as 40 Kcal/mole. The rate ratio for hydrazine, using the data from Table 16 is

$$\frac{k_{het}}{k_h} = 2.51 \times 10^{-3} \exp\left(\frac{40,000}{RT}\right) \qquad (6)$$

Equation (6) is plotted in Figure 47 to indicate the temperature region over which catalytic effects are expected to contribute to the decomposition initiation process. Prior to propellant injection, the thruster is maintained at a holding temperature of approximately 773°K. The initial propellant slug impinging on the screen pack has its temperature raised to approximately 523°K. The rate ratio from Equation (6) is about 10^4. The corresponding homogeneous rate at 523°K is, from Equation (3), 7×10^{-14}. This slight acceleration in reaction rate is sufficient to prevent propellant "channeling" through the screen pack. An incremental penetration into the screen pack is associated with a region of higher temperature resulting from the energy liberated by the initial molecular decomposition. A thermo-kinetic barrier is created to prevent subsequent propellant penetration. A necessary condition for establishment of this barrier is that the first and second derivatives of temperature with respect to screen pack distance are positive, i.e.,

$$\frac{dT}{dx} > 0, \quad \frac{d^2T}{dx^2} > 0 \qquad (7)$$

Specification of the sufficient condition requires that: (1) the kinetic reaction rates are accelerated to the extent that the heat released by decomposition is equal to or greater than that required for propellant vaporization; and (2) that the heat is made available for the vaporization process. "Flooding" will eventually occur if only sufficient condition 1 is met. The thermo-kinetic barrier will be established and will move backwards towards the injector end if the heat released by decomposition

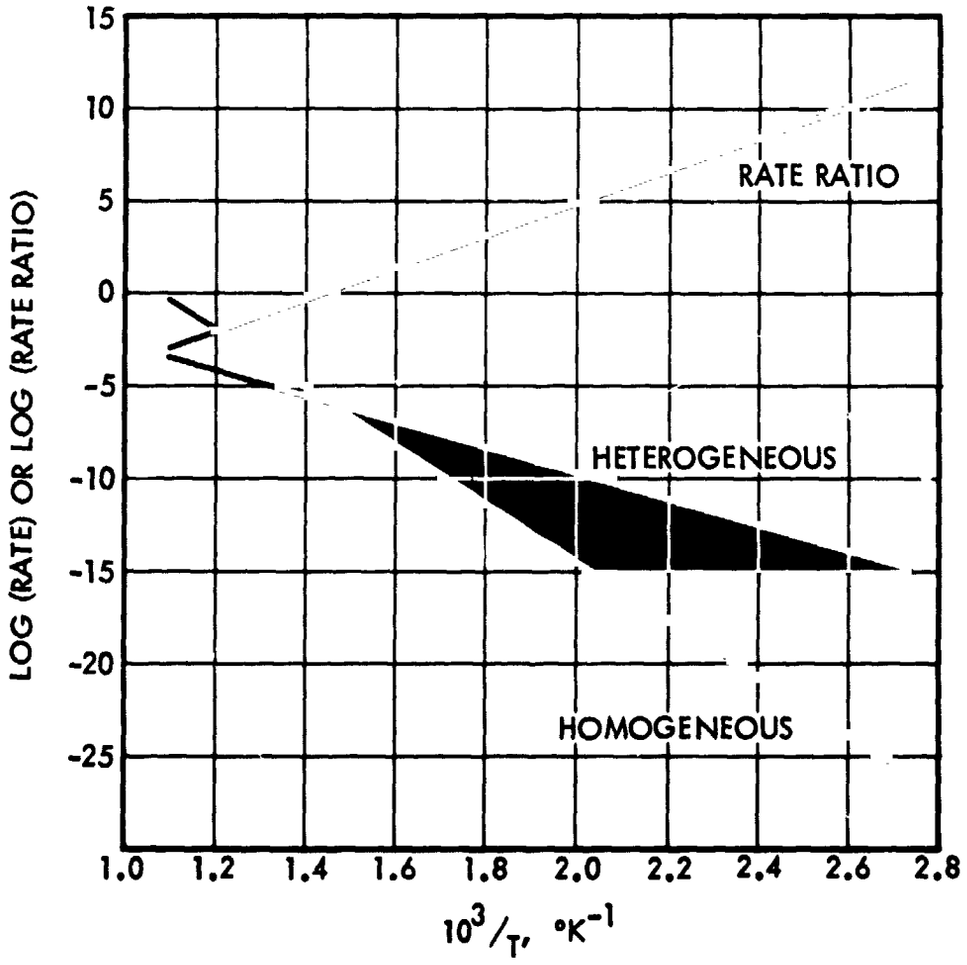

Figure 47. Comparison of Heterogeneous and Homogeneous Reaction Rates

exceeds that required by vaporization (assuming sufficient condition 2 is satisfied).

The transition from initiating decomposition through barrier establishment to true steady-state ignition is accompanied by high frequency chamber pressure oscillations at propellant injection and a final chamber pressure increases over the nominal steady-state value (overshoot). This transient period, commonly called "cook-off," occurs within a few milliseconds. This mode of electrothermal thruster operation is significant for the following reasons:

- Homogeneous decomposition kinetics are promoted in the head space with a resultant increase in delivered performance.
- The energy liberated by propellant decomposition is made available to vaporize and initiate decomposition of a substantial amount of propellant in the head space.
- Chamber pressure roughness (thrust variation) is greatly attenuated during steady-state operation and the pulsed-mode impulse-bit levels and reproducibility are better than those of other small monopropellant thrusters.

The steady-state hydrazine performance data for four thruster configurations are presented in Figure 48. The baseline thruster configuration (Figure 9) gave non-optimal hydrazine performance. Performance levels were increased by providing an additional 0.25 cm head space length. The two configurations yielding the lowest performance levels had the standard head space, but contained 180 to 400 platinum screens packed in sleeves up to 2.54 cm length. The pulsed-mode performance levels of the baseline versus the large head space configuration are shown in Figure 49. The maximum chamber temperatures at a pulse rate of one per second are indicated at each datum point. The holding temperature (810°K) and injection pressure (1.724 MN/m^2) were identical for each configuration.

Two effects are responsible for the differences in hydrazine performance presented in Figures 48 and 49. They are:

SYMBOL	CONFIGURATION
■	LARGE HEAD, 60 SCREENS, 0.5 cm PACK
▲	BASELINE, 60 SCREENS, 0.5 cm PACK
⬢	BASELINE, 180 SCREENS, 1.02 cm PACK
●	BASELINE, 400 SCREENS, 2.54 cm PACK

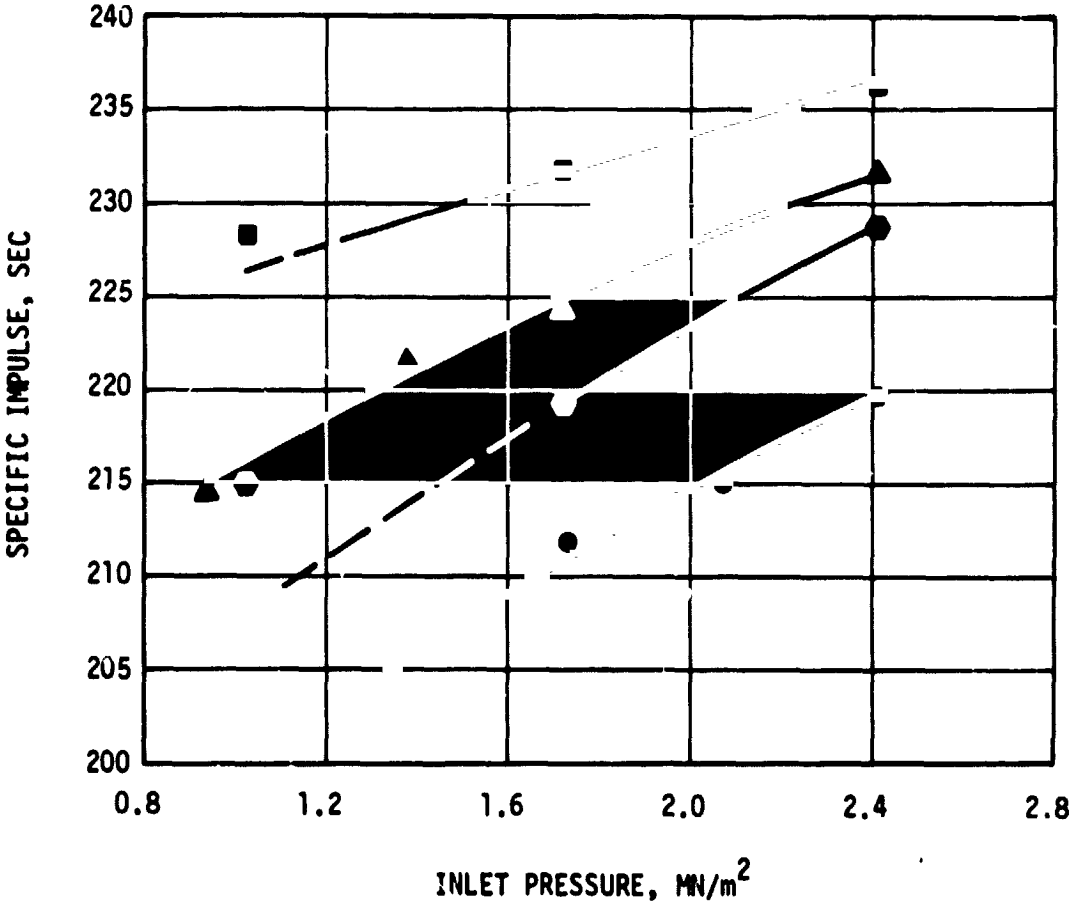

Figure 48. Configurational Hydrazine Performance Data, Steady-State

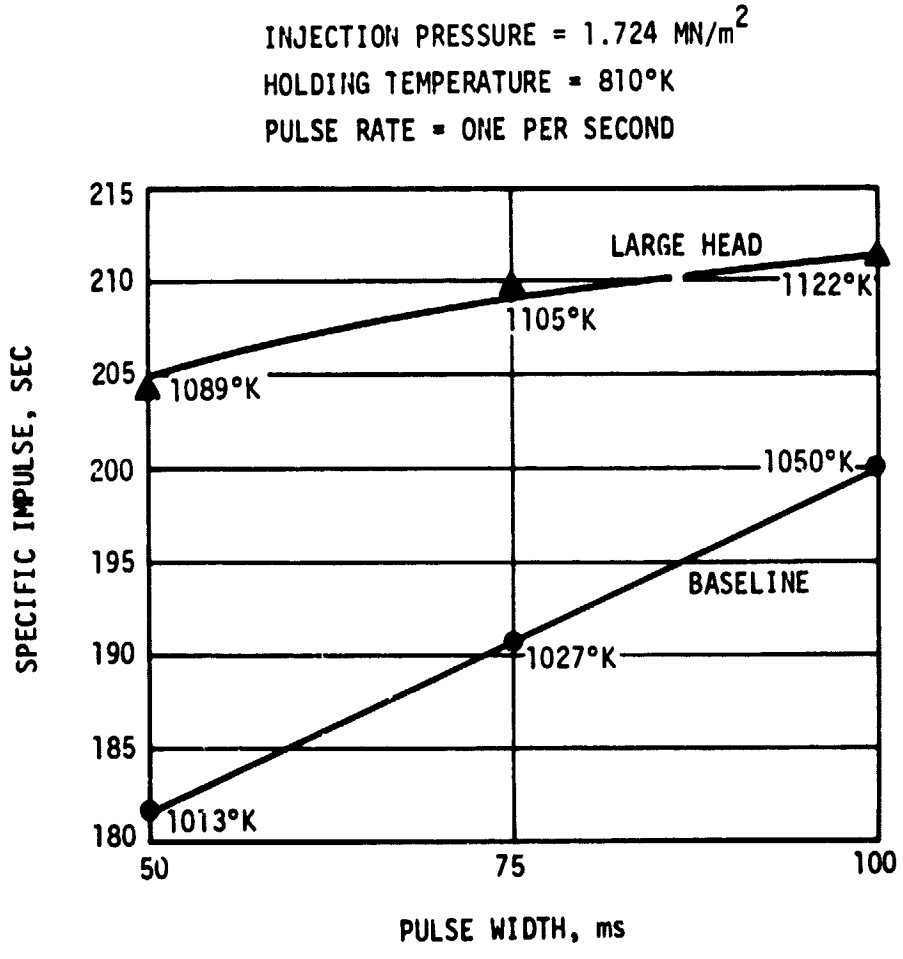

Figure 49. Configurational Hydrazine Performance Data, Pulsed-Mode

1. Homogeneous hydrazine decomposition with the subsequent heterogeneous dissociation of ammonia (large head and long screen packs).

2. Heterogeneous hydrazine decomposition which accelerates ammonia dissociation plus the subsequent heterogeneous dissociation of ammonia (baseline).

The higher performance levels of the large head space thruster were caused by promoting homogeneous hydrazine decomposition in a free volume. The fraction of ammonia produced by a pure homogeneous process is solely a function of the reaction temperature. The homogeneous dissociation of ammonia does not occur in any appreciable quantity below 1400°K[7,8] for typical thruster residence times. Ammonia dissociation in the electrothermal thruster is initiated by the platinum screens and other thrust chamber materials. A high catalytically active material such as Shell 405 will produce a 50% ammonia dissociation level at temperatures as low as 700°K.[8] A quantitative estimate of the activity level of platinum for ammonia dissociation in the electrothermal thruster geometry is not presently available. The effect of screen pack length on the endothermic dissociation of ammonia is readily seen by the thruster temperature distributions in Figure 50. The long screen pack assemblies produced a higher thrust chamber pressure drop which also promoted homogeneous decomposition kinetics in the head space. Temperature data for four configurations are compared in Table 17. The nominal difference between the head and nozzle temperatures was 30°K for the baseline (60 screen) configuration. The corresponding difference for the 400 screen thruster was 200°K. Only a small portion of the "heat loss" may be attributed to thermal conduction and radiation effects. The major portion represents heat expended to dissociate ammonia. The resultant performance loss is seen in Figure 48 and Table 17.

Decomposition in the baseline configuration was mixed-mode. The data suggested that although partial homogeneous kinetics occurred in the head space, heterogeneous decomposition was taking place within the screen pack. A higher fraction of ammonia can be dissociated when the heat liberated

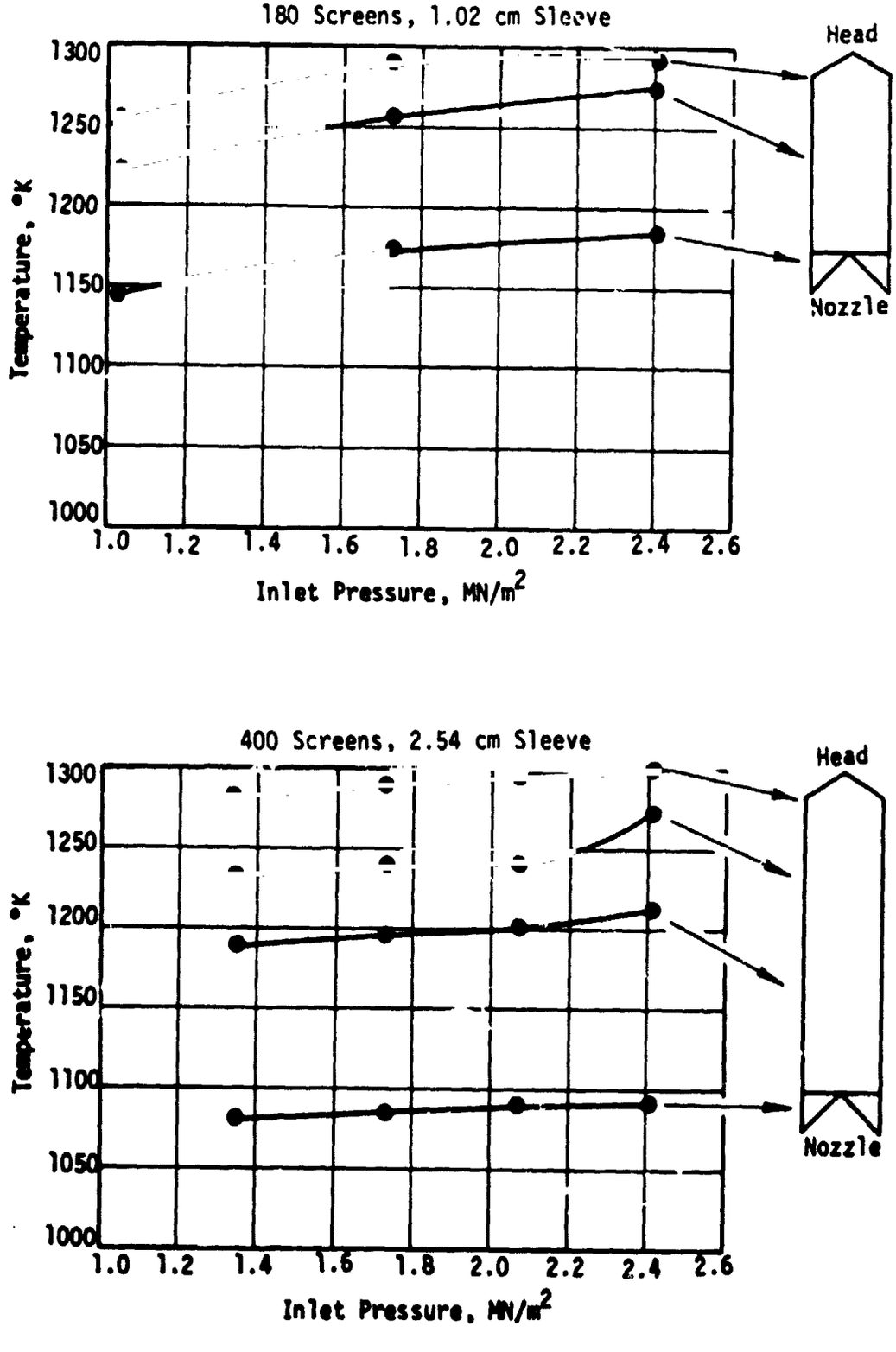

Figure 50. Thruster Temperature Distributions with Long Screen Packs

Table 17. Configurational Hydrazine Performance Data (Steady-State)

		Injection Pressure = 1.724 MN/m^2 Holding Temperature = 810°K		Temperatures, °K		
Designation	Configuration	Thrust mN	Specific Impulse Sec	Head	Middle	Nozzle
Large Head	60 screens, 0.76 cm sleeve additional 0.25 cm head space	315	232	1255	-	1222
Baseline	60 screens, 0.5 cm sleeve	314	224	1233	-	1200
Medium Pack	180 screens, 1.02 cm sleeve	267	220	1289	1255	1171
Long Pack	400 screens, 2.54 cm sleeve	259	212	1289	1217	1083

from hydrazine decomposition occurs near a catalytically active material. The localized decomposition process removes heat that would normally increase the reaction product enthalpy. The net result is macroscopically observed as a performance loss.

5.2.2 Carbonaceous Propellants

An apparent paradox is created when the thruster performance with propellants containing UDMH or MMH is compared to that of hydrazine. Thermo-chemical computations predict similar levels of performance; homogeneous reaction kinetics are faster for UDMH and MMH than for hydrazine; the formation and vaporization energies of the three propellants are similar. Steady-state operation of the carbonaceous propellants with the baseline thruster configuration resulted in "flooding." Little or no decomposition occurred during such tests. Longer thrust chamber residence times and higher thermal input levels (holding temperatures) were required to initiate and sustain decomposition of the carbonaceous propellants. This paradox is resolved by consideration of the kinetic model presented for hydrazine decomposition. Three cases are presented:

1. MMH decomposition. Worst case operating conditions were experienced (highest holding temperature).

2. Mixtures of hydrazine with MMH and UDMH. The role of hydrazine is discussed.

3. Mixture of hydrazine monopropellants (MHM). The role of ammonia is explained.

An evaluation of carbon accumulation follows discussion of the above cases.

MHM Decomposition

The "flooding" phenomena experienced with MMH during early thruster tests is represented schematically in Figure 51. The temperature-time history, Figure 51a, illustrates the general thermal degradation. The head temperature would decrease immediately at propellant valve actuation. The nozzle temperature would remain at or near the holding temperature

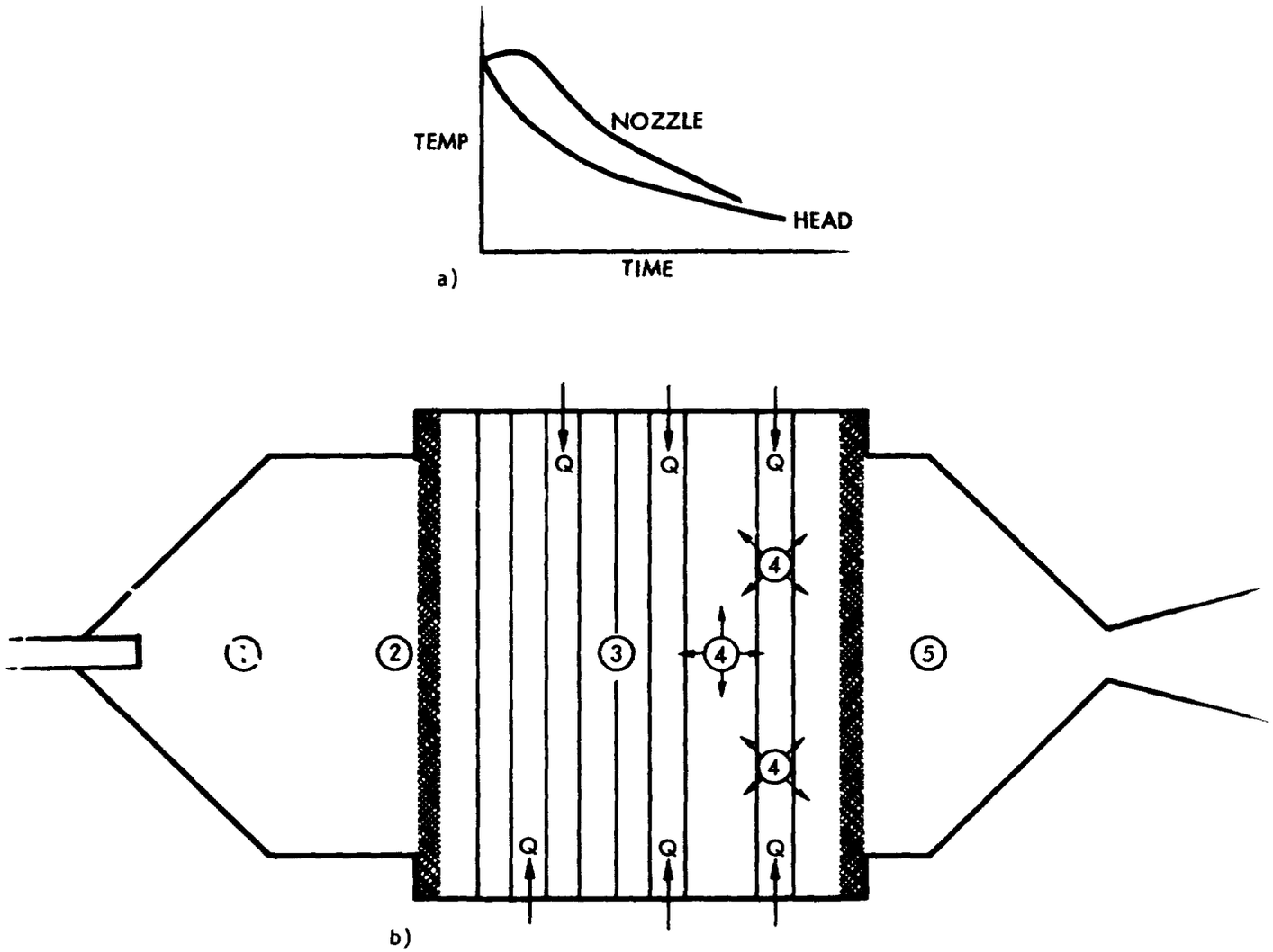

Figure 51. Flooding Characteristics During Operation With MMH

for a few seconds and then decrease. Continued operation in this mode would eventually produce liquid expulsion through the nozzle. The processes occurring within the thruster are explained below with reference to Figure 51b:

1. Propellant is admitted to the thrust chamber. A limited amount of vaporization occurs.

2. Propellant contacts the screen pack. Energy stored by the platinum screens is utilized to continue the vaporization process and supply a limited amount of heat to increase the vapor temperature.

3. The final stages of vaporization occur. The platinum screens store a limited amount of heat. Heat must be transferred from the thrust chamber walls and heaters to the propellant via the platinum screens.

4. The first parcel of vaporized propellant has its temperature elevated to a point where decomposition can occur. Decomposition is initiated thermally. The platinum screens have little effect in reducing the homogeneous activation energy. Energy released by decomposition is sufficient to raise the combustion gas enthalpies and the nozzle section temperature. The necessary condition required to establish a thermo-kinetic barrier is satisfied. However, the sufficient condition is not. Energy cannot be supplied to cause localized vaporization and decomposition.

5. Subsequent propellant entering the thrust chamber cannot be vaporized and elevated to a temperature at which the decomposition rate is appreciable. Undecomposed propellant vapor is exhausted through the nozzle. The "flooding" process is complete with the eventual expulsion of liquid through the nozzle.

Very high holding temperatures with short screen packs or reduced holding temperatures with long screen packs enabled sustained decomposition. The net effect was to elevate the propellant to a temperature where decomposition could be initiated and sustained. In the former case (high T_{hold}, short packs), the necessary thermal input was achieved in a shorter time*; whereas, a longer time was necessary at reduced holding temperature.

The MMH decomposition process with long screen packs is represented schematically in Figure 52. The temperature-time history, Figure 52a, reflects that a substantial time lapse was required to establish a thermo-kinetic barrier. The processes (Figure 52b) are:

1. Propellant injection

2. Vaporization complete. Decomposition begins but is slow. The additional screen pack length allows substantial propellant heating and the main decomposition front occurs towards the nozzle end. The nozzle temperature rises while the head temperature continues to decay.

3, 4. Heat liberated from decomposition is transferred back through the screen pack (3) and along the thruster walls (4). The thermo-kinetic barrier is established in the lower portion of the screen pack. Heat transferred by the conduction processes (3) and (4) is sluggish and inefficient.

5. The thermo-kinetic barrier moves towards the thruster's head end as more heat is made available for vaporization by the conduction process. An increase in head temperature is accompanied by a slight decrease in nozzle temperature. The true steady-state condition, i.e.,

*Time in the sense of this discussion is implied to mean dwell, contact, residence, or reactor time.

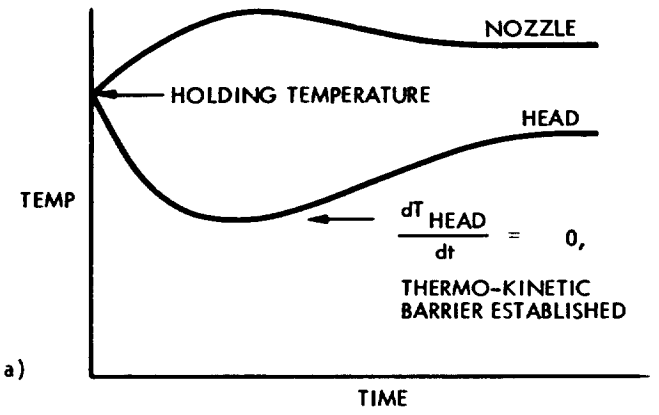

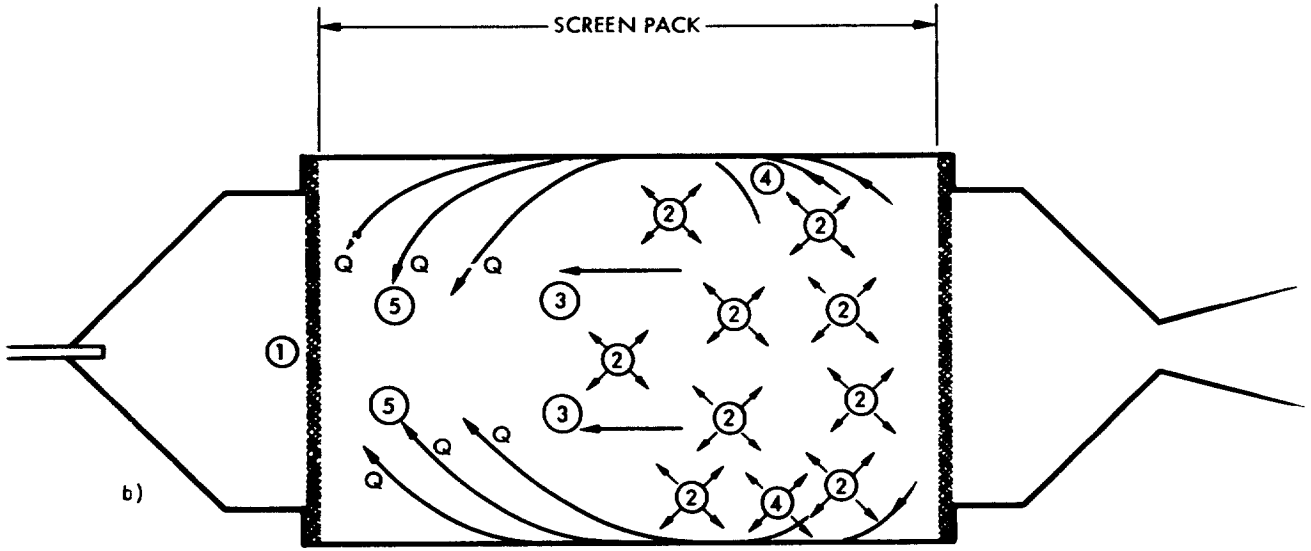

Figure 52. MMH Decomposition Process With Long Screen Pack

$T_{noz} > T_{head}$, suggested that the head space, which is critical for operation with hydrazine is not nearly as effective for operation with MMH.

Mixtures of Hydrazine with MMH and UDMH

The net effect of adding hydrazine to MMH or UDMH is to allow a decrease in the screen pack length. Hydrazine decomposes more readily than either MMH or UDMH. The heat released by hydrazine decomposition is made available to vaporize and heat the carbonaceous component without relying on extensive and inefficient heat transfer by conduction. The internal "heat source" decreases the physical separation between the vaporization and decomposition fronts, reduces the holding power, and significantly decreases the time required to establish a thermokinetic barrier.

Tests with Aerozine-50 (50% N_2H_4-50% UDMH) and 50% N_2H_4-50% MMH established that the catalytic activity of platinum was higher for UDMH than for MMH. Lower holding temperatures and shorter screen pack assemblies were possible with Aerozine-50.

Mixture of Hydrazine Monopropellants (MHM)

Ammonia in the MHM mixture depresses the freezing point of hydrazine mixtures and also reduces the internal "heat source" effect (35 percent versus 50 percent hydrazine). The real advantage is in suppressing carbon deposition (discussed next).

Carbon Accumulation

A summary of the thrust chamber regions where carbon deposited is presented in Table 18 for all carbonaceous propellants tested. The qualitative observations indicated that the Haynes 25 retaining screen had a very high catalytic effect in dissociating the carbonaceous gas species. The physical form of carbon buildup in the surfaces of the nozzle inlet section raised questions as to the mechanism of formation. It is doubtful that pyrolysis of the decomposition gases could account for the buildup. The logical source was the high velocity ablation of

Table 18. Regions of Carbon Deposition (Steady-State)

Propellant	Injector (Haynes 25)	Head Space	Screen Platinum Screens	Pack Haynes 25 Retainer	Nozzle Inlet Section	Throat	Nozzle
MHM	None	None	None	Very Slight	None	None	None
50% N_2H_4-50% MMH	None	Slight	None	Extensive	Slight	None	None
MMH	None[1]	None	None[2]	Moderate	Slight	None	None
Aerozine-50	None	Slight	Moderate[2]	Extensive	Moderate	None	None

NOTES: (1) One injector was plugged during off design pulsed-mode operation. Holding temperature 1143°K. Injection pressure 0.31 MN/m^2.

(2) Only outer periphery affected.

semicoherent graphite deposits previously formed on the Haynes 25 retaining screen. This process is illustrated in Figure 53. All Haynes 25 surfaces in the nozzle section have the same initial catalytic activity for carbon-bearing molecules. A very thin layer of carbon deposits on the nozzle-inlet surfaces. The catalytic activity of those surfaces ceases (Figure 53a). Carbon deposits non-uniformly on the Haynes 25 retaining screen. The buildup of an initial layer is faster on the side where a stagnation region is created by the high velocity decomposition gases (rear side facing the nozzle). The front side of the Haynes 25 screen remains catalytically active. Gas molecules are catalyzed by that surface but pyrolysis is not complete. Carbon accumulates toward the rear side (Figure 53b). The powdery carbon deposits are ablated away by the decomposition gases. Much of the carbon swept away is intercepted by the nozzle inlet section. Carbon does not accumulate in the nozzle throat due to the very high gas velocities.

Carbon deposition following operation with the MHM blend was minimal, even on the Haynes 25 retaining screen. The addition of ammonia plays an important role in suppressing carbon formation. The tendency of a decomposition gas mixture to approach equilibrium is severely inhibited. The kinetic mechanism is not well understood. However, it is suspected that an intermediate step which forms gases that are easily pyrolyzed takes place only to a limited degree.

5.2.3 Hydrazine-Hydrazine Azide

Kinetic data on the decomposition characteristics of azide mixtures are not available. Rough operational characteristics increase with an increase in the hydrazine azide content. Stable operation with the azide blend was achieved by empirical means. Two phenomena were observed when operating with the baseline configuration: low frequency spiking and high frequency instability. These effects were absent after screen pack modifications rendered the head space less effective in promoting decomposition. Slightly higher holding temperatures were required to reduce rough start characteristics (923°K for the azide blend versus 810°K for

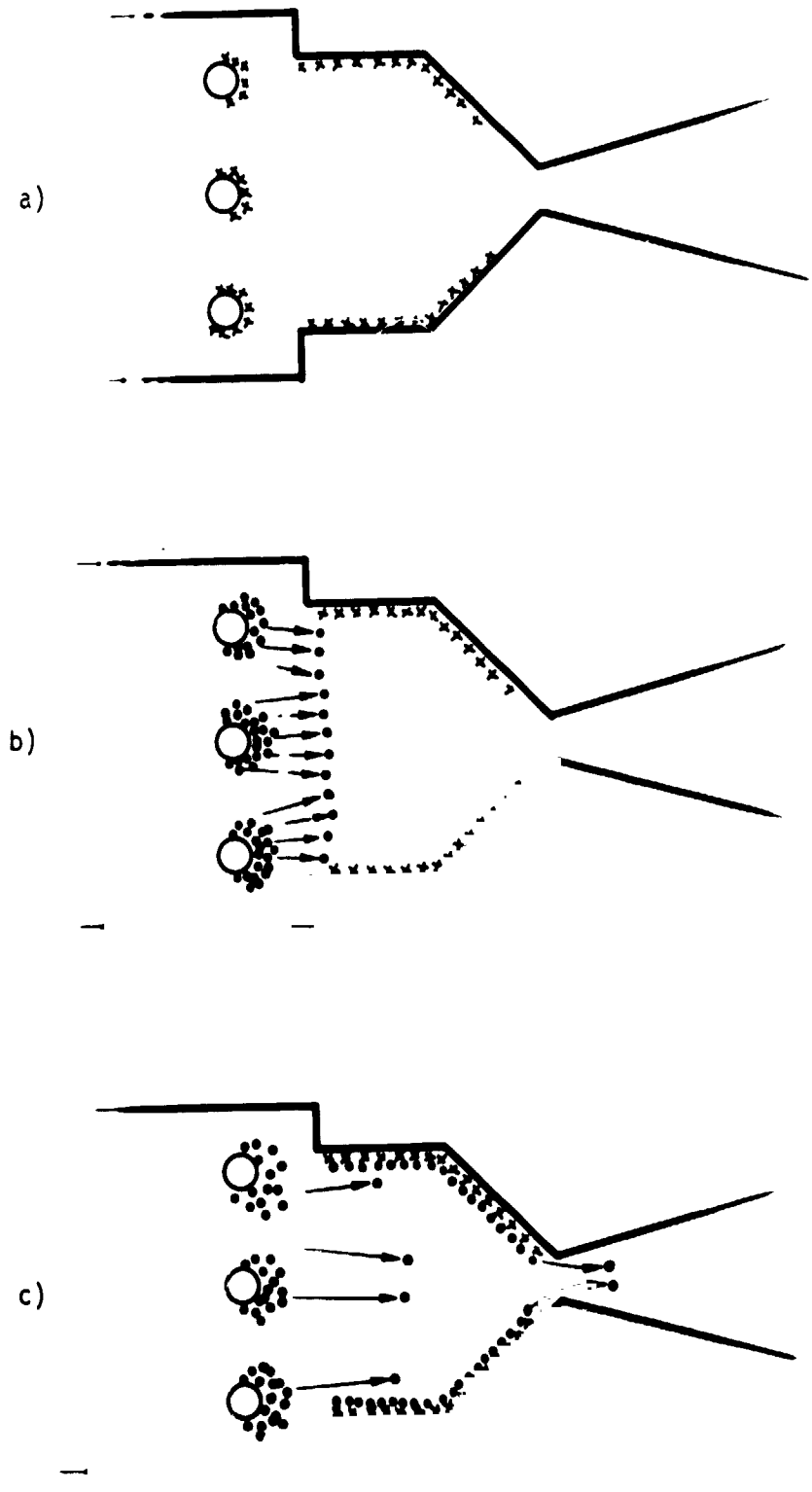

Figure 53. Mechanism of Carbon Deposition on Nozzle Inlet Section

hydrazine). These factors indicated that the vaporization and decompcsition processes were distributed non-uniformly within the thruster. The hydrazine component of the mixture has a tendency to vaporize before the azide component. The hydrazine azide content is thus concentrated above the initial value of 23 percent. Complete vaporization of the remaining high-azide-content liquid occurs further into the screen pack. Subsequent decomposition of the hydrazine azide is abnormally rapid which gives rise to high frequency instabilities. A periodic coupling of these instabilities creates large, low frequency chamber pressure fluctuations.

The overall decomposition process is bimodal. Hydrazine decomposition constitutes one mode and occurs in a normal manner. The other mode is the unstable decomposition of hydrazine azide. Rough operation is caused by the oscillatory benavior of the unstable mode. Thruster screen pack modifications reduced the bimodal operating characteristics by reducing the extent of hydrazine vaporization in the head space.

6.0 RECOMMENDATIONS

6.1 PROPELLANT SELECTION

Three monopropellant categories warrant advanced development with the electrothermal thruster concept. These monopropellants are listed below:

1. TRW-formulated mixture of hydrazine monopropellants (MHM)
2. 77 percent hydrazine - 23 percent hydrazine azide
3. Monomethylhydrazine and binary mixtures of hydrazine and monomethylhydrazine.

The performance levels of Aerozine-50 are very adequate, but the freezing point reduction (7.1°K) relative to hydrazine does not appear to justify advanced development when the minimum freezing point reduction of the above three monopropellants is 19°K.

All three propellants are suitable for operation with the electrothermal thruster concept. The highly-contaminated azide blend used in the feasibility demonstration gave higher performance than hydrazine. TRW feels that the electrothermal thruster concept offers a current solution to problems encountered with high performance azide blends and catalytic thrusters. The carbonaceous propellants have adequate performance, very low freezing points, and are not compatible with catalytic thrusters.

6.2 THRUSTER DESIGN

The design criteria for the advanced monopropellant electrothermal thruster is dictated by flight application requirements. The design should have:

1. Small physical size and low thermal mass to minimize power consumption and thermal transient times
2. High impulse-bit reproducibility
3. High component reliability and design simplicity.

TRW has demonstrated the ability to design a flightworthy electrothermal hydrazine thruster (EHT). The design, performance and reliability of the EHT is currently state-of-the-art. The knowledge gained during EHT development combined with that of the present study described herein places TRW in a unique position to evaluate the flight applicability of electrothermal thrusters with low freezing point monopropellants.

The modular monopropellant demonstration thruster (Figure 9) serves as a reference point for the design of a flightworthy thruster.

6.2.1 Alternate Injection Concepts

A sound injector design is the first critical step in a liquid propellant thruster. The requirement for both pulsed-mode and steady-state operation places additional design constraints. The current TRW electrothermal injector design meets the pulsed-mode and steady-state requirements by:

1. Providing the necessary pressure drop to limit the instantaneous flow rate immediately after valve opening
2. Decoupling the supply system from chamber pressure oscillations
3. Providing a small dribble volume
4. Preventing two-phase flow conditions which may result in propellant decomposition in the injector.

Areas that require improvement for operation with the carbonaceous propellants are:

1. Methods to increase propellant distribution and vaporization as soon as the propellant enters the thrust chamber
2. Alternate injector materials having a lower catalytic activity than Haynes 25.

The injector cannot be designed to produce a "shower-head" flow pattern in the thrust chamber due to the small mass flow rates. The thrust chamber heat transfer characteristics have not yet allowed

sufficient hot gas recirculation to break up the propellant stream. The propellant injection velocity cannot be lowered by an increase in injector diameter without upsetting the delicate heat transfer balance designed to eliminate two-phase flow conditions. An energy balance on the incoming propellant stream indicates which parameters must be adjusted to render the stream unstable, i.e., to effect breakup. A critical velocity, v^*, below which the propellant stream will be unstable is obtained by a balance between the kinetic and surface energies of the propellant stream. The kinetic energy per unit length of a circular stream of diameter d, and density ρ, is:

$$K.E. = \frac{1}{2} mv^2 = \frac{\rho \pi d^2}{8} v^2 \tag{8}$$

The surface energy per unit length is:

$$S.E. = \sigma A_s = \sigma \pi d \tag{9}$$

where A_s is the surface area and σ is the surface tension. The critical velocity, v^*, is obtained by equating the kinetic energy to the surface energy:

$$v^* = \left(\frac{8\sigma}{\rho d}\right)^{1/2} \tag{10}$$

The stream is unstable at velocities lower than that predicted by Equation (10). Hot gas recirculation influences Equation (10) by lowering the surface tension proportionally more than the associated decrease in density. A change in the injector aspect ratio (i.e., elliptical or convoluted shapes) can reduce the breakup velocity by increasing the effective diameter at the point of injection.

Alternate injector materials should be evaluated for long term pulsed-mode operation. Haynes 25 has proven adequate for hydrazine operation, but its catalytic activity may promote carbon deposition during "boil-off" conditions between pulses.

The Haynes 25 injector must be replaced for long term operation with the hydrazine-hydrazine azide propellant. Haynes 25 is adequate for steady-state operation where the injector remains at a relatively cool 520°K. However, pulsed-mode operation precludes the use of Haynes 25. A small amount of propellant remains in the injector after valve closure. Hydrazine vaporization leaves a high-azide-content liquid residue on the injector surface. The rate of corrosive attack by the liquid is orders of magnitude higher than that corresponding to a normal gas-metal reaction. Noble metal alloys are the logical material replacement for the Haynes 25 injector.

6.2.2 Thrust Chamber and Nozzle Section Variables

Only minor modifications of the demonstration thruster are required for long term operation with the azide blend. The head space and screen pack geometry requirements for stable operation were determined during the feasibility study. The Haynes 25 retaining screen will be replaced by iridium or by a high-iridium-content noble metal alloy. Iridium is highly resistant to attack by nitrogen and hydrogen environments. The stress/rupture properties at maximum possible operating temperatures (<1370°K) are superior to those of tungsten, molybdenum, tantalum, and Haynes 25.[9] The tensile strength of iridium is 324 MN/m^2 at 1370°K. This compares with tensile strengths of 400 MN/m^2 for tungsten and 240 MN/m^2 for molydenum at the same temperature.[9,10] Thruster body material changes do not appear necessary. The thruster body is not as susceptible to the nitriding environment as the injector and the Haynes 25 retaining screen. Negligible thruster body corrosion occurred during feasibility testing with the azide blend.

The primary thrust chamber design goal for operation with the carbonaceous propellants is to reduce the holding power requirements to an acceptable level. A reduction in the characteristic chamber length, L^* (ratio of chamber volume to throat area), will greatly increase the pulsed-mode performance. The inefficient heat transfer characteristics encountered during steady-state operation must be eliminated to effect significant L^* reductions. Composite screen pack assemblies of varying

materials and densities to initiate decomposition early in the flow process should be investigated. A desirable composite assembly should consist of catalytically active initiation screens near the injector with high conductivity material sandwiched between the initiator screens and a non-catalytic structural support screen. A true composite screen pack assembly combined with alternate injection techniques should produce a viable solution to steady-state requirements without sacrificing pulsed-mode performance.

Nozzle section variables such as inlet and throat sections contours will be easily evaluated using the modular design. A full evaluation of carbon deposition and ablation behavior in the nozzle section may be investigated at low cost.

6.3 THRUSTER FABRICATION

Fabrication techniques for joining all base-metal alloy components are fully developed with no problem areas. Techniques for joining noble to base-metal components require minor refinement. A braze evaluation program was initiated during the later stages of EHT development. A Pt-10 Ir injector exhibited grain boundary embrittlement with a loss of ductility after a two cycle braze to Haynes 25. Silicon was identified as the major contaminant. The cobalt used in manufacturing Haynes 25 contains silicon as a contaminant. It is not anticipated that electron beam welding will eliminate silicon contamination. Three alternate fabrication methods can be investigated at minimal cost:

1. Silicon-free "Haynes 25" made from isostatic powder compaction and thermomechanical processing. A Pt-10 Ir injector is brazed using a cobalt-palladium alloy (Palco).
2. Standard Haynes. Zirconia (ZrO_2) stabilized platinum injector brazed with Palco.
3. Silicon-free "Haynes 25" - zirconia stabilized platinum injector.

The zirconia stabilized platinum is attractive by virtue of a small grain structure stabilized by a dispersion of sub-micron ZrO_2 particles. TRW has produced numerous alloys by powder metallurgical techniques and no development effort is involved in manufacturing a bar from which to machine thrust chamber parts.

TRW is currently investigating an alternate thermal insulation to WRP-X. The new insulation, designated ZYF Zircar (Union Carbide), has numerous advantages over WRP-X. Type ZYF is composed of yttria (Y_2O_3) stabilized zirconia and has the following properties:

1. Zero shrinkage up to 1720°K. WRP-X has a linear shrinkage of 4 percent after 24 hours at 1370°K
2. Vapor pressure less than 10^{-9} N/m^2 at 1620°K
3. Thermal conductivity one-half that of WRP-X
4. ZYF Zircar easily conforms to irregular surfaces and does not require auxiliary molding fixtures.

This insulation will be evaluated for the flight model design.

6.4 THRUSTER CHARACTERIZATION TESTS

Each configurational prototype should be performance tested to determine the effect of parameter variations such as

a) Injector geometry and propellant dispersal

b) Injector material and fabrication techniques

c) Head space

d) Screen pack geometry and materials - packing density and characteristic chamber length

e) Thruster geometry on holding temperature

Extensive thruster exhaust gas measurements should be performed during all test phases. A quadrapole, residual gas analyzer (RGA, Electronic Associates, Inc.) is used to continuously monitor the exhaust gas composition. The analyzer head is enclosed in a separate and portable vacuum

system. The minimum detectable partial pressure is approximately 10^{-13}. The RGA output displays a spectrum showing mass peak heights for various mass numbers. Gas decomposition in the analyzer head is corrected by quantifying the "cracking-pattern" of pure gases.

7.0 CONCLUSIONS

Four propellants other than MIL-grade hydrazine were identified that do not require an excessive trade-off between freezing point and performance and are not compatible for use with the more conventional catalytic type thrusters. These propellants are 76% hydrazine - 24% hydrazine azide, Aerozine-50, 50% hydrazine - 50% monomethylhydrazine, and a TRW-formulated mixture of 35% hydrazine - 50% monomethylhydrazine - 15% ammonia.

A modular, three piece thruster designed and fabricated for use with MIL-grade hydrazine was ideally suited for the rapid performance evaluation of the above mentioned propellants.

The electrothermal thruster concept is suitable for operation with hydrazine azide mixtures and propellants containing carbonaceous species. Steady-state specific impulse levels exceeded 200 sec for all propellants tested. The pulsed-mode program goal of 175 sec specific impulse was exceeded by the azide blend for pulse widths greater than 50 ms and was met by the carbonaceous propellants for pulse widths greater than 100 ms. Specific thruster modifications will deliver 175 sec specific impulse for the carbonaceous propellants at pulse widths as low as 50 ms.

The initiation of decomposition was different for hydrazine and the carbonaceous propellants. Hydrazine decomposition was initiated by the combined effects of thermal excitation and catalysis, whereas decomposition of the carbonaceous propellants was initiated by thermal excitation. A complex heat transfer problem existed with the original thruster geometry. Vaporization and decomposition fronts were not located in the same proximity. Longer screen pack assemblies were required to satisfy the heat transfer conditions necessary for sustained steady-state operation. Thruster design changes are possible that will eliminate the need for long thrust chamber lengths. Steady-state operation can be maintained at lower holding power levels. An increase in pulsed-mode performance will be realized with redesigned thruster configurations.

The performance levels of hydrazine thrusters are increased by promoting homogeneous, gas-phase decomposition kinetics in a free volume head space. The endothermic dissociation of ammonia is suppressed in the homogeneous decomposition mode. More thermal energy is available to increase the exhaust gas kinetic energy.

The feasibility of operating small thrust level electrothermal thrusters with monopropellants other than MIL-grade hydrazine has been conclusively demonstrated. An advanced development phase is warranted to fully realize the potential of applying the electrothermal thruster concept to low freezing point monopropellants.

8.0 NEW TECHNOLOGY

The electrothermal thruster concept has been demonstrated to be feasible for operation with propellants other than MIL-grade hydrazine. The modular design of the monopropellant demonstration thruster resulted in substantial fabrication cost savings and enhanced technical efforts during the Evaluation Test Program Phase. The design is novel in electrothermal hydrazine thruster technology.

A secondary task of the Evaluation Test Program was to obtain baseline hydrazine performance data for all new thruster configurations. One thruster configuration provided substantial performance increases over previous electrothermal hydrazine thrusters. An analysis of the data generated from the several configurations yielded an increased level of understanding the hydrazine decomposition process. The model presented to describe the electrothermal hydrazine decomposition process may be applied to other technology areas. These areas include catalytic hydrazine thruster and gas generator technologies.

9.0 REFERENCES

1. "Monopropellant Hydrazine Resistojet, Engineering Model Fabrication and Test Task Summary Report." TRW Systems Group, Redondo Beach, California, Report 20266-6024-RO-00, March 1973.

2. "Propellant, Hydrazine." Military Specification MIL-P-26536C, May 1969.

3. "Cleaning and Packing of Fluid System Components." TRW Systems Group, Redondo Beach, California, Specification PR2-2, Table 1, Level 2.

4. "Propellant, Hydrazine-uns-Dimethylhydrazine (50% N_2H_4-50% UDMH)." Military Specification MIL-P-27402B.

5. "Propellant, Monomethylhydrazine." Military Specification MIL-P-27404A, Amendment 2, June 1970.

6. Benson, S. W. and H. E. O'Neal. Kinetic Data on Gas Phase Unimolecular Reactions, National Bureau of Standards Publication NSRDS-NBS 21, Washington, D.C., 1970.

7. Eberstein, I. J. "The Gas Phase Decomposition of Hydrazine Propellants," Department of Aerospace and Mechanical Sciences, Princeton University, New Jersey, Technical Report No. 708, 1964.

8. Martignoni, P., et al. "The Thermal and Catalytic Decomposition of Ammonia and Hydrazine," Army Propulsion Laboratory and Center, U.S. Army Missile Command, Redstone Arsenal, Alabama, Report No. RK-TR-70-2, January 1970.

9. Semchyshen, M. and J. J. Harwood (Eds.). Refractory Metals and Alloys, Interscience, New York, 1961.

10. Douglass, R. W. and R. J. Jaffee. "Elevated-Temperature Properties of Rhodium, Iridium and Ruthenium," Proc. ASTM, Vol. 62, p. 627, 1962.

APPENDIX A

A.1 SHOCK SENSITIVITY

The two standard methods of determining shock sensitivity are the drop-weight and JANNAF card gap tests.

The drop-weight test for liquids assumes that an explosion is initiated by the adiabatic compression of the gas volume present with the sample. A small amount (0.030 cc) of propellant is enclosed in a 0.060 cc cavity formed by a steel cup, an elastic ring and a steel diaphragm. A piston rests on the diaphragm and contains a vent hole which is blocked by the steel diaphragm. A weight is dropped onto the piston. Explosion is indicated by a ruptured diaphragm and loud noise. The sensitivity value for a given sample is the potential energy (height x weight) at which the probability of explosion is fifty percent.

The standard JANNAF card gap test assembly consists of a 25.4 mm diameter by 76.2 mm long schedule 40 steel cup with a 0.051 mm polyethylene film mounted in the bottom of a cardboard support assembly. A 50 gram tetryl pellet is placed below and touching the polyethylene bottom; a blasting cap is placed below and touching the tetryl pellet. The test liquid is placed in the cup and a 101.6 mm x 101.6 mm x 9.5 mm cold-rolled mild steel plate is placed, unattached, atop the cup. The tetryl charge is detonated by activation of the blasting cap. Test liquid detonation due to the hydrodynamic shock from the tetryl charge produces a 25.4 mm diameter hole in the mild steel witness plate. No plate damage is observed with non-detonable materials (e.g. water). Results are expressed as the number of cellulose acetate cards that must be placed between the tetryl donor charge and the cup bottom such that the donor shock will be sufficiently attenuated to give a 50% statistical chance of test material detonation.

A.2 DETONATION PROPAGATION

Standard ICRPG detonation propagation tests are performed by containing the test liquid in a section of 6.35 mm 347 stainless steel tubing having a 0.89 mm wall thickness. The tube fits into a reservoir through

a 25.4 mm diameter opening. A 50-gram pentolite booster is used with a number 8 electric blasting cap to detonate the reservoir fluid. The criterion for a positive test is the complete destruction of the 6.35 mm acceptor tube.

A.3 THERMAL STABILITY

Propellant thermal stability is measured by the standard ICRPG thermal stability test and by differential scanning calorimetric methods. Results of the standard tests are regarded as practical values and the differential scanning calorimetric test results are considered as limiting values. Only the standard ICRPG test will be described.

The ICRPG test fixture consists of a stainless steel cylinder which has a 5.59 mm diameter and is 38.1 mm long. The bottom is closed and a compression-fitted shielded thermocouple is employed. The fixture is charged with 0.5 cc of propellant and closed at the top with a 0.076 mm thick SS diaphragm. The assembly is then placed in a bath which is heated at a constant rate of 10°K/min. A second thermocouple and an X-Y recorder are connected with the sample thermocouple so as to yield a plot of differential temperature (sample temperature minus bath temperature) versus bath temperature. Exothermic reactions appear as positive peaks, while endothermic reactions appear as negative peaks. The results are reported in terms of the temperature at which significant thermal activity is observed.

Long term thermal storability is measured by the rate of gas evolution over a specified period of time. Results are usually given for a particular material in units of psi/day.

A.4 TOXICITY

Exposures are expressed as concentration and exposure duration for exposure to vapors in the air; and as dosages referred to as a fraction of body weight for ingestion. In tests on animals, the lethal dosage is defined as that which kills 50 percent of the test subjects. The dosage is expressed as LD_{50} in milligrams of substance per kilogram of body

weight (mg/kg). The concentration of vapors in air is expressed in terms of parts of vapor per million parts of air (ppm).

A.5 MATERIALS COMPATIBILITY

The compatibility classification is based on the rating scheme recommended by the Defense Metals Information Center. Table A1 presents the rating scheme used in this report.

Table A1. Materials Compatibility Classification

Class	Corrosion Rate mm/Year	Decomposition	Usage Limitations
A	Less than 0.0254	None	No limitations. Typical use involves constant contact with the fuel. Metals can be considered for long term storage.
B	0.0254 to 0.127	Slight degradation over a period of time.	Restricted to transient or limited contact. Not recommended for long term storage.
C	0.127 to 1.27	Limited decomposition may occur on contact.	May be used in areas where brief contact can occur. Not recommended for use where contact occurs regularly.
D	More than 1.27	Considerable decomposition may occur. May cause ignition or explosion.	Metals are totally unsuitable for use under any conditions. Contact may create a hazardous condition.

APPENDIX B

A complete set of monopropellant demonstration thruster drawings is included in this appendix.

(1)	Gasket	X412586-1
(1)	Gasket-Screen Pack	X412582-1
(1)	Body, Monopropellant Demonstration Thruster	X412581-1
(1)	Sleeve-Threaded, Monopropellant Demonstration Thruster	X412579-1
(1)	Nozzle, Monopropellant Demonstration Thruster	X412578-1
(1)	Tube, Barrier-EHT	X409236-1
(60)	Screen	X412580-15
(1)	Screen	X412580-14
(1)	Sleeve	X412580-13
(1)	Tube	X412580-12
(1)	Tube	X412580-11
(1)	Plate, Seal-EHT	X409383-1
(1)	Seal, Tube-EHT	X410563-1
(1)	Sleeve, Injector	X409240-9

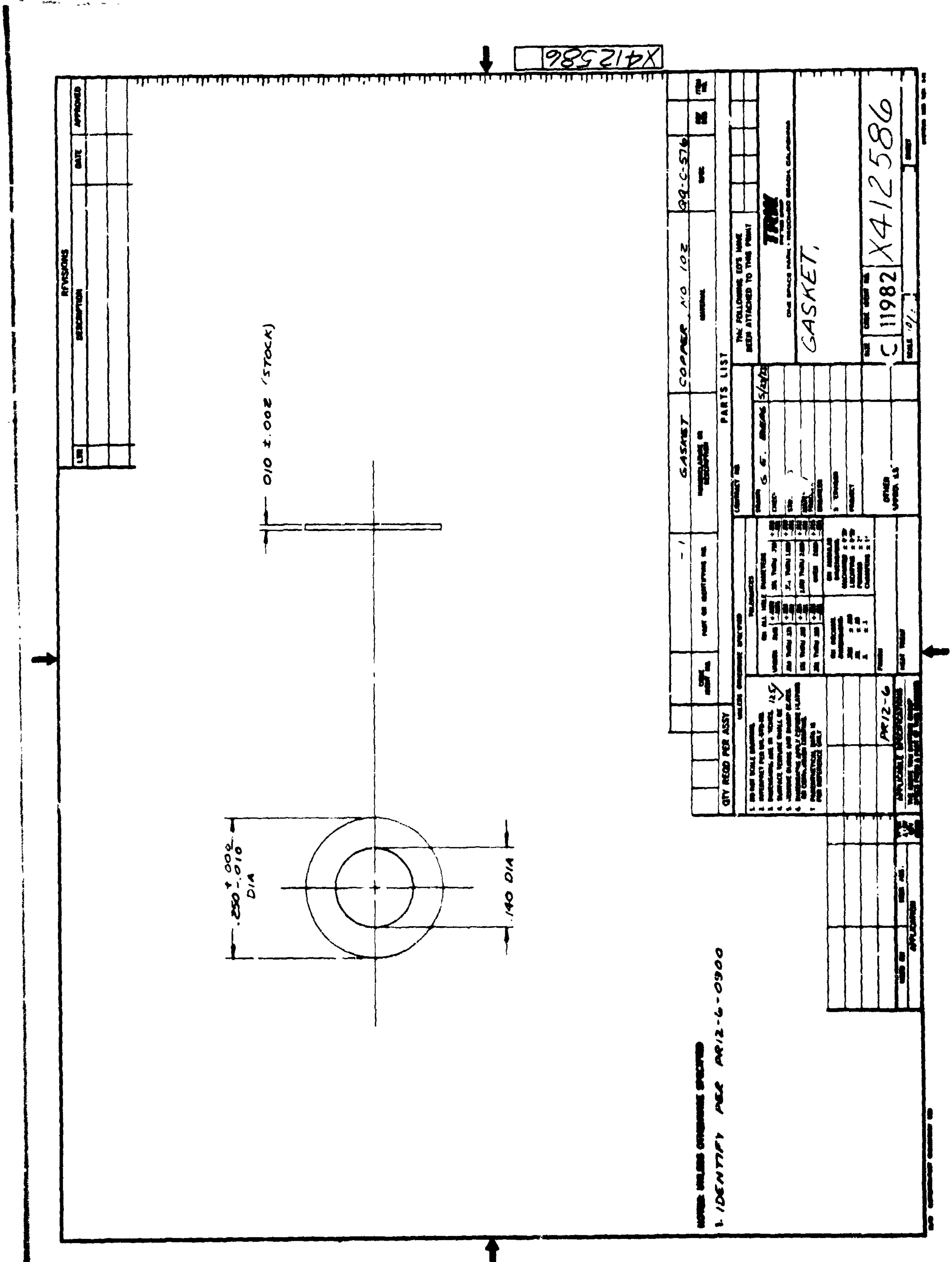
X412586
REVISIONS
DESCRIPTION
DATE
APPROVED
.010 ±.002 (STOCK)
.250 +.002 -.010 DIA
.140 DIA
NOTES: UNLESS OTHERWISE SPECIFIED
1. IDENTIFY PER PR12-6-0900
GASKET
COPPER NO 102
QQ-C-576
PARTS LIST
QTY REQD PER ASSY
PR12-6
THE FOLLOWING EO'S HAVE BEEN ATTACHED TO THIS PRINT
TRW
GASKET,
C
11982
X412586

REVISIONS			
LTR	DESCRIPTION	DATE	APPROVED

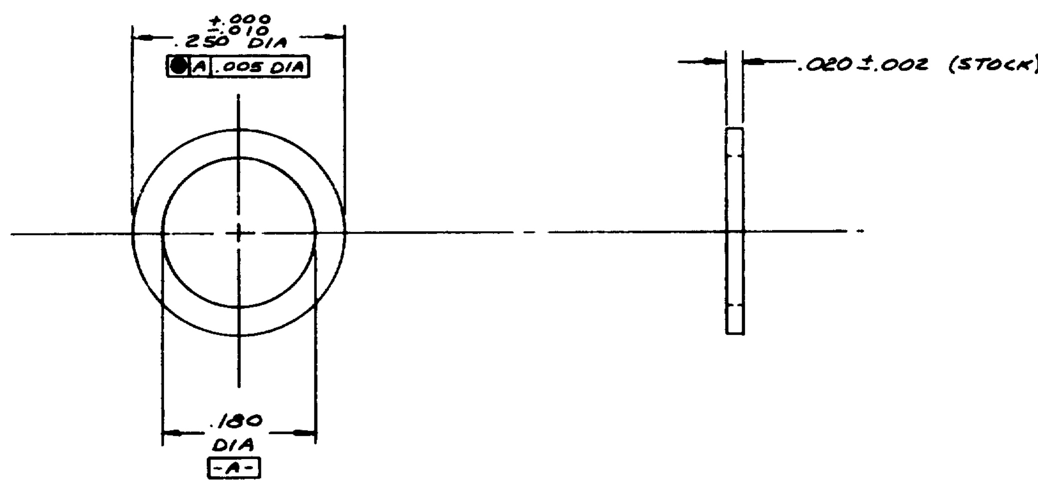

NOTES: UNLESS OTHERWISE SPECIFIED

1. IDENTIFY PER PR12-6-0900

CODE IDENT NO.	PART OR IDENTIFYING NO.	NOMENCLATURE OR DESCRIPTION	MATERIAL	SPEC
	-1	GASKET	COPPER, NO. 102	QQ-C-576

QTY REQD PER ASSY — PARTS LIST

UNLESS OTHERWISE SPECIFIED

1. DO NOT SCALE DRAWING.
2. INTERPRET PER MIL-STD-100.
3. DIMENSIONS ARE IN INCHES.
4. SURFACE TEXTURE SHALL BE 125
5. REMOVE BURRS AND SHARP EDGES.
6. DIMENSIONS APPLY BEFORE PLATING OR CONVERSION COATING.
7. PARENTHETICAL DATA IS FOR REFERENCE ONLY.

TOLERANCES — ON ALL HOLE DIAMETERS; ON DECIMAL DIMENSIONS: .XXX ± .010, .XX ± .03, .X ± .1; ON ANGULAR DIMENSIONS: MACHINED ± 0°30', LOCATING ± 0°30', FORMED ± 2°, CHAMFERS ± 5°

FINISH

HEAT TREAT

APPLICABLE SPECIFICATIONS: PR12-6

THE ABOVE TRW SYSTEMS GROUP SPECS FORM A PART OF THIS DRAWING

APPLICATION: USED ON / NEXT ASSY

CONTRACT NO.

DRAWN G. E. BEK 5/21/75

CHECKED / STRUCTURES / MATERIAL/PROCESS ENGINEER / SUPERVISOR / PROJECT / OTHER APPROVALS

THE FOLLOWING ED'S HAVE BEEN ATTACHED TO THIS PRINT

TRW SYSTEMS GROUP — ONE SPACE PARK • REDONDO BEACH, CALIFORNIA

GASKET - SCREEN PACK,

SIZE C — CODE IDENT NO. 11982 — X412582

SCALE 10/1 — SHEET

X412582

REVISIONS			
LTR	DESCRIPTION	DATE	APPROVED

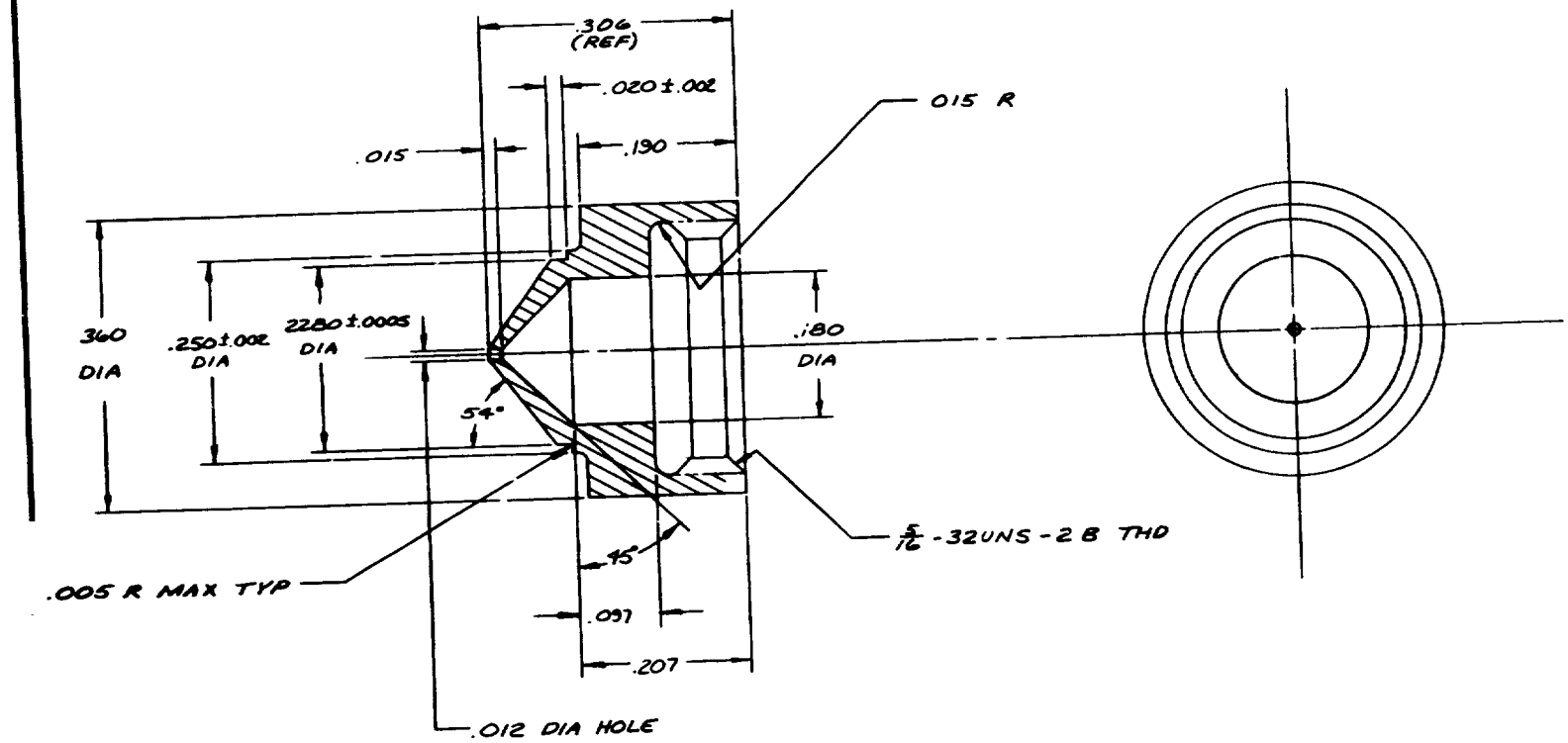

X412581

NOTES: UNLESS OTHERWISE SPECIFIED

1. IDENTIFY PER PR12-G-0900

QTY REQD PER ASSY	CODE IDENT NO.	PART OR IDENTIFYING NO.	NOMENCLATURE OR DESCRIPTION	MATERIAL	SPEC	SIZE DWG	ITEM NO.
		-1	BODY	L-605 (HAYNES 25) BAR	AMS 5759		

PARTS LIST

UNLESS OTHERWISE SPECIFIED

1. DO NOT SCALE DRAWING.
2. INTERPRET PER MIL-STD-100.
3. DIMENSIONS ARE IN INCHES.
4. SURFACE TEXTURE SHALL BE 125 ✓
5. REMOVE BURRS AND SHARP EDGES.
6. DIMENSIONS APPLY BEFORE PLATING OR CONVERSION COATING.
7. PARENTHETICAL DATA IS FOR REFERENCE ONLY.

TOLERANCES

ON ALL HOLE DIAMETERS

UNDER .064	+.0005 −.0000	.501 THRU .750	+.003 −.000
.064 THRU .125	+.001 −.000	.751 THRU 1.000	+.003 −.001
.126 THRU .250	+.002 −.000	1.001 THRU 2.000	+.003 −.002
.251 THRU .500	+.003 −.000	OVER 2.000	+.003 −.003

ON DECIMAL DIMENSIONS: .XXX ± .005; .XX ± .02; .X ± .1

ON ANGULAR DIMENSIONS: MACHINED ± 0°30'; LOCATING ± 0°30'; FORMED ± 2°; CHAMFERS ± 5°

FINISH

HEAT TREAT

APPLICABLE SPECIFICATIONS: THE ABOVE TRW SYSTEMS GROUP SPECS FORM A PART OF THIS DRAWING

PR12-G

CONTRACT NO.

DRAWN	G.E. BERG	5/21/75
CHECKED		
STRUCTURES		
MATERIALS/PROCESS		
ENGINEER		
SUPERVISOR		
PROJECT		

OTHER APPROVALS

THE FOLLOWING ECO'S HAVE BEEN ATTACHED TO THIS PRINT

TRW SYSTEMS GROUP
ONE SPACE PARK • REDONDO BEACH, CALIFORNIA

BODY - MONOPROPELLANT DEMONSTRATION THRUSTER

SIZE	CODE IDENT NO.	
C	11982	X412581

SCALE 10/1 SHEET

USED ON APPLICATION	NEXT ASSY	NEXT ASSY QTY

REVISIONS			
LTR	DESCRIPTION	DATE	APPROVED

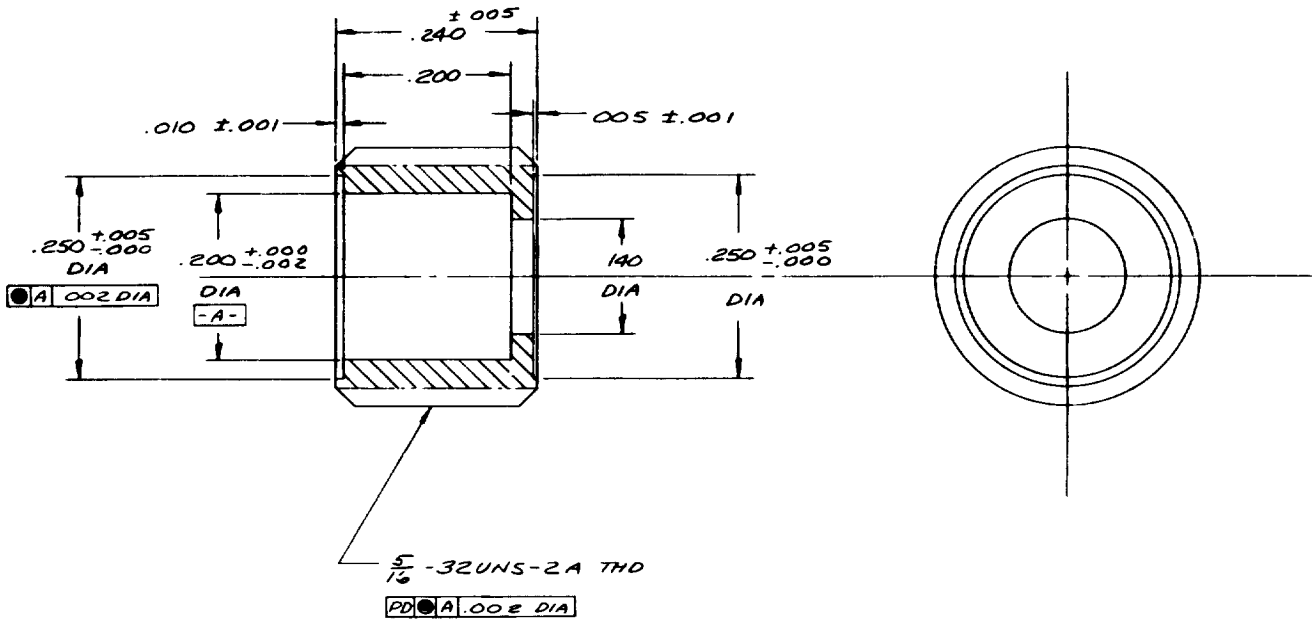

127

X412579

NOTES: UNLESS OTHERWISE SPECIFIED

1. IDENTIFY PER PR12-6-0900

CODE IDENT NO.	PART OR IDENTIFYING NO.	NOMENCLATURE OR DESCRIPTION	MATERIAL	SPEC	REF DES	ITEM NO.
	-1	SLEEVE	L-605 (HAYNES 25) BAR	AMS 5759		

QTY REQD PER ASSY

PARTS LIST

UNLESS OTHERWISE SPECIFIED

1. DO NOT SCALE DRAWING.
2. INTERPRET PER MIL-STD-100.
3. DIMENSIONS ARE IN INCHES.
4. SURFACE TEXTURE SHALL BE 125
5. REMOVE BURRS AND SHARP EDGES.
6. DIMENSIONS APPLY BEFORE PLATING OR CONVERS OR COATING.
7. PARENTHETICAL DATA IS FOR REFERENCE ONLY

TOLERANCES

ON ALL HOLE DIAMETERS

UNDER .014	+.0020 -.0005	.501 THRU .750	+.000 -.001
.014 THRU .125	+.004 -.001	.751 THRU 1.000	+.000 -.001
.126 THRU .250	+.005 -.001	1.000 THRU 2.000	+.012 -.001
.251 THRU .500	+.006 -.001	OVER 2.000	+.015 -.005

ON DECIMAL DIMENSIONS: .XXX ± .010, .XX ± .03, .X ± .1

ON ANGULAR DIMENSIONS: MACHINED ± 0°30', LOCATING ± 0°30', FORMED ± 1°, CHAMFERS ± 5°

FINISH

HEAT TREAT

CONTRACT NO.

DRAWN G E BERG 5/21/70

CHECKED

STRUCTURES

MATERIAL/ PROCESS

ENGINEER

SUPERVISOR

PROJECT

OTHER APPROVALS

THE FOLLOWING EO'S HAVE BEEN ATTACHED TO THIS PRINT

TRW SYSTEMS GROUP
ONE SPACE PARK • REDONDO BEACH, CALIFORNIA

SLEEVE - THREADED, MONOPROPELLANT DEMONSTRATION THRUSTER

SIZE	CODE IDENT NO.	
C	11982	X412579

SCALE 10/1 SHEET

USED ON NEXT ASSY APPLICATION	NEXT ASSY QTY REQD	APPLICABLE SPECIFICATIONS
		PR12-6

THE ABOVE TRW SYSTEMS GROUP SPECS FORM A PART OF THIS DRAWING

REVISIONS			
LTR	DESCRIPTION	DATE	APPROVED

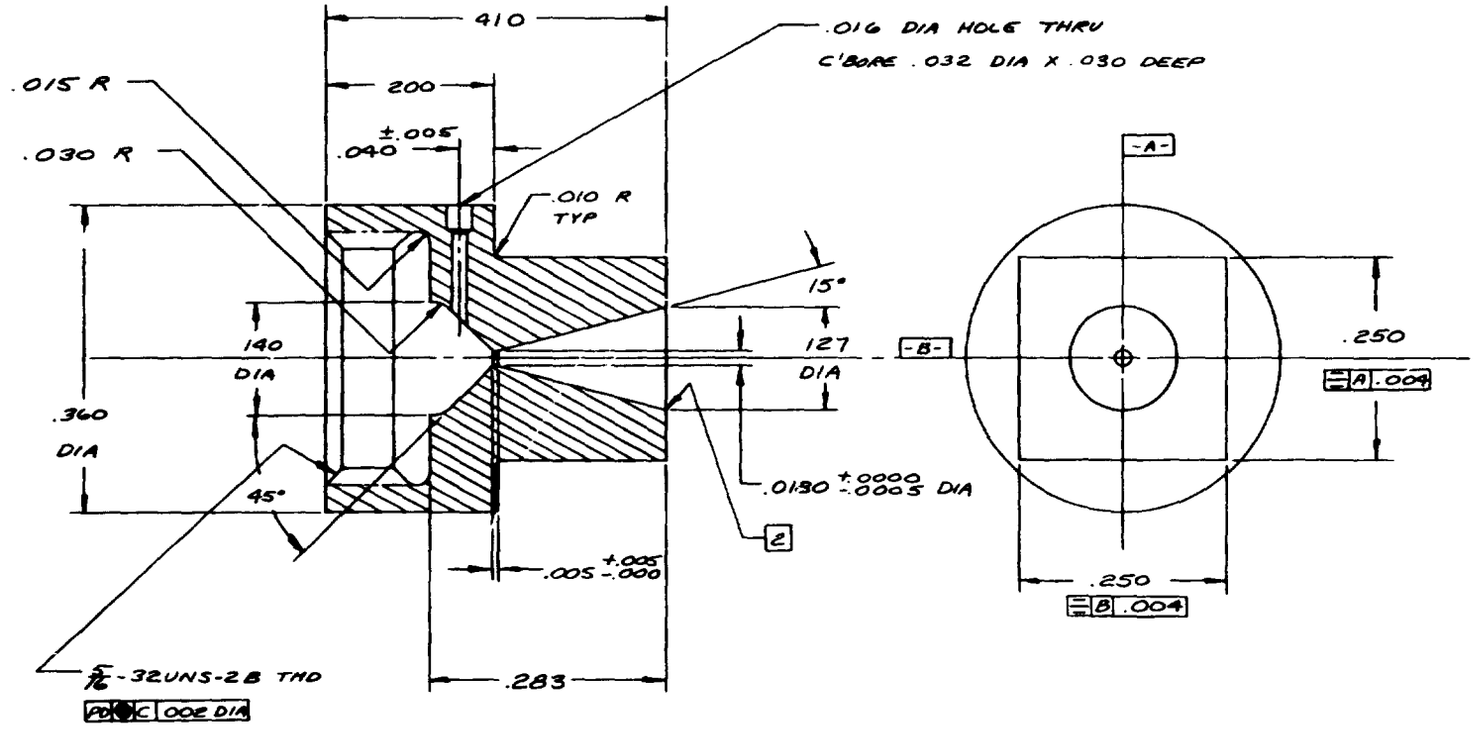

X412578

NOTES: UNLESS OTHERWISE SPECIFIED

1. IDENTIFY PER PR12-6-0900
2. REMOVE BURR BUT DO NOT BREAK SHARP CORNER.

ITEM NO.	QTY REQD PER ASSY	CODE IDENT NO.	PART OR IDENTIFYING NO.	NOMENCLATURE OR DESCRIPTION	MATERIAL	SPEC	REF DES
			-1	NOZZLE	L-605 (HAYNES 25) BAR	AMS 5759	

PARTS LIST

UNLESS OTHERWISE SPECIFIED
1. DO NOT SCALE DRAWING.
2. INTERPRET PER MIL-STD-100.
3. DIMENSIONS ARE IN INCHES.
4. SURFACE TEXTURE SHALL BE 125
5. REMOVE BURRS AND SHARP EDGES.
6. DIMENSIONS APPLY BEFORE PLATING OR CONVERSION COATING.
7. PARENTHETICAL DATA IS FOR REFERENCE ONLY.

TOLERANCES
ON ALL HOLE DIAMETERS

UNDER .064	+.0000 -.0005	.501 THRU .750	+.000 -.001
.064 THRU .125	+.001 -.000	.751 THRU 1.000	+.000 -.002
.126 THRU .250	+.002 -.000	1.000 THRU 2.000	+.001 -.002
.251 THRU .500	+.003 -.000	OVER 2.000	+.003 -.003

ON DECIMAL DIMENSIONS: .XXX ± .005; .XX ± .01; .X ± .1
ON ANGULAR DIMENSIONS: MACHINED ± 0°30'; LOCATING ± 0°30'; FORMED ± 2°; CHAMFERS ± 5°

FINISH
HEAT TREAT

CONTRACT NO.

DRAWN	G E BERG	5/10/73
CHECKED		
STRUCTURES		
MATERIAL/ PROCESS		
ENGINEER		
SUPERVISOR		
PROJECT		

OTHER APPROVALS

THE FOLLOWING ECR'S HAVE BEEN ATTACHED TO THIS PRINT

TRW
ONE SPACE PARK • REDONDO BEACH, CALIFORNIA

NOZZLE - MONOPROPELLANT DEMONSTRATION THRUSTER

SIZE	CODE IDENT NO.	
C	11982	X412578

SCALE 10/1 SHEET

USED ON	NEXT ASSY	APPLICATION

APPLICABLE SPECIFICATIONS
THE ABOVE TRW SPECIFICATIONS GRADE NOTES FORM A PART OF THIS DRAWING

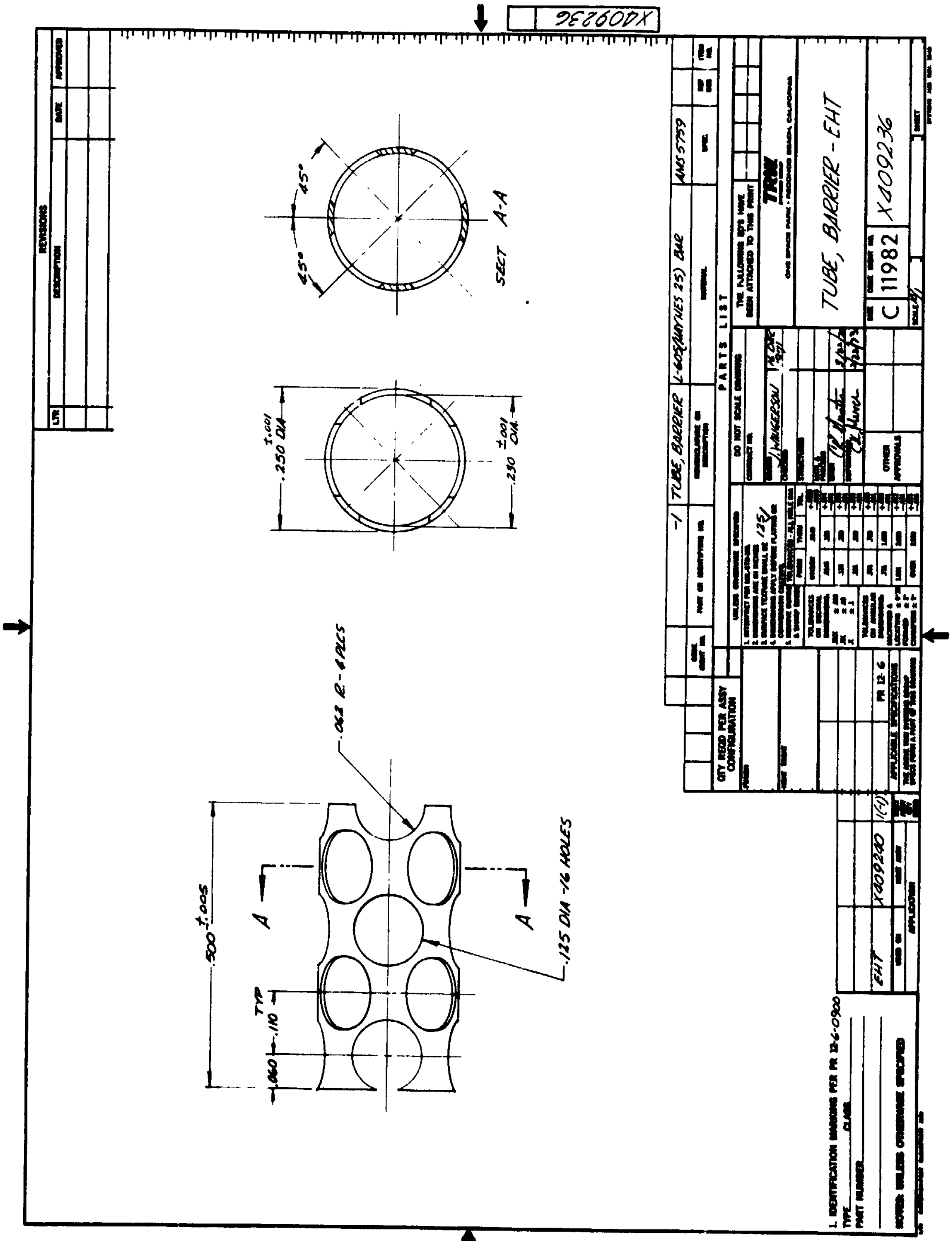
REVISIONS
PARTS LIST
-1 TUBE, BARRIER
L-605 (HAYNES 25) BAR
AMS 5759
DO NOT SCALE DRAWING
TRW
TUBE, BARRIER - EHT
C 11982
X409236
SECT A-A
45°
.250 DIA ±.001
.230 ±.001 DIA
.062 R - 4 PLCS
.125 DIA -16 HOLES
.500 ±.005
TYP
.110
.060
A
EHT
X409240
PR 12-6
1. IDENTIFICATION MARKING PER PR 12-6-0900
NOTES: UNLESS OTHERWISE SPECIFIED

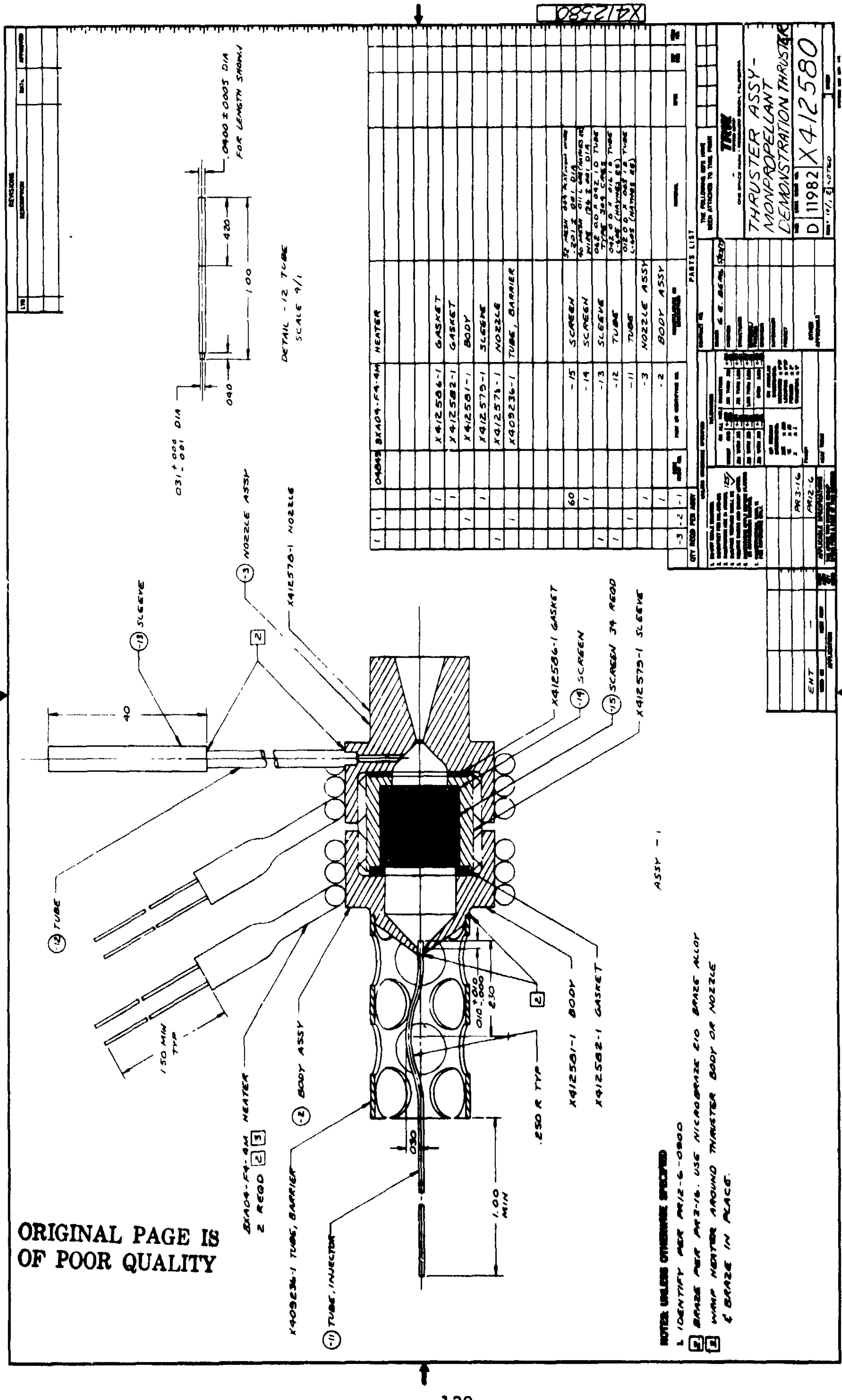

ORIGINAL PAGE IS
OF POOR QUALITY

REVISIONS			
LTR	DESCRIPTION	DATE	APPROVED

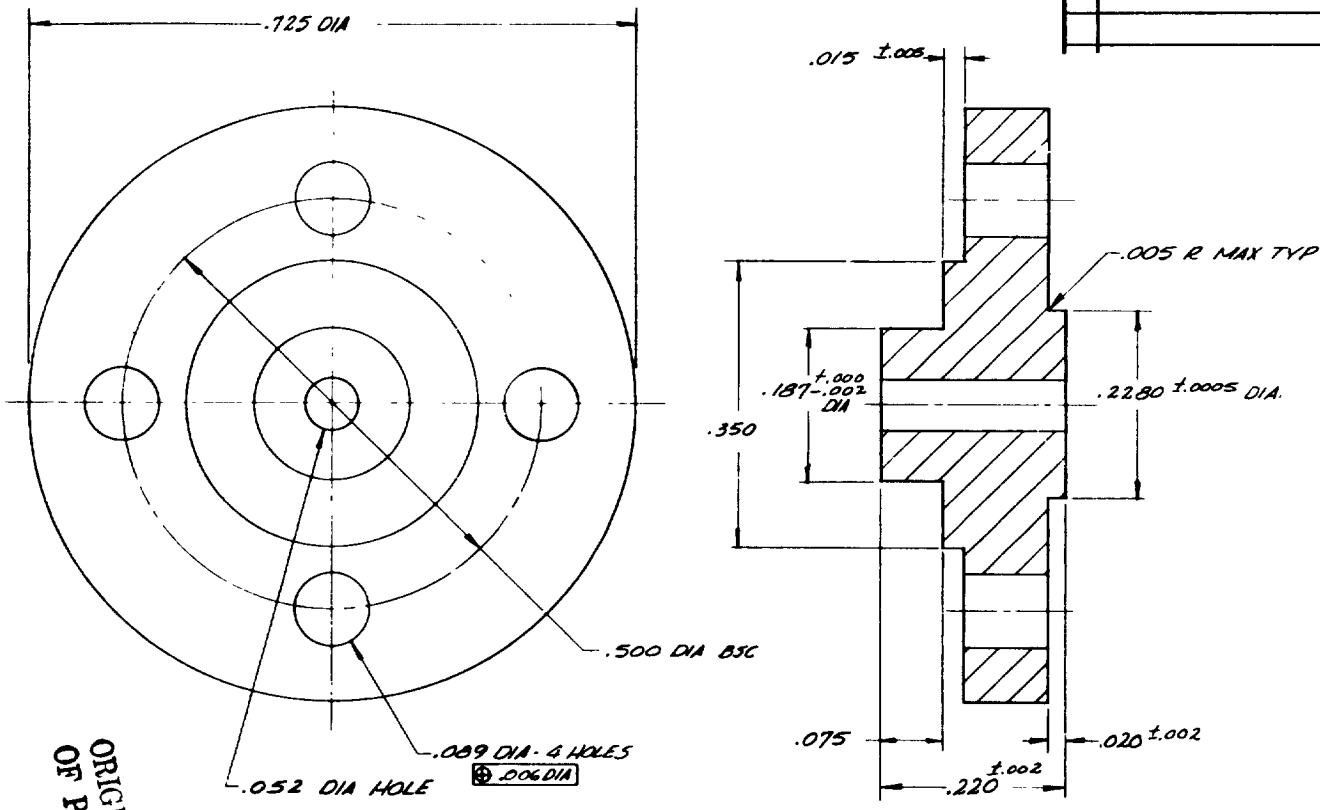

ORIGINAL PAGE IS OF POOR QUALITY

X409383

CODE IDENT NO.	PART OR IDENTIFYING NO.	NOMENCLATURE OR DESCRIPTION	MATL/DIMN.	SPEC.	REF DES	ITEM NO.
	-1	SEAL R	TYPE 304 CRES BAR	AMS5759		

PARTS LIST

QTY REQD PER ASSY CONFIGURATION

UNLESS OTHERWISE SPECIFIED
1. INTERPRET PER MIL-STD-100.
2. DIMENSIONS ARE IN INCHES
3. SURFACE TEXTURE SHALL BE 125/
4. DIMENSIONS APPLY BEFORE PLATING OR CONVERSION COATING.
5. REMOVE BURRS & SHARP EDGES

TOLERANCES - ALL HOLE DIA	FROM	THRU	TOL.
UNDER	.0469		±.0005
.0469	.125		±.001
.125	.250		±.002
.251	.375		±.003
.376	.750		±.004
.751	1.000		±.005
1.001	2.000		±.007
OVER	2.000		±.010

TOLERANCES ON DECIMAL DIMENSIONS: .XXX ± .010; .XX ± .03; .X ± .1

TOLERANCES ON ANGULAR DIMENSIONS: MACHINED & LOCATING ± 0°30'; FORMED ± 2°; CHAMFERS ± 5°

DO NOT SCALE DRAWING
CONTRACT NO.

DRAWN	J.WINGERSON	21 DEC 1971
CHECKED		
STRUCTURES		
MATL & PROCESS		
ENGR		
SUPERVISOR		

OTHER APPROVALS

THE FOLLOWING ED'S HAVE BEEN ATTACHED TO THIS PRINT

TRW
ONE SPACE PARK • REDONDO BEACH, CALIFORNIA

PLATE, SEAL - EHT

SIZE	CODE IDENT NO.	
C	11982	X409383

SCALE 9/1 SHEET

1. IDENTIFICATION MARKING PER PR 12-6-0900
TYPE CLASS
PART NUMBER
NOTES: UNLESS OTHERWISE SPECIFIED

EHT	X009240	1(4)
USED ON	NEXT ASSY	QUAN PER NEXT ASSY
APPLICATION		

PR 12-6
APPLICABLE SPECIFICATIONS
THE ABOVE TRW SYSTEMS GROUP SPECS FORM A PART OF THIS DRAWING

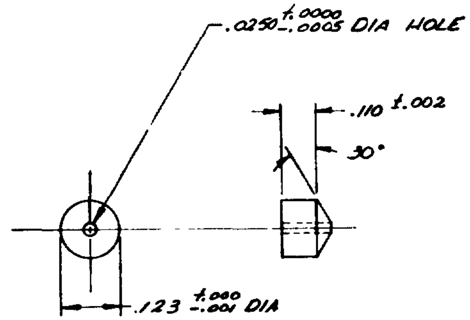

ORIGINAL PAGE IS

NOTES: UNLESS OTHERWISE SPECIFIED

1. IDENT. MARKING PER PR 12-6-0900

QTY REQD PER ASSY	CODE IDENT NO.	PART OR IDENTIFYING NO.	NOMENCLATURE OR DESCRIPTION	MATERIAL	SPEC	ITEM NO.
		-1	SEAL	TEFLON ROD	MIL-P-19468	

PARTS LIST

THE FOLLOWING EO'S HAVE BEEN ATTACHED TO THIS PRINT

TRW — ONE SPACE PARK • REDONDO BEACH, CALIFORNIA

SEAL, TUBE - EHT

SIZE C | CODE IDENT NO. 11982 | X410563

SCALE NONE

APPLICATION: EHT | 1(-1) | PR 12-6

APPLICABLE SPECIFICATIONS

X410563

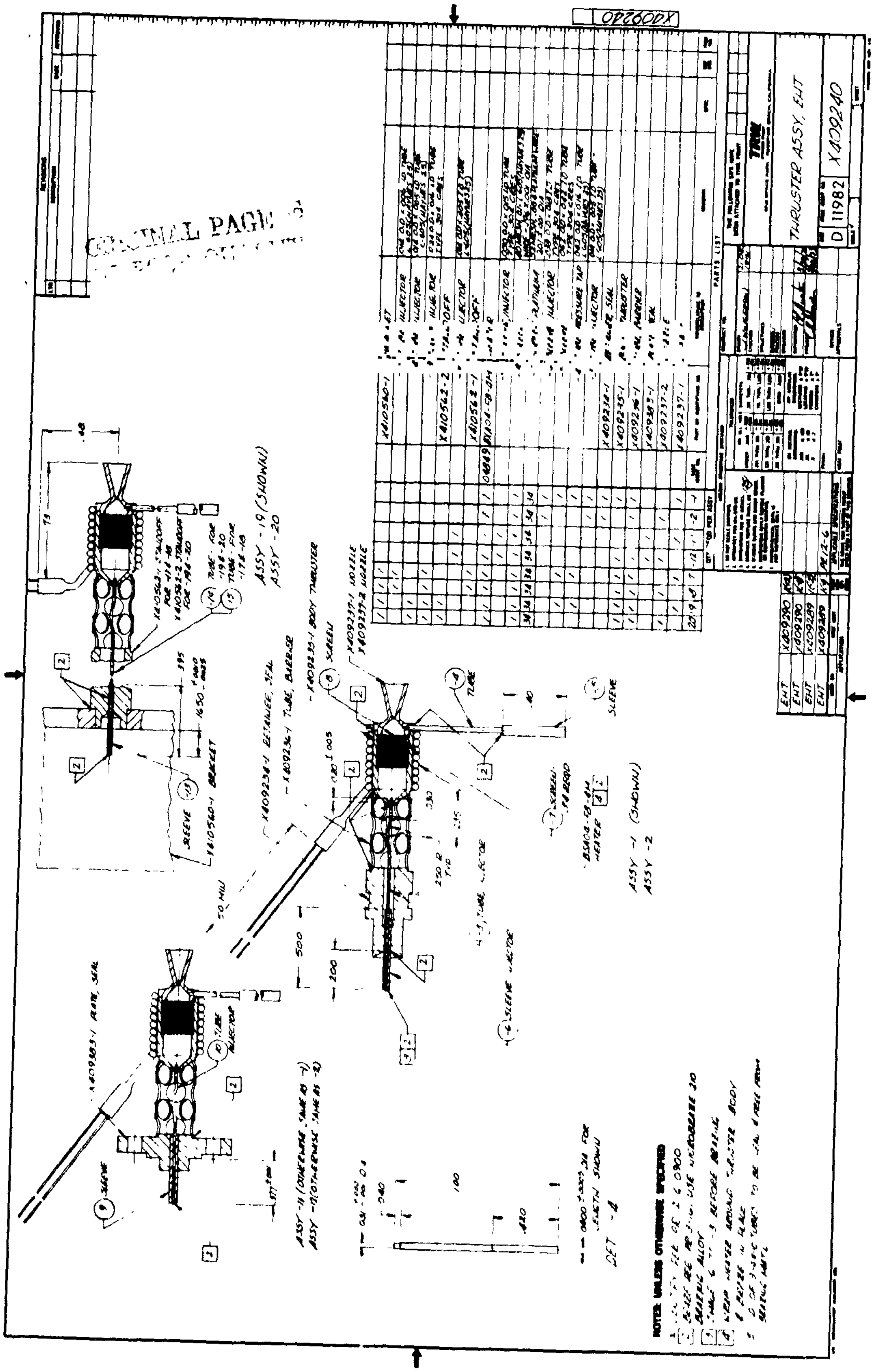

ORIGINAL PAGE IS
OF POOR QUALITY
THRUSTER ASSY, EHT
D 11982 X409240
X409240
PARTS LIST
ASSY -19 (SHOWN)
ASSY -20
ASSY -1 (SHOWN)
ASSY -2
NOTES: UNLESS OTHERWISE SPECIFIED